Functional and therapeutic effects of viscumins in the treatment of experimental glioblastoma

Dissertation

zur Erlangung des Grades eines
Doktors der Naturwissenschaften

der Mathematisch-Naturwissenschaftlichen Fakultät
und
der Medizinischen Fakultät
der Eberhard-Karls-Universität Tübingen

vorgelegt
von

Sonja Schötterl
aus Schwäbisch Gmünd, Deutschland

Juli - 2018

Tag der mündlichen Prüfung: 21.01.2019

Dekan der Math.-Nat. Fakultät: Prof. Dr. W. Rosenstiel
Dekan der Medizinischen Fakultät: Prof. Dr. I. B. Autenrieth

1. Berichterstatter: Prof. Dr. Ulrike Naumann
2. Berichterstatter: Prof. Dr. Peter Ruth

Prüfungskommission: Prof. Dr. Ulrike Naumann
Prof. Dr. Peter Ruth
Prof. Dr. Robert Feil
Prof. Dr. Stephan Huber

Erklärung / Declaration:

Ich erkläre, dass ich die zur Promotion eingereichte Arbeit mit dem Titel:
„Functional and therapeutic effects of viscumins in the treatment of experimental glioblastoma“
selbständig verfasst, nur die angegebenen Quellen und Hilfsmittel benutzt und wörtlich oder inhaltlich übernommene Stellen als solche gekennzeichnet habe. Ich versichere an Eides statt, dass diese Angaben wahr sind und dass ich nichts verschwiegen habe. Mir ist bekannt, dass die falsche Abgabe einer Versicherung an Eides statt mit Freiheitsstrafe bis zu drei Jahren oder mit Geldstrafe bestraft wird.

I hereby declare that I have produced the work entitled “Functional and therapeutic effects of viscumins in the treatment of experimental glioblastoma”, submitted for the award of a doctorate, on my own (without external help), have used only the sources and aids indicated and have marked passages included from other works, whether verbatim or in content, as such. I swear upon oath that these statements are true and that I have not concealed anything. I am aware that making a false declaration under oath is punishable by a term of imprisonment of up to three years or by a fine.

Tübingen, den ....

Datum / Date Unterschrift /Signature

Statement of contributions according to § 9 (2):

As a PhD student I supervised the following students that produced data used in my dissertation “Functional and therapeutic effects of viscumins in the treatment of experimental glioblastoma”:

- Vivien Veninga
  p. 68, Figure 13B: Parts of the ELISA were performed by Vivien Veninga.
- Jennifer Theresia Miemietz
  p.55, Table 2 and p. 56, Figure 6: Staining of CD75s in GBM cells and tissue and correlation analysis of CD75s expression and ML-mediated cytotoxicity were performed by J. T. Miemietz.

Furthermore, parts of the animal experiments were evaluated in collaboration with the Neurological Institute, Edinger Institute, Frankfurt/Main.

- Naita Maren Wirsik
  p.83, Figure 21C: Evaluation of tumor proliferation, invasion, and apoptosis of brain HE stainings

Additionally, the murine hippocampal slice cultures (HSC) from C57BL/6 mice were prepared and provided by Ingrid Ehrlich, Hertie Institute for Clinical Brain Research and Center for Integrative Neuroscience (Tübingen, Germany; p.26).

All other data presented in this dissertation were collected by me.

Table of Contents

List of abbreviations

Abbreviation	Meaning
ABC	ATP-binding cassette
ANGPT1	Angiopoetin-1
APC	Antigen-presenting cell
APS	Ammonium persulfate
ATM	Ataxia telangiectasia mutated serine/threonine kinase
ATR	Ataxia telangiectasia and Rad3 related protein
ATP	Adenosine 5′-triphosphate
Avi	Aviscumine
BBB	Blood-brain barrier
BCL2	B-cell lymphoma 2
BER	Base excision repair
BLC	B lymphocyte chemoattractant
BrdU	5-Bromo-2-deoxyuridine
BRMS1	Breast cancer metastasis suppressor 1
BSA	Bovine serum albumin
CASP8	Caspase-8
CCL24	Chemokine ligand 24
CCNB	Cyclin B
CCND	Cyclin D
CDKN1A	Cyclin-dependent kinase inhibitor 1A, p21
CDKN1B	Cyclin-dependent kinase inhibitor 1B, p27
cDNA	Complementary DNA
CM	Conditioned medium
CNS	Central nervous system
COX-2	Cyclooxygenase-2
CSF3	Colony-stimulating factor 3
Ct	Cycle threshold

CTLA4	Cytotoxic T lymphocyte-associated antigen-4
CV	Crystal violet
CXCL5	C-X-C motif chemokine 5
CX3CL1	Chemokine (C-X3-C motif) ligand 1
d	Days
DAPI	4,6-Diamidino-2-phenylindol
DAMPs	Damage-associated molecular patterns
DC	Dendritic cell
DMEM	Dulbecco's modified eagle's medium
DMSO	Dimethyl sulfoxide
DNA	Deoxyribonucleic acid
dNTP	Deoxynucleoside triphosphate
DSB	Double-strand breaks
DTT	1,4-Dithiothreitol
E2F1 / E2F2	E2F transcription factor 1 / 2
e.g.	*Exempli gratia* / for example
EBM-2	Endothelial basic medium
ECL	Enhanced chemiluminescence
ECM	Extracellular matrix
EDTA	Ethylenediaminetetraacetic acid
EGF	Epidermal growth factor
EGFR	Epidermal growth factor receptor
EGFRvIII	Epidermal growth factor receptor version III
EGM-2	Endothelial growth medium
EGTA	Ethylene glycol-bis(2-aminoethylether)-N,N,N′,N′-tetraacetic acid
ELISA	Enzyme-linked immunosorbent assay
ENG	Endoglin
EPHB2	EPH receptor B2
FBS	Fetal bovine serum
FC	Fold change
FGF2	Fibroblast growth factor 2

FITC	Fluoresceinisothiocyanate
GAPDH	Glycerinealdehyde-3-phosphate dehydrogenase
GBM	Glioblastoma
GM-CSF	Granulocyte monocyte colony-stimulating factor
GMP	Good manufacturing practice
GSC	Glioblastoma stem cell
HBVP	Primary human brain vascular pericytes
hCEMC/D3	Human brain endothelial cells
HE	Haematoxylin eosin
HDAC	Histone deacetylase
HMOX1	Heme oxygenase 1
HRP	Horseradish peroxidase
HSC	Hippocampal slice cultures
i.p.	Intraperitoneal
IDH	Isocitrate dehydrogenase
IFN-γ	Interferon-γ
IL	Interleukin
ISC P	ISCADOR P
ISC Qu	ISCADOR Qu
KDR	Kinase insert domain receptor / VEGFR2
KISS1R	KISS1 receptor
K-ML	Korean viscumin
MDR	Multi-drug resistance
ME	Mistletoe extracts
MEM	Modified eagle's medium
MGMT	O^6-methylguanin-DNA-methyltransferase
MHC	Major histocompatibility complex
MICA	MHC class I polypeptide-related sequence A
MIG	Monokine induced by gamma interferon
MIP-1α	Macrophage inflammatory protein alpha
miR	MicroRNA

ML	Mistletoe lectins / viscumins
MMP	Matrix metalloproteinase
MMR	Mismatch repair
mRNA	Messenger RNA
MTA1	Metastasis associated 1
MT-MMP	Membrane type matrix metalloproteinase
MTT	Thiazolyl blue tetrazolium bromide
NK cell	Natural killer cell
NMDA	N-Methyl-D-aspartate
NME	NME/NM23 nucleoside diphosphate kinase 1
NMRI	Rj:NMRI-Foxn1^{nu}/Foxn1^{nu}
NP-40	Igepal
o/n	Over night
PBMC	Peripheral blood mononuclear cell
PBS	Dulbecco's phosphate buffered saline
PCR	Polymerase chain reaction
PD	Programmed cell death
PDGFRA	PDGF receptor A
PDL	Programmed cell death ligand
PE	Phycoerythrin
PGS	Pericyte growth supplement
PI	Propidium iodide
PPP2CA	Protein phosphatase 2 catalytic subunit alpha
P/S	Penicillin (100 U/ml)/streptomycin (100 µg/ml)
PTEN	Phosphatase and tensin homolog
PTGS	Prostaglandin-endoperoxide synthase
PVDF	Polyvinylidene fluoride
QoL	Quality of life
R	Relation coefficient
RB1	Retinoblastoma protein
RBL1	Retinoblastoma like protein

RCTs	Randomized control trials
RIP	Ribosome-inactivating protein
RNA	Ribonucleic acid
RT	Room temperature
RTF	Regeneration and tolerance factor
RT-qPCR	Quantitative real time PCR
s.c.	Subcutaneous
SDS	Sodium dodecyl sulfate
SDS-PAGE	Sodium dodecyl sulfate - polyacrylamide gel electrophoresis
SELE	Selectin E / CD62E
SERPINB5	Serpin family B member 5
SFM	Serum free medium
SMAD	Mothers against DPP homolog
TECK	Thymus-expressed chemokine / CCL25
TEMED	Tetramethylethylenediamine
TERT	Telomerase
TGFB / TGF-β	Tumor growth factor β
TGFBR / TGF-βR	Tumor growth factor β receptor
TIMP	Tissue inhibitor of metalloproteinase
TMZ	Temozolomide
TNF	Tumor necrosis factor
TP53	Tumor protein p53
Treg	Regulatory T cell
Tris	Trizma
TTF	Tumor-treating fields
ULBP2	UL16 binding protein 2
VCAM	Vascular cell adhesion molecule
VEGF	Vascular endothelial growth factor
VT	Viscotoxins
WHO	World health organization

Summary

Glioblastoma (GBM) is the most aggressive primary brain tumor, leading to death in less than 15 months despite tumor resection, radiation, and chemotherapy. The development of new and effective treatment options is therefore crucial. Mistletoe extracts (ME) have been used in complementary and alternative cancer therapy for decades. Mistletoe lectins I-III, also called viscumins (ML), and viscotoxins are the main active components, providing anti-cancer activity by different mechanisms including immuno-modulation, dose-dependent cytotoxicity, and mitigation of tumor cell motility. In clinical trials, viscumin treatment of cancer patients led to an improvement in the quality of life and to prolonged survival for some tumor entities. Here we show anticancer effects of the ME ISCADOR Qu, the recombinant ML-1 Aviscumine, and native ML-1. We found that each of the three viscumins reduced cell proliferation but even to a different extent. The reduction in proliferation was accompanied by changes in glioma cell cycle distribution and gene expression. In higher concentrations viscumins induced cell death in GBM cells *in vitro*. Nevertheless, at the same concentration we observed no toxic effects in organotypic mouse brain cultures *in situ*. The viscumin receptor CD75s was expressed in all tested GBM cell lines so far and its level of expression correlated well with the cell's vulnerability towards viscumin induced cell death. We detected CD75s in 6 out of 7 human GBM tissues but not in human and murine healthy brain tissue. This makes viscumins suitable for a localized drug application in the brain. Viscumins significantly reduced glioma cell motility and the expression and activity of cancer motility-associated factors in GBM cell lines. Viscumins also provided beneficial immune-stimulating effects. They enhanced the vulnerability of GBM cells towards natural killer (NK) cell and T cell mediated killing. Besides, in GBM cells viscumins altered the expression of immune response related genes that are associated to pro-inflammatory processes. Furthermore, we found synergistic therapeutic effects in GBM cells if viscumins were used in combination with irradiation and chemotherapy. Additionally, adjuvant viscumin therapy prolonged the survival of glioma bearing

mice in two different mouse models. In mice, serum levels of pro-inflammatory cytokines were increased after ISCADOR Qu injections. These findings provide the basis for clinical trials to investigate the therapeutic efficacy of adjuvant viscumin treatment in glioblastoma patients.

1. Introduction

1.1 Glioblastoma (GBM)

GBM is the most malignant brain tumor in adults with an incidence rate of approximately 3 per 100,000 persons in the US and European countries. This is the highest incidence rate of all brain tumors and rises to about 8 per 100,000 in the group of over 55 years old persons [1]. The prognosis of GBM patients is infaust; the one year survival rate is currently 37.2% and the five year survival only 5.1% [2]. In the last decade, GBM standard therapy consists of maximal safe tumor resection, radiotherapy, and chemotherapy using temozolomide (TMZ). The median survival is 12.1 months after surgery and radiotherapy and rises to 14.6 months if TMZ therapy is added [3]. No significant improvements with drug therapy were achieved in the last years despite testing several novel therapeutic approaches. Due to advances in surgery and radiotherapy the median survival could be increased to 18-20 months [4]. Nevertheless, for elderly patients (> 70 years) the median survival did not improve and is still only 4 months [5]. GBM are preferentially located at frontal and temporal lobes and show massive necrosis and haemorrhage (see Figure 1). It is also possible that the GBM cells invade over the *corpus callosum* to the contralateral hemisphere. Typical symptoms of GBM are partial or generalised seizures, focal neurological deficits, cognitive dysfunction, elevated intracranial pressure and edema leading to headache, vomiting, nausea, drowsiness, and visual deficits [6]. The incurable nature of GBM and the bad prognosis originates from its strongly invasive, angiogenic, and immunosuppressive features. Furthermore, GBM and especially recurrent GBM are mainly multi-drug and radiation resistant. New treatment approaches are therefore essential to improve the treatment of this malignant brain tumor.

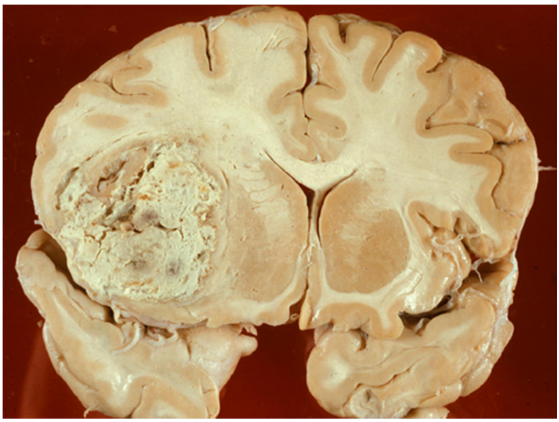

Figure 1: Formalin fixed brain containing a GBM on the left hemisphere with necrosis and haemorrhage. Source: http://neuropathology-web.org/chapter7/chapter7bGliomas.html, status from 24.06.2018.

1.1.1 GBM classification

In 2016 the world health organisation (WHO) renewed the classification of central nervous system (CNS) tumors [7]. From now on, not only histological but also molecular parameters are used for classification. According to the new classification GBM belong to the group of diffuse astrocytic and oligodendroglial tumors. As shown in Figure 2, this group includes astrocytic tumors WHO grade II and III, oligodendrogliomas WHO grade II and III, diffuse gliomas of childhood, and WHO grade IV GBM.

GBM are subdivided into isocitrate dehydrogenase (IDH)-wildtype, IDH-mutant, and not otherwise specified (NOS) if the IDH status cannot be tested. IDH-wildtype GBM largely correlate with *de novo* primary GBM and IDH-mutant GBM with secondary GBM developing from lower grade gliomas [8]. IDH-wildtype GBM are more common in older patients with a median age of 62 years at diagnosis, while IDH-mutant GBM affect younger patients with a median age of 44 years. IDH-wildtype tumors count for 90% of GBM cases. Additionally, these tumors are further divided into giant cell GBM, gliosarcoma, and epithelioid GBM (for review see [9]).

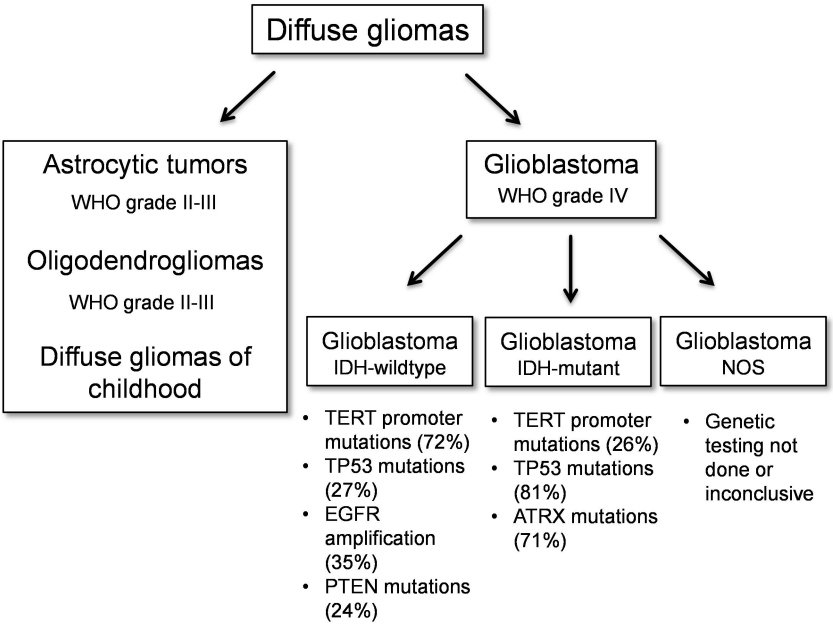

Figure 2: Classification of diffuse gliomas. Isocitrate dehydrogenase (IDH)-wildtype and IDH-mutant GBM not only differ in their IDH status but also in telomerase (TERT) promoter mutations, epidermal growth factor receptor (EGFR) amplification, and tumor protein p53 (TP53), ATRX, and Phosphatase and tensin homolog (PTEN) mutation status. Modified from [7].

1.1.2 Therapy resistance

One general problem of treating brain tumors is the blood-brain barrier (BBB) that protects the tumor from many anti-cancer drugs like doxorubicin, vincristine, or erlotinib. Resistance towards these drugs is also induced by overexpression of transmembrane ATP-binding cassette (ABC) transporters, which are responsible to export foreign substances [10, 11]. High activity of these transporter leads to the so called multi-drug resistance (MDR). The best option to treat GBM is therefore to use drugs that can cross the BBB, like the lipophilic TMZ. TMZ, sold as Temodal®, is an orally administered DNA alkylating agent that modifies DNA or RNA at N^7 and O^6

sites on guanine and the N^3 on adenine by the addition of methyl groups. The methylated sites can remain mutated, can be fixed by DNA mismatch repair (MMR), can be removed by base excision repair (BER), or can be dealkylated by enzymes such as O^6-methylguanine methyl transferase (MGMT). When MGMT and BER proteins are expressed, GBM cells become resistant to TMZ [12, 13]. MGMT silencing by promotor methylation is a predictive factor for the impact of GBM therapy. The median overall survival increases from 12.2 to 18.2 months if the MGMT promotor is methylated [13].

Another mode of resistance results from the hypoxic tumor environment. GBM cells are largely resistant to acidosis present at low oxygen levels that result from fast GBM cell proliferation and the subsequent low supply of nutrients and oxygen due to low blood vessel density [14]. The distance of hypoxic GBM cells to the vasculature makes them often unreachable for anti-cancer drugs. Furthermore, many of these drugs rely on the formation of reactive oxygen species (ROS), but ROS formation is reduced in hypoxic conditions due to low oxygen supply. Finally, hypoxic GBM cells become inactive and stop to proliferate. This way tumor cells escape the effects of anti-proliferative drugs (for review see [15, 16]).

Glioblastoma stem cells (GSCs) are another major cause for GBM drug resistance and tumor recurrence. In the tumor these cells occur in low frequency and show self-renewing features, express stem cell markers, and hold multi-lineage potential (for review see [17]). GSCs are highly resistant towards most therapy approaches [18, 19]. Targeting these cells is a promising future approach to treat GBM. Furthermore, several microRNAs, small noncoding RNAs regulating gene expression, are differentially expressed in GBM cells and are associated to GBM drug resistance. MicroRNA (miR)-21 is overexpressed in GBM and prevents TMZ induced apoptosis of GBM cells [20]. miR-195, miR-455, and miR-10a* are upregulated in GBM and linked to TMZ resistance [21]. Besides, some miRNAs are associated with the vulnerability of GBM cells towards chemotherapy. miR-200a-3p is downregulated in GBM and its overexpression leads to increased TMZ sensitivity [22]. MGMT expression is downregulated by miR-181d, and also miR-211 and miR-130a can influence GBM chemosensitivity [23-25]. Taken together, GBM drug resistance is

determined by several features, including the integrity of the BBB, ABC transporters, MGMT, MMR, BER, hypoxia, GSCs, and microRNAs.

1.1.3 Migration and invasion

The invasive growth and the ability of GBM cells to migrate away from the tumor core make a complete surgical resection of GBM nearly impossible. GBM cells that invade into the surrounding tissue also escape focal irradiation and might cause GBM recurrence. In GBM several mechanisms are involved that enhance tumor cell migration and invasion. Important aspects are the degradation and remodelling of the extracellular matrix (ECM), alterations of the cytoskeleton, the hypoxia induced switch from proliferation towards migration, cell shrinkage to reduce the cell volume, reduced cellular adhesion, and alterations in the expression of transcription factors, ion channels, proteases, chemokines, and cytokines (for review see [26]).

The degradation of the ECM is essential for invasive processes since this way glioma cells conquer the space they need to migrate. Responsible for this degradation are matrix metalloproteinases (MMPs), secreted or membrane-anchored endoproteinases that can be grouped according to their substrate specificity (e.g. gelatinases or collagenases). The expression of the more than 20 MMP family members in the normal brain is very low, and enhanced expression is normally disease associated [27]. In GBM, MMPs are mainly overexpressed and activated. The expression of the gelatinases MMP-2 and MMP-9 is especially important for GBM invasion and correlates with GBM grade and progression [28, 29]. MMP-2 and MMP-9 can activate latent tumor growth factor-β (TGF-β/TGFB) leading to a feedback loop where TGF-β induces MMP-2 and MMP-9 expression [30-32]. The membrane-anchored MMP-14 activates MMP-2 by cleaving the pro-peptide. MMP-2 is not solely expressed on GBM cells but also on surrounding microglia cells [33-35]. Besides MMP-2 and -9, MMP-3, -7, -12, -13, -16, -19, and -26 are overexpressed in GBM cells and are mainly linked to enhanced glioma invasion [36-43]. The four tissue inhibitors of metalloproteinases (TIMP) members, TIMP1-4, can inhibit but also help to activate MMPs. For example, TIMP-2 forms a complex with MMP-14 and pro-MMP-2 that enhances MMP-2

activation [35, 44]. Because TIMPs are able to activate and to inhibit MMPs, their function during GBM migration and invasion remains unclear.

TGF-β is massively secreted by GBM cells. TGF-β not only supports the activation of MMPs but also promotes a general pro-migratory GBM cell phenotype [45]. TGF-β 1-3 are members of the TGF-β cytokine family. Mainly TGF-β1 and TGF-β2 hold key functions in tumor progression [46]. They bind to the TGF-β receptor (TGF-βR/TGFBR) I complex, leading to the phosphorylation of TGF-βRII subsequently inducing the phosphorylation of mothers against DPP homolog (SMAD) 2/3. Finally, this complex regulates gene expression in the nucleus [47]. TGF-β influences the interaction of GBM cells with the ECM also by upregulating versican and integrin αvβ3, thereby enhancing migration [48, 49]. Through upregulation of miR-10a/b, TGF-β suppresses phosphatase and tensin homolog (PTEN) in GBM [50]. TGF-β expression is also enhanced after irradiation, thereby inducing a more invasive GBM phenotype [51]. Although the migration and invasion of GBM is of great importance and research was focused on GBM cell motility for long time, no therapy is currently available that targets invaded GBM cells or reduces GBM migration.

1.1.4 Immunosuppressive mechanisms

In GBM patients several pathways and mechanisms lead to a local, tumor-associated suppression of the immune system. One the one hand an intact BBB limits the entry of immune cells into the brain. On the other hand GBM cells actively enforce immunosuppression (for review see [52]). In the healthy brain only few immune cells are present, but if the BBB is disrupted due to a pathological condition, the permeability for immune cells increases [53-55]. Antigens from the brain drain towards lymph nodes into the body where antigen-presenting cells (APC) present them to naïve T cells [56]. Upon activation T cells upregulate α4 and β1 integrins which enables them to bind to vascular cell adhesion molecule (VCAM)-1 on vascular cells and to cross the BBB [57, 58].

Also regulatory T cells (Tregs) are among the immune cells that are attracted by the tumor. Tregs are anti-inflammatory T cells that help to maintain tolerance to self-

antigens and to inhibit autoimmunity. In GBM patients the increase of Tregs in the tumor area and blood is linked to a worse prognosis and to the tumor grade [59, 60]. The amount of GBM infiltrating Tregs could be reduced by inhibiting TGF-β signalling [61]. TGF-β provides not only pro-migratory functions as described in the previous chapter but is additionally a strongly immunosuppressive cytokine in GBM. It induces the differentiation of $CD4^+$ T cells into Tregs, inhibits granzyme B and interferon-γ expression in $CD8^+$ T cells, and downregulates the expression of the activating receptor NKG2D on NK cells [62-65]. Furthermore, TGF-β reduces the expression of NKG2D ligands like MHC class I polypeptide-related sequence A (MICA) or UL16 binding protein 2 (ULBP2) on the cell surface of GBM cells [66]. Several other immunosuppressive factors are secreted by GBM cells like the vascular endothelial growth factor (VEGF), interleukin (IL)-10, arginase, nitric oxide, prostaglandin E-2, and the regeneration and tolerance factor (RTF) [67-72].

Macrophages and microglia cells are the main infiltrating immune cells found in GBM. They count for up to 12% of the tumor bulk and are manipulated by GBM cells to secrete pro-tumorigenic factors [73]. Macrophages can be differentiated into M1 macrophages that harbor anti-tumorigenic functions and secrete pro-inflammatory cytokines, or alternatively into immunosuppressive M2 macrophages. Glioma secreted TGF-β modulates macrophages to differentiate into the M2 phenotype [74]. These M2 macrophages secrete TGF-β, epidermal growth factor (EGF), VEGF, MMP-2, and MMP-9, thereby fostering GBM immunosuppression, migration, and angiogenesis [75-78].

GBM cells do not only secrete immunosuppressive factors but also express cell surface proteins that interact with immune cells to prevent an immune response. The most prominent example is programmed cell death ligand (PDL)-1 that binds to programmed cell death (PD)-1 on activated T cells and induces T cell exhaustion. This mechanism protects GBM cells from cytotoxic T cell attacks [79, 80]. CD95L is another protein expressed on GBM cells. It binds to its receptor on T cells where it induces apoptosis [81, 82]. Furthermore, GBM cells inhibit immune cells by expressing non-classical major histocompatibility complex (MHC) class I proteins [83, 84]. Even the hypoxic tumor environment and certain tumor metabolites are

immunosuppressive and lead to T cell apoptosis and anergy [85-87]. To understand and circumvent the immunosuppressive mechanisms in GBM will help to successfully develop novel GBM immunotherapeutic approaches.

1.1.5 New therapy options

Since the introduction of the current standard therapy for GBM that includes maximal safe surgical resection, radiation, and TMZ-based chemotherapy, many new therapy approaches have been tested. Unfortunately, most of them did not provide benefit in the overall survival of GBM patients. Treatment strategies like intensifying or prolonging TMZ application, blocking angiogenesis by application of the anti-VEGF antibody bevacizumab (Avastin), or application of the αvβ3/αvβ5 integrin inhibitor cilengitid in combination with standard therapy, were unfortunately not successful [88-91]. New therapy strategies combine tumor-treating fields (TTF) with GBM standard therapy. In TFF, alternating electrical fields are used to disrupt cell division. With this approach a significant increase in overall survival could be achieved in GBM patients [92].

Currently, immune therapies using tumor vaccines or immune checkpoint inhibitors are tested in clinical trials. For the constitutively active, truncated epidermal growth factor receptor version III (EGFRvIII), which is expressed in many GBM, the phase III ACT IV clinical trial using the vaccine rindopepimut was terminated ahead of schedule because the therapy failed to prolong the overall survival of the GBM patients, although previous trials were promising [93]. The company Northwest Biotherapeutics currently started a phase III clinical trial using DCVax®-L, a dendritic cell vaccine, in combination with standard therapy (ClinicalTrials.gov identifier: NCT00045968). In this trial autologous dendritic cells are pulsed with tumor lysates to promote anti-tumor immune-responses. The aim of immune checkpoint inhibitors is to block suppressive signals from the tumor that would lead to T cell anergy, exhaustion, or apoptosis. At the moment, ipilimumab, a cytotoxic T lymphocyte-associated antigen-4 (CTLA4) antibody and nivolumab, a PD-1 antibody, are tested in phase III clinical trials (ClinicalTrials.gov Identifier: NCT02017717). For these antibody therapies adverse

side effects have to be controlled closely because inflammatory and autoimmune events occurred. Other emerging GBM therapies include adoptive immunotherapy [94], oncolytic virus therapy [95, 96], as well as nanoparticles that are loaded with anti-tumoral agents [97]. Besides, targeting microRNAs and GSCs might have therapeutic potential in the future (for review see [17, 98]).

1.2 Extracts of *Viscum album* plants

The European mistletoe (*Viscum album* L) is an hemiparasite growing on a wide range of host trees [99]. Aqueous extracts of *Viscum album* L were used the first time in the 1920s to treat cancer. This idea is based on the considerations of Rudolf Steiner, the creator of anthroposophy. The first *Viscum album* extract (ME) was generated 1917 by the physician Ita Wegman [100]. Since 1926 this extract is called ISCADOR, and it is still produced today. Currently, ME like ISCADOR, Iscucin, Helixor, or abnobaVISCUM are manufactured as anticancer agents by several companies. Every company uses different plant parts, harbours the plant at different seasons, or uses different extraction and fermentation methods. In addition, the companies offer several ME dependent on the host tree. Five types of ISCADOR are available: ISCADOR Qu (oak tree), ISCADOR M (apple tree), ISCADOR P (pine tree), ISCADOR A (fir tree), and ISCADOR U (elm tree) [101]. Variations in the plant material and the manufacturing process lead to tremendous differences in the molecular content of ME. In general, ME contain about 1000 different proteins, polysaccharides, triterpenes, and flavonoids [102]. The anticancer activity is mainly produced by mistletoe lectins (ML), also called viscumins 1-3 and by viscotoxins (VT).

1.2.1. Viscumins

ML 1-3 are glycosylated proteins present in most ME. They consist of an A- and B-chain connected via disulfide bonds and belong in the group of type 2 ribosome-inactivating proteins (RIP) [103]. The A-chain is a highly specific N-glycosidase that

inhibits protein synthesis by catalytically inactivating ribosomes [104, 105]. The B-chain is a carbohydrate binding lectin that, in case of ML-1, specifically binds the sialic acid containing ganglioside CD75s [106]. This binding is probably necessary for the cellular uptake, as a direct correlation between ML-1 toxicity and the receptor ganglioside was suggested [107]. The uptake mechanism is not fully understood, but it is believed to be similar to that of ricin, which is also a type 2 RIP and a structural analogue of ML-1 (for review see [108]).

The main anticancer activity is mediated by ML-1, which is the best characterized ML so far. Several ME are standardized to their ML-1 content, thus enhancing reproducible effects [109]. In *in vitro* studies ML-1 was cytotoxic for tumor cell lines, inducing apoptosis and inhibiting tumor cell proliferation of cancer cells derived from leukemia, breast cancer, colon cancer, melanoma, and hepatocellular carcinoma [110-116]. In F98 rat GBM cells, ML-1 reduced cell proliferation, and our group showed that the ML-rich ME ISCADOR Qu has cytotoxic and anti-proliferative effects in human GBM cell lines [117, 118]. ME and ML are furthermore described to modulate the cell cycle distribution of tumor cells. Besides, ME and ML provide anti-angiogenic function due to the induction of cell death in endothelial cells [119-124]. One obvious key function of ML-1 as type 2 RIP is to inhibit protein synthesis, but it modifies gene expression of cancer cells, too [125]. Our group showed altered gene expression in GBM cells upon treatment with ML-rich ISCADOR Qu. Many pro-tumorigenic genes were downregulated and anti-tumorigenic genes upregulated [118]. Especially the expression of migration associated genes like MMPs or TGF-β was downregulated, and, presumably a result of this reduced expression, GBM cell migration was mitigated. In total, ML-1 provides several direct effects on tumor cells, including induction of cell death, inhibition of proliferation and angiogenesis, modulation of gene and protein expression, and reduction of tumor cell motility.

Apart from the effects on cancer cell lines, ML-1 has been described to stimulate immune cells and to thereby enhance anti-tumoral immune responses. ML-1 induces the release of cytokines from immune cells like tumor necrosis factor (TNF)-α, IL-1, IL-5, IL-6, IL-10, and granulocyte monocyte colony-stimulating factor (GM-CSF) [126-130]. ML-1 induced IL-2 secretion was described for immune cells, but also the

opposite was reported [131, 132]. Contrarily and as it was expected by immunologists, interferon (IFN)-γ secretion in PBMCs was not influenced by ML-1 treatment [131]. The induction of TNF-α, IL-1α, IL-1β, and IL-6 was more specifically described for monocytes and macrophages as an inflammatory response to ML-1, whilst lymphocytes did not secrete IL-1β after ML-1 treatment [133-135]. In addition, after ME treatment an increase of IL-4 and a decrease of IFN-γ were reported for CD4+ and CD8+ T cells [136, 137].

ML-1 also changes the activity and maturation of immune cells. ME stimulated the maturation of dendritic cells (DC). In a mouse model, low doses of ML-1 increased DC tumor infiltration, whilst high doses of ML-1 led to DC apoptosis [138-140]. Additionally, the anti-tumoral activity of macrophages was enhanced by ME, but no effect was seen with pure ML-1 [141, 142]. The Korean viscumin (K-ML) that shows strong homology to ML-1 (> 90% A-chain, > 80% B-chain) increased macrophage activity [143, 144]. K-ML also modulates lymphocytes and NK cells [143]. Upon ML-1 treatment T cells show more proliferation, faster maturation, and stronger activation [145, 146]. Nevertheless, high ML concentrations can induce lymphocytic cell death [131, 147]. Mechanisms why ME and ML provide immune-stimulatory activity are based on the upregulation of CD95L in CD4+, CD8+ T cells, and CD19+ B cells [148], but enhanced T cell migration was also observed [149]. Additionally, our group and others showed an enhancement of NK cell mediated tumor cell killing by ME and ML [118, 150, 151]. The effect of ME on NK cells is not only related to ML-1, as other ME ingredients like viscotoxins and rhamnogalacturonan also enhance NK cell mediated lysis of tumor cells [152-154]. Summing up, ML-1 influences the immune system in several ways, including the induction of cytokine expression and secretion to promote inflammatory and anti-tumoral immune responses but also by stimulating DC, monocytes, macrophages, NK cells, and T cells.

ME and ML-1 showed anti-tumoral effects in many murine tumor models [155]. In melanoma, a ME applied as a single intraperitoneal (i.p.) injection inhibited tumor growth [156]. Immune-deficient mice transplanted with human ovarian cancer cells and treated with recombinant ML-1 survived longer [157]. In a urinary bladder carcinoma mouse model intravesical ME application enhanced survival [158].

Intraperitoneally applied ISCADOR M or subcutaneous (s.c.) injections of recombinant ML-1 showed anti-carcinogenic and anti-metastatic effects as well as prolonged survival in sarcoma bearing mice [159, 160]. ML showed anti-tumoral effects when provided orally to mice with non-Hodgkin lymphoma [161]. Other tumors in which ME or ML provided anti-tumoral effects, at least in mouse models, were pancreatic cancer, breast cancer, acute lymphoblastic leukemia, and Ehrlich carcinoma [162-165]. Our group showed reduced tumor growth upon ISCADOR Qu treatment in a subcutaneous GBM mouse model [118]. Furthermore, ML-1 reduced the tumor volume in an intracerebral F98 rat brain tumor model [117].

Aviscumine is a recombinant, non-glycosylated ML-1 produced in *E. coli* (Melema Pharma AG). The advantage to use Aviscumine lays in the fact that the application of a defined single substance avoids the complexity and the component variation of ME. *In vitro* Aviscumine provides cytotoxic effects on tumor cells and shows synergism if used in combination with chemotherapeutics and radiation [166-168]. Aviscumine also showed promising results in phase I clinical trials where infusions or injections (s.c.) were well tolerated [169-171]. In a phase II study with stage IV metastatic melanoma patients Aviscumine was clinically active [172]. Eck et al. did not find differences between glycosylated and recombinant, non-glycosylated ML-1 [173]. Nonetheless, in the present study one goal was to compare the anti-cancer effects of Aviscumine, ISCADOR Qu, and native, purified ML-1.

1.2.2. Viscotoxins

Viscotoxins (VT) are small (~ 5 kDa), cytotoxic proteins that belong to the group of plant thionins. Their original function is to protect plants against bacteria and fungi [174]. VT are cysteine rich and form three disulfide bonds which are highly conserved within the VT family [175]. The VT A1, A2, A3, and B are present in ME and play, next to ML, a role in mediating anticancer effects [176]. It is suggested that VT bind to DNA since their structure contains a helix-turn-helix motif [177]. Whether this is true and plays a role in mediating anticancer effects is not known. There is much more insight into the interaction of VT with cell membranes. VT are positively surface

charged, which allows an interaction with negatively charged heads of phospholipids [177-179]. This interaction leads to membrane stiffness, changes in fluidity, and finally to membrane defects and disruption [178, 179]. In a comparison of cytotoxicity, VT A2 and A3 act similar, while VT B is less active, although all VT have highly conserved 3D structures [180]. These findings indicate that unspecific membrane lysis leads to the cytotoxic effects of VT.

Not only cytotoxic effects are described for VT. If patients are treated with VT they develop an immunological response and form VT antibodies [181]. Furthermore, VT increase NK cell mediated killing of tumor cells, probably by enhancing tumor cell membrane destabilization [152]. Finally, granulocyte activity can be enhanced by VT treatment [182, 183]. Whether VT can also stimulate other types of immune cells remains elusive.

1.2.3. Clinical trials

So far more than 80 clinical trials using ME or ML were conducted for many tumor entities [184]. Several systematic reviews summarizing the results are available. In 2003 Ernst et al. reviewed ten randomized control trials (RCTs) and came to the conclusion that only the studies with a "weak" design found benefits for ME, especially an improvement in quality of life (QoL). "Stronger" designed studies did not show a benefit of ME/ML on survival or QoL [185]. In 2008 Horneber et al. came to similar findings also reviewing RCTs. They included 21 trials and found only weak evidence for a survival benefit and some benefit for improved QoL for breast cancer patients during chemotherapy [184]. Kienle and Kiene published several systematic reviews and came to more promising result. They published that in 26 RCTs 22 showed an improvement in QoL, no change was reported in three cases, and one did not present results [186]. Furthermore, they concluded that a survival benefit is shown in 8 of 17 trials (RCTs and non-RCTs), but due to poor study design the results must be considered with caution [187]. For breast and gynecological cancer they evaluated 35 trials (19 RCTs and 16 non-RCTs). 22 trials tested survival and of these 12 trials showed a statistically significant survival benefit and the remaining trials showed

either a trend or no changes. 24 trials tested the QoL also during chemotherapy. 21 of these trials reported significant improvements in the QoL [188]. Finally, Ostermann et al. evaluated 49 studies using ISCADOR. By evaluating the hazard ratios with a random effect meta-analysis they found that ISCADOR treatment is associated with a significant prolonged survival [189].

Many of the clinical trials were of poor quality and lack proper documentation, especially the very old studies lack transparency and a clear description of ME usage. Also small sample sizes and unclear inclusion/exclusion criteria make the interpretation of the results difficult [189]. In the studies many different ME (providing either very high or very low ML content) were used and the treatment protocols differed, sometimes it is not even clear which ME was used [185]. This makes the interpretation and the comparison of these trials difficult. Assessment of the effects of every available ME and well-designed clinical trials of high quality would be necessary to make a clear statement whether ME (and which) have a positive effect on the survival and the QoL of cancer patients.

For glioma results from solely one study with only 38 patients is currently available. 20 patients received ME and standard therapy and 18 patients received standard therapy alone. In this study a significant prolongation of survival after ME treatment for grade III & IV gliomas is shown [190]. Apart from the small sample size, the trial enrolled patients with different glioma grades. The survival time differs hugely between these grades, but it is not mentioned how these patients were distributed between the treatment and the control group. This unknown patient distribution alone can lead to the reported survival benefits and limits the overall significance of the study. A clinical trial with GBM patients only remains to be done.

1.2.4. ME/ML-1 usage, routes of application, and side effects

The standard route of ME application are subcutaneous injections. The anthroposophical approach is to start with low to homeopathic doses of the extracts and to increase the doses in a period of several weeks until an optimal tolerated dose is reached. Subcutaneous ME/ML-1 injections are tolerated well by patients. Known side

effects include flue like symptoms, fever, headache, fatigue, gastrointestinal symptoms, and local reactions at the injection site (for review see [191]). Especially the very common local reddening at the injection side makes blinded clinical trials almost impossible.

Sometimes ME or ML are also applied i.v. as an off-label intervention. Reasons for this route of application is (i) a missing response to s.c. injections, (ii) to induce fever and stimulate the immune system, and (iii) that it might be a last option for high-risk and advanced stage cancer patients [192]. In clinical trials only the recombinant ML-1 Aviscumine (applied i.v.) was tested so far. For intravenous infusion with ME/ML-1 flue like symptoms, fatigue, fever, shivering, nocturia, urticaria, erythema, pruritus, and liver toxicity were reported [169, 170, 192]. Pseudoallergic and allergic reactions are reported more frequently after i.v. infusion compared to s.c. injections [192].

The much rarer applied off-label intratumoral ME/ML-1 therapy also leads to mild or moderate side effects including fever, gastrointestinal disorders, pain, headache, dyspnea, hypertension, and erythema, which occur more frequently than in the other routes of application, probably due to the generally higher doses of ME/ML-1 used for intratumoral injections (for review see [193]). So far, no clinical trial using intratumoral ME/ML-1 injections was performed, although this route of application could lead to the best anti-cancer effects and attraction of immune cells to the tumor.

1.3 Aim of the thesis

Because of the very aggressive features of GBM, the 14-16 months median survival time for GBM patients, even with best and newest available therapies, is unchanged for years. Therefore, the development of new therapy approaches is utterly important. Lately, natural compounds that can be used as adjuvant cancer agents are running more and more in the focus of attention. In German-speaking countries *Viscum album*-based drugs are used for decades in the treatment of nearly all types of cancer, but little is known about their effects if used as adjuvant GBM therapeutics. Therefore, I pursued the goal to understand more about the complex anti-cancer functions of viscumins in the context of GBM. To achieve this goal, three different viscumin-based drugs were used. ISCADOR Qu is a ME generated from plants growing on oak trees and contains high ML concentrations. Aviscumine is a recombinant, not glycosylated ML-1 produced in *E-Coli* and purified to good manufacturing practice (GMP) quality. Native ML-1 was isolated from plants growing on ash trees. Different aspects of the anti-cancer functions of the three drugs were analyzed *in vitro* and *in vivo* using two different GBM mouse models. Firstly, the cytotoxicity of the viscumins in GBM cell lines, non-neoplastic cells, primary cell lines, and in murine hippocampal slice cultures were determined. Next, the effects of viscumins on proliferation and cell cycle distribution were evaluated. Thirdly, viscumin-mediated modulation of motility-associated genes expression in GBM cells and the influence of viscumins on glioma cell migration were analyzed. Fourthly, and since viscumins are known to be immune-stimulatory agents, their effects on the activity of NK cells and T cells, on the immune cell-mediated killing of GBM cells, as well as their ability to change the expression of immune response related genes were tested. Finally, viscumins are normally given as adjuvant therapeutics in cancer patients. For this, the therapeutic effect of viscumins, if used as adjuvant therapeutics in combination with tumor irradiation and TMZ was evaluated both *in vitro* and in glioma bearing mice. These experiments were performed to facilitate the basis for clinical trials where the anti-GBM effects of viscumins will be further investigated and it will be decided whether viscumins can be used as effective adjuvant therapeutics to treat glioma.

2. Material and methods

2.1 Materials

2.1.1 Equipment

Equipment	Manufacturer
10 / 100 / 1000 µl pipettes	Eppendorf (Hamburg, Germany)
7500 Fast Real time PCR	Applied Biosystems (Darmstadt, Germany)
Accu Jet Pipette Pro Controller	Hirschmann (Eberstadt, Germany)
Axio Imager Z1 fluorescent microscope	Carl Zeiss (Oberkochen, Germany)
Biofuge Pico centrifuge	Heraeus (Hanau, Germany)
Biorad Immunoblot Equipment	Biorad (Munich, Germany)
ChemiDoc™ Imaging System	Biorad (Munich, Germany)
CO_2 Incubator	Sanyo (Munich, Germany)
CyAn ADP flow cytometer	Beckman Coulter (Krefeld, Germany)
Eclipse TS100 microscope	Nikon (Kingston, UK)
ELISA reader Thermo Electron Multiscan EX	Thermo Electron Corporation (Karlsruhe, Germany)
Gammacell-40 Irradiator	MDS Nordion (Toronto, Canada)
Hamilton 10 µl syringe, 701 N, 26s ga, ps 2	Hamilton (Bonaduz, Switzerland)
Hera Safe Clean Bench	Heraeus (Hanau, Germany)
Imager.Z1	Carl Zeiss (Oberkochen, Germany)
LSM 510 META Confocal microscope	Carl Zeiss (Oberkochen, Germany)
MACS MultiStand	Miltenyi (Bergisch Gladbach, Germany)
MilliQ Integral (ultrapure water preparation)	Millipore/Merck (Darmstadt, Germany)
MiniMACS Separator	Miltenyi (Bergisch Gladbach, Germany)

Mithras LB940 Fluorimeter	Berthold Technologies (Bad Wildbad, Germany)
Mouse stereotaxic instrument	Stoelting (Dublin, Ireland)
Multifuge 3 S-R centrifuge	Heraeus (Hanau, Germany)
Multipipettes	Eppendorf (Hamburg, Germany)
NanoDrop ND 1000	Peqlab (Erlangen, Germany)
Neubauer cell counting chamber	Marienfeld (Bad Mergentheim, Germany)
Power Pac power supply unit	Biorad (Munich, Germany)
Thermomixer Comfort	Eppendorf (Hamburg, Germany)
Wallac Victor 1420 Multilabel counter	PerkinElmer (Rodgau, Germany)

2.1.2 Consumables

Consumable	Manufacturer
Amicon centrifugal filter units 3 kDa NMGG	Millipore (Schwalbach, Germany)
Assay plate white, 96 well format	Corning (New York, USA)
Cell culture flasks T25 / T75 / T125	Greiner Bio-One (Frickenhausen, Germany)
Cell culture insert 8.0 µm pore size, 24 well format	Becton Dickinson (Heidelberg, Germany)
Cell scraper	Corning (New York, USA)
Combitips advanced 2.5 / 5 ml	Eppendorf (Hamburg, Germany)
ELISA Kit RayBio® Human VEGF or TGF-ß 1 & 2	RayBiotech (Norcross, GA, USA)
Falcon centrifuge tubes 15 / 50 ml	Corning (New York, USA)
Filter paper	Peqlab (Erlangen, Deutschland)
Microlance 3 needles	Becton Dickinson (Heidelberg, Germany)
Microscope slides 76x26 mm	R. Langenbrick (Emmendingen, Germany)
Microscopical cover slips	R. Langenbrick (Emmendingen, Germany)
Mouse Inflammation Array G1 (Catalog number: AAM-INF-G1-8)	RayBiotech (Norcross, GA, USA)

MS columns	Miltenyi (Bergisch Gladbach, Germany)
MycoAlert mycoplasma detection kit	Lonza (Cologne, Germany)
NK cell isolation kit, human	Miltenyi (Bergisch Gladbach, Germany)
PERMA-HAND silk suture, black braided, 6-0, 11 mm, 3/8 circle	Ethicon (Somerville, NJ, USA)
Pipette tips	Ratiolab (Dreieich, Germany)
Polypropylene tubes 1.3 / 5 ml	Greiner Bio-One (Frickenhausen, Germany)
PVDF 0.45 transfer membrane	Serva (Heidelberg, Germany)
Reaction tubes 0.5 / 1.5 / 2 ml	Greiner Bio-One (Frickenhausen, Germany)
RNA-Isolation kit	Macherey-Nagel (Düren, Germany)
RT-qPCR adhesive film	Biozym Scientific (Hessisch Oldendorf, Germany)
RT-qPCR plates	Thermo Fisher Scientific (MA, USA)
Serological pipettes 5 / 10 / 25 ml	Corning (New York, USA)
Surgical blades, sterile	B. Braun (Melsungen, Germany)
Syringe with Sub-Q needle 1 ml	Becton Dickinson (Heidelberg, Germany)
Syringes Inject-F/Inject Solo 1-20 ml	B. Braun (Melsungen, Germany)
TaqMan array human cyclins & cell cycle regulation 96-well plate (Catalog number: 4418768)	Thermo Fisher Scientific (MA, USA)
TaqMan array human immune response 96-well plate (Catalog number: 4414073)	Thermo Fisher Scientific (MA, USA)
TaqMan array human tumor metastasis 96-well plate (Catalog number: 4414098)	Thermo Fisher Scientific (MA, USA)
Water (ultrapure)	Milli Q Integral (Millipore/Merck, Darmstadt, Germany)
Well plates 6 / 12 / 24 / 48 / 96	Becton Dickinson (Heidelberg, Germany)
Zymogram gel 10%	Biorad (Munich, Germany)

2.1.3 Chemicals, media, and reagents

Material	Manufacturer
1,4-Dithiothreitol (DTT)	Sigma-Aldrich (Taufkirchen, Germany)
5-Bromo-2-deoxyuridine (BrdU)	Sigma-Aldrich (Taufkirchen, Germany)
5-Sulfosalicylacid	Merck (Darmstadt, Germany)
Accutase	PAA Laboratories (Cölbe, Germany)
Acetic acid	Merck (Darmstadt, Germany)
ACK lysis buffer	Thermo Fisher Scientific (MA, USA)
Acrylamide	Carl Roth (Karlsruhe, Germany)
Adenosine 5′-triphosphate disodium salt (ATP)	Sigma-Aldrich (Taufkirchen, Germany)
Ammonium persulfate (APS)	Carl Roth (Karlsruhe, Germany)
Ascorbic acid	Sigma-Aldrich (Taufkirchen, Germany)
Bicoll	Merck (Darmstadt, Germany)
BIOMYC-1 / 2 / 3 antibiotic solution 100X	PromoCell (Heidelberg, Germany)
Bovine serum albumin (BSA)	Carl Roth (Karlsruhe, Germany)
Bradford reagent	Carl Roth (Karlsruhe, Germany)
Bromophenol blue	Merck (Darmstadt, Germany)
Calcium chloride	Sigma-Aldrich (Taufkirchen, Germany)
Coenzyme A, trilithium salt	Merck (Darmstadt, Germany)
Collagen I, rat tail	Enzo Life Sciences (New York, USA)
Coomassie brilliant blue R250	Merck (Darmstadt, Germany)
Crystal violet (CV)	Merck (Darmstadt, Germany)
D-glucose	Sigma-Aldrich (Taufkirchen, Germany)
Dimethyl sulfoxide (DMSO)	Carl Roth (Karlsruhe, Germany)
D-Luciferin	Sigma-Aldrich (Taufkirchen, Germany)
D-Luciferin sodium salt	Promega (Madison, USA)
dNTP´s 20 mM	Peqlab (Erlangen, Germany)
Dulbecco’s modified eagle’s medium	Sigma-Aldrich (Taufkirchen, Germany)

(DMEM)	
Dulbecco's phosphate buffered saline (PBS)	Sigma-Aldrich (Taufkirchen, Germany)
Endothelial basic medium (EBM-2)	Lonza (Basel, Switzerland)
Endothelial growth medium (EGM-2)	Lonza (Basel, Switzerland)
Ethanol 99%	Merck (Darmstadt, Germany)
Ethylene glycol-bis(2-aminoethylether)-N,N,N′,N′-tetraacetic acid (EGTA)	Sigma-Aldrich (Taufkirchen, Germany)
Ethylenediaminetetraacetic acid (EDTA)	Sigma-Aldrich (Taufkirchen, Germany)
Fetal bovine serum (FBS)	Sigma-Aldrich (Taufkirchen, Germany)
Formamide	Merck (Darmstadt, Germany)
Gamunex 10%	Grifols (Barcelona, Spain)
Glycerol	Carl Roth (Karlsruhe, Germany)
Glycine	Carl Roth (Karlsruhe, Germany)
Gly-Gly	Sigma-Aldrich (Taufkirchen, Germany)
Goat serum	Sigma-Aldrich (Taufkirchen, Germany)
H_2O_2	Carl Roth (Karlsruhe, Germany)
Haematoxylin	Merck (Darmstadt, Germany)
Horse serum	Sigma-Aldrich (Taufkirchen, Germany)
Human serum	Sigma-Aldrich (Taufkirchen, Germany)
Hygromycin B	Invivogen (Toulouse, France)
Igepal (NP-40)	Sigma-Aldrich (Taufkirchen, Germany)
Insulin	Sigma-Aldrich (Taufkirchen, Germany)
Isopropanol	Merck (Darmstadt, Germany)
K_2HPO_4	Carl Roth (Karlsruhe, Germany)
L-Glutamine 200 mM	Sigma-Aldrich (Taufkirchen, Germany)
Magnesium sulfate	VWR (Darmstadt, Germany)
Matrigel matrix basement membrane	Corning (New York, USA)
Methanol	VWR (Darmstadt, Germany)
M-MLV reverse transcriptase	Promega (Madison, USA)
M-MLV RT 5xBuffer	Promega (Madison, USA)

Modified eagle's medium (MEM)	Sigma-Aldrich (Taufkirchen, Germany)
Mouse IgG_1 isotype control	Covance (Dedhan, USA)
Mouse IgM κ isotype control	BioLegend (Fell, Germany)
Mowiol 4-88	Carl Roth (Karlsruhe, Germany)
NaN_3	Carl Roth (Karlsruhe, Germany)
N-Methyl-D-aspartate (NMDA)	Sigma-Aldrich (Taufkirchen, Germany)
Normal rabbit IgG	Santa Cruz Biotechnology (Heidelberg, Germany)
Oligo dT-nucleotide 100 µM	Sigma-Aldrich (Taufkirchen, Germany)
Paraformaldehyde	AppliChem (Darmstadt, Germany)
Penicillin/Streptomycin (100x)	PAA Laboratories (Cölbe, Germany)
Pericyte medium	ScienCell (San Diego, USA)
Poly-L-lysine hydrobromide	Sigma-Aldrich (Taufkirchen, Germany)
Ponceau S	Merck (Darmstadt, Germany)
Propidium iodide (PI)	Sigma-Aldrich (Taufkirchen, Germany)
Protein marker	PanReac AppliChem (Darmstadt, Germany)
Proteinase inhibitor cocktail set III Chalbio.	EMD Chemicals (San Diego, USA)
Recombinant human IL-2	ImmunoTools (Friesoythe, Germany)
Recombinant human VEGF-A	ImmunoTools (Friesoythe, Germany)
Ribonuclease A from bovine pancreas	Sigma-Aldrich (Taufkirchen, Germany)
RPMI1640 medium HEPES modification	Sigma-Aldrich (Taufkirchen, Germany)
Skim milk powder	Carl Roth (Karlsruhe, Germany)
Sodium chloride	Merck (Darmstadt, Germany)
Sodium citrate	Merck (Darmstadt, Germany)
Sodium dodecyl sulfate (SDS)	Carl Roth (Karlsruhe, Germany)
ß-Mercaptoethanol	Carl Roth (Karlsruhe, Germany)
Sybr Green PCR master mix	Thermo Fisher Scientific (MA, USA)
TaqMan gene expression master mix	Thermo Fisher Scientific (MA, USA)
Temozolomide (TMZ)	Sigma-Aldrich (Taufkirchen, Germany)

Tetramethylethylenediamine (TEMED)	Carl Roth (Karlsruhe, Germany)
Thiazolyl blue tetrazolium bromide (MTT)	Sigma-Aldrich (Taufkirchen, Germany)
Trichloroacetic acid	Merck (Darmstadt, Germany)
Tricine	AppliChem (Darmstadt, Germany)
Triton X-100	Sigma-Aldrich (Taufkirchen, Germany)
Trizma base (Tris)	Sigma-Aldrich (Taufkirchen, Germany)
Trizma hydrochloride (Tris HCl)	Sigma-Aldrich (Taufkirchen, Germany)
Trypan blue 0.4%	Sigma-Aldrich (Taufkirchen, Germany)
Trypsin-EDTA	Sigma-Aldrich (Taufkirchen, Germany)
Tween-20	Carl Roth (Karlsruhe, Germany)
VECTASHIELD Antifade mounting medium with DAPI	Vector laboratories (Burlingame, USA)
VECTASHIELD HardSet mounting medium with DAPI	Vector laboratories (Burlingame, USA)
WesternBright ECL HRP substrate	Advansta (California, USA)

2.1.4 Antibodies flow cytometry

Antibody	Manufacturer
APC anti-human CD25 (BC96)	BioLegend (Fell, Germany)
APC anti-human CD56 (5.1H11)	BioLegend (Fell, Germany)
APC anti-human CD8 (SK1)	BioLegend (Fell, Germany)
APC anti-human CD95 (DX2)	BioLegend (Fell, Germany)
APC anti-human HLA-G (87-G)	BioLegend (Fell, Germany)
FITC AnnexinV	BioLegend (Fell, Germany)
FITC anti-BrdU (3D4)	BioLegend (Fell, Germany)
FITC anti-human CD4 (RPA-T4)	BioLegend (Fell, Germany)
FITC anti-human HLA-DR, DP, DQ (Tu39)	BioLegend (Fell, Germany)
Pacific blue anti-human CD3 (UCHT1)	BioLegend (Fell, Germany)
Pacific blue anti-human HLA-A, B, C (W6/32)	BioLegend (Fell, Germany)

PE anti-human CD273 (24F.10C12)	BioLegend (Fell, Germany)
PE anti-human CD274 (29E.2A3)	BioLegend (Fell, Germany)
PE anti-human FoxP3 (206D)	BioLegend (Fell, Germany)
PE/Cy7 anti-human CD40 (5C3)	BioLegend (Fell, Germany)
PE/Cy7 anti-human CD69 (FN50)	BioLegend (Fell, Germany)

2.1.5 Antibodies immunoblot

Antibody	Manufacturer
Goat anti-mouse IgG-horseradish peroxidase (HRP), secondary antibody	Santa Cruz Biotechnology (Heidelberg, Germany)
Goat anti-rabbit IgG-HRP, secondary antibody	Santa Cruz Biotechnology (Heidelberg, Germany)
Mouse anti-human MMP-2	Oncogene (Massachusetts, USA)
Mouse monoclonal anti-human GAPDH	Santa Cruz Biotechnology (Heidelberg, Germany)
Mouse monoclonal anti-human MMP-9	Santa Cruz Biotechnology (Heidelberg, Germany)
Mouse polyclonal anti-human TIMP-2	R&D Systems (Minneapolis, USA)
Rabbit monoclonal anti-human MMP-14	Epitomics (Burlingame CA, USA)
Rabbit polyclonal anti-human SMAD2/3	Cell Signaling (Danvers, MA, USA)
Rabbit polyclonal anti-human α-Tubulin	Santa Cruz Biotechnology (Heidelberg, Germany)

2.1.6 Antibodies immunofluorescent staining and blocking

Antibody	Manufacturer
Donkey polyclonal anti-mouse IgG H&L Alexa Fluor 594	Abcam (Cambridge, UK)
Goat anti-mouse IgG H&L DyLight 488	Thermo Fisher Scientific (MA, USA)
Goat anti-mouse IgM TexasRed	Santa Cruz Biotechnology (Heidelberg, Germany)
Goat anti-mouse IgM FITC	Santa Cruz Biotechnology (Heidelberg, Germany)
Goat anti-rabbit IgG H&L Alexa Fluor 488	Invitrogen (Carlsbad, USA)
Mouse anti-human NKp30 (CD337, P30-15)	BioLegend (Fell, Germany)
Mouse anti-human NKp44 (CD336, P44-8)	BioLegend (Fell, Germany)
Mouse anti-human NKp46 (CD335, 9E2)	BioLegend (Fell, Germany)
Mouse monoclonal anti-human CDw75 (ZB55)	Santa Cruz Biotechnology (Heidelberg, Germany)
Mouse monoclonal anti-human NKG2D (CD314, 149810)	R&D Systems (Minneapolis, USA)
Rabbit polyclonal anti-ML	ISCADOR AG (Arlesheim, Switzerland)

2.1.7 *Viscum album* extracts and lectins

The plant extracts ISCADOR P and Qu were kindly provided by ISCADOR AG (Arlesheim, Switzerland). ISCADOR P was harvested from plants growing on pine trees, whilst ISCADOR Qu was generated from plants growing on oak trees. The concentrations of the extracts were 200 mg/ml (P) and 20 mg/ml (Qu). To achieve a comparable viscotoxin concentration in the ISCADOR Qu_{20} extracts, charge numbers 5141/02 and 5228 were mixed 1:1 (= ISCADOR Qu_{20} mix). For the experiments the ISCADOR Qu charges 3108/1, 4080/3 and the ISCADOR Qu_{20} mix were used.

Mistletoe extract	Charge number	ML [ng/ml]	Viscotoxins [µg/ml]
ISCADOR Qu_{20}	3108/1	1630	62
ISCADOR Qu_{20}	4080/3	1095	48
ISCADOR Qu_{20}	5141/02	415	67
ISCADOR Qu_{20} spez.	5228	1430	12
ISCADOR Qu_{20} mix		922.5	39.5
ISCADOR P_{200}	5191	<5	75.2

Aviscumine (ME-503), a recombinant ML-1 produced in *E. coli*, was kindly donated by MELEMA Pharma GmbH (Hamburg, Germany). The ML concentration was 0.93 mg/ml (Charge 004/03/030200).

Isolated native ML-1 (ML-1) from plants grown on ash trees (summer harvest) was kindly provided by C. Heyder (Abnoba GmbH, Pforzheim, Germany) in a concentration of 4.6 mg/ml.

2.1.8 Murine hippocampal slice cultures

Murine hippocampal slice cultures (HSC) from C57BL/6 mice were prepared at postnatal day 5-7 as described and were kindly provided by Ingrid Ehrlich, Hertie Institute for Clinical Brain Research and Center for Integrative Neuroscience (Tübingen, Germany) and used after at least one week in culture [194].

2.1.9 Cell lines and primary cells

Name	Description	Source
HBVP	Primary human brain vascular pericytes isolated from human brain tissue	ScienCell (San Diego, USA)
hCMEC/D3	Immortalized human endothelial cells isolated from human temporal lobe	B. Weksler (Weill Cornell Medical Collage, New

	microvessels	York, USA)
LN-308	Human astrocytoma cell line ($p53^{-/-}$)	N. de Tribolet (Lausanne, Switzerland)
LN-319	Human astrocytoma cell line ($p53^{WT}$)	N. de Tribolet (Lausanne, Switzerland)
LNT-229	Human GBM cell line ($p53^{WT}$)	N. de Tribolet (Lausanne, Switzerland)
LNT-229 Luc	LNT-229 cells stably transfected by the luciferase expression vector pGL4.14-HSV-Luc	
MZ-18	Human GBM cell line ($p53^{mut/mut}$)	H. Hetschko (Frankfurt, Germany)
NIH/3T3	Murine embryonic fibroblast cell line	ATCC (Manassas, USA)
PBMC	Primary human peripheral blood mononuclear cells isolated from blood	
RPMI 8866	Human lymphoblastoid cell line from blood, B lymphocyte origin	Sigma-Aldrich (Taufkirchen, Germany)
SMA-560	Murine astrocytoma cell line	D. Bigner (Duke University, Durham, NC, USA)
SVGA	Immortalized human fetal astrocytes	R. Atwood (Brown University, Providence, Rhode Island, USA)
T98G	Human GBM cell line ($p53^{mut/mut}$)	ATCC (Manassas, USA)
U87MG	Human GBM cell line ($p53^{WT}$)	ATCC (Manassas, USA)

2.1.10 Primer

Stock solution: 100 µM

Storage: -20 °C

Manufacturer: Sigma Aldrich (Taufkirchen, Germany)

Name	Sequence in 5'-3' orientation
hu_ANGPT1 fwd	CGGTGAATATTGGCTGGGG
hu_ANGPT1 rev	GTCATACTGTAATAGGCTCGGTT
hu_ATM fwd	CCGAATGTTTTGGGGCAGTG
hu_ATM rev	TTTTCTCCGTTAGCCACGCA
hu_BCL2 fwd	GGTGAACTGGGGGAGGATTG
hu_BCL2 rev	GCCCAGACTCACATCACCAA
hu_CCNB2 fwd	GAGTTACAACCAGAGCAGCACA
hu_CCNB2 rev	TCCTCAGGTGTGGGAGAAGGA
hu_CCNB3 fwd	GAGATGACCCATGAGACCCTGT
hu_CCNB3 rev	CCACACGAGGTGAGTTGTGCT
hu_CCND1 fwd	TGAGGGACGCTTTGTCTGTC
hu_CCND1 rev	GCCTTTGGCCTCTCGATACA
hu_CCND2 fwd	CTGGGTGCTGTCTGCATGTT
hu_CCND2 rev	AGGTTCCACTTCAACTTCCCC
hu_CCND3 fwd	CCGAAACTTGGCTGAGCAGA
hu_CCND3 rev	GTGTTTACAAAGTCCGCGCC
hu_CDKN1A fwd	GATGACAAGCAGAGAGCCCC
hu_CDKN1A rev	ACTCCCCACATAGCCCGTAT
hu_CDKN1B fwd	TCGGGGTCTGTGTCTTTTGG
hu_CDKN1B rev	AGACACTCGCACGTTTGACA
hu_ENG fwd	CAAAGGCCTCGTCCTGCCC
hu_ENG rev	GGGGAACGCGTGTGCGAG
hu_EPHB2 fwd	CCACTCATCATCGGCTCCTC
hu_EPHB2 rev	GCTCAAACCCCCGTCTGTTA

hu_GAPDH fwd	TGCACCACCAACTGCTTAGC
hu_GAPDH rev	GGCATGGACTGTGGTCATGAG
hu_HDAC6 fwd	AAGGTCGCCAGAAACTTGGT
hu_HDAC6 rev	TGGGGGTTCTGCCTACTTCT
hu_HMOX1 fwd	CAGGCTCCGCTTCTCCGATG
hu_HMOX1 rev	GGAGCCAGCATGCCTGCATTC
hu_IL1B fwd	GCTCGCCAGTGAAATGATGG
hu_IL1B rev	GGTGGTCGGAGATTCGTAGC
hu_IL6 fwd	TTCCTGCAGAAAAAGGCAAAGA
hu_IL6 rev	AAAGCTGCGCAGAATGAGATG
hu_IL8 fwd	GTGGAGAAGTTTTTGAAGAGGGC
hu_IL8 rev	CACTTCATGTATTGTGTGGGTCT
hu_IL10 fwd	CTTGATGTCTGGGTCTTGGTT
hu_IL10 rev	GCTGGAGGACTTTAAGGGTTA
hu_IL12A fwd	CCAGAAGGCCAGACAAACTCTA
hu_IL12A rev	GCCAGGCAACTCCCATTAGTT
hu_KDR fwd	GTCCTAGAGCGTGTGGCACC
hu_KDR rev	CATGATCTGTGGAGGGGGATT
hu_MMP14 fwd	CGGCCCTTTCCAGCCTCTG
hu_MMP14 rev	GAGGTCTGAGGGTCCTGCC
hu_MMP2 fwd	CCAGAGACAGTGGATGATGCC
hu_MMP2 rev	GGAGTCCGTCCTTACCGTCAA
hu_MMP9 fwd	TTCAGGGAGACGCCCATTTC
hu_MMP9 rev	AACCGAGTTGGAACCACGAC
hu_MTA1 fwd	CCCAGTAGGGGTCTGGCAAA
hu_MTA1 rev	GGTAGGACTTCCCGTTGAGC
hu_NME fwd	TTTGTGTGTCTGCCTCCCCT
hu_NME rev	AGCCGGAGTTCAAACCTAAGC
hu_PPP2CA fwd	TGGTGGTCTCTCGCCATCTA
hu_PPP2CA rev	TGACCACAGCAAGTCACACA
hu_PTGS1 fwd	TCTTGCTGTTCCTGCTCCTG

hu_PTGS1 rev	GTCACACTGGTAGCGGTCAA
hu_PTGS2 fwd	GTTCCACCCGCAGTACAGAA
hu_PTGS2 rev	AGGGCTTCAGCATAAAGCGT
hu_SELE fwd	GCCTGCAATGTGGTTGAGTG
hu_SELE rev	GGTACACTGAAGGCTCTGGG
hu_SERPINB5 fwd	CATCCAGGTCTTTGTGCTCCT
hu_SERPINB5 rev	GGGCCTGGAGTCACAGTTATC
hu_TGFB1 fwd	GCCCTGGACACCAACTATTG
hu_TGFB1 rev	CGTGTCCAGGCTCCAAATG
hu_TGFB2 fwd	CAAAAGCCAGAGTGCCTGAA
hu_TGFB2 rev	CAGTTACATCGAAGGAGAGC
hu_TGFBR2 fwd	GGAGTTTCCTGTTTCCCCCG
hu_TGFBR2 rev	AGGGAAGCTGCACAGGAGTC
hu_TIMP2 fwd	GTTTATCTACACGGCCCCCT
hu_TIMP2 rev	TCGGCCTTTCCTGCAATGAG
hu_TNF fwd	CACAGTGAAGTGCTGGCAAC
hu_TNF rev	AGGAAGGCCTAAGGTCCACT
hu_VEGF fwd	GGCCTCCGAAACCATGAACT
hu_VEGF rev	TTCTGCCCTCCTCCTTCTGC

2.1.11 Software

Software	Manufacturer
qPCR 7500 Software v 4.2.0.	Applied Biosystems (Darmstadt, Germany)
Ascent Software 2.6	Thermo Fisher Scientific (MA, USA)
Axiovision SE64	Carl Zeiss (Oberkochen, Germany)
Excel Office	Microsoft (Redmond, WA, USA)
Fiji is just ImageJ	Johannes Schindelin, Albert Cardona, Mark Longair, Benjamin Schmid, and others
FlowJo V10	FlowJo, LLC (Ashland, OR, USA)

Image Lab Version 6.0	Biorad (Munich, Germany)
JMP 13	SAS (Böblingen, Germany)
NanoDrop 1000	Thermo Fisher Scientific (MA, USA)
OriginPro 8	OriginLab Corporation (Northampton, MA, USA)
Power Point Office	Microsoft (Redmond, WA, USA)
Word Office	Microsoft (Redmond, WA, USA)

2.2 Methods

2.2.1 Cell culture

Murine and human GBM cell lines as well as murine NIH/3T3 cells were maintained in DMEM supplemented with 10% inactivated FBS and 1% penicillin (100 U/ml)/streptomycin (100 µg/ml; P/S). Human brain endothelial cells (hCMEC/D3) were used until passage 35 and maintained in EBM-2 supplemented with EGM-2 growth factors in cell culture flasks coated with 100 µg/ml rat tail collagen I. Primary human brain vascular pericytes (HBVPs) were maintained in pericyte basal medium supplemented with 2% inactivated FBS, 1% of pericyte growth supplement (PGS) and 1% P/S in cell culture flasks coated with 19 µg/cm^2 Poly-L-lysine. RPMI 8866 cells as well as human PBMCs were maintained in RPMI1640 medium supplemented with 2 mM glutamine plus 1% P/S and either 5% human serum for T cell expansion or 10% FBS. All cells were kept at saturated humidity in 5% CO_2 at 37°C.

RPMI8866 cells and human PBMCs were cultured as suspension cultures, all other cell lines grew adherently. To use adherent cells the medium was removed, the cells were washed once with PBS and detached 2-3 min after the addition of trypsin-EDTA. Detached cells were resuspended in medium supplemented with the appropriate sera, growth factors, and antibiotics. Suspension cells were centrifuged (5 min, 1200 rpm), the medium was removed, and the cell pellet was resuspended in complete medium. Cell numbers were determined by mixing the cell suspension 1:1 with trypan blue to stain dead cells. Viable cells were counted using a Neubauer cell counting chamber and seeded accordingly. To reduce the amount of cultured cells, the cells were split 1:2

up to 1:10. For freezing, the cells were suspended in freezing media (the appropriate culture medium, supplemented with 1% P/S, 40% FBS, 10% DMSO) and stored at -80°C for short term or at -150°C for long term storage. To take frozen cells in culture, the cells were thawed in a 37 °C water bath and suspended in complete medium. After 24 h the medium was changed to remove residual DMSO.

2.2.2 Mycoplasma detection

All cell lines were regularly checked for mycoplasma contamination using the Lonza MycoAlert mycoplasma detection kit. In brief, 500 µl cell culture supernatant was centrifuged (5 min, 2000 rpm) and 40 µl was transferred into a well of a 96-well white assay plate. 40 µl of MycoAlert reagent was added, incubated for 5 min, and luminescence was measured using a luminometer (value A). Subsequently, 40 µl MycoAlert substrate was added, incubated for 10 min and luminescence was measured again (value B). If value B was equal or higher than value A, the cells were ranked to be mycoplasma positive according to the manufacturer's protocol. Mycoplasma positive cells were treated with BIOMYC antibiotic solution 1-3 according to the manufacturer's instructions and were analyzed again. Only mycoplasma free cells were used in experiments.

2.2.3 Clonogenic survival assay

The efficiency of cancer cells to grow up to colonies that origin from single cells was measured by seeding 500 cells/well (LNT-229) or 2500 cells/well (LN-308) in 6-well plates. The cells were treated as indicated and cell growth was stopped if colonies became visible (approximately > 50 cells). Colonies were stained with crystal violet and were counted manually.

2.2.4 Crystal violet staining

The density of adherently growing cells was measured using crystal violet staining. The medium was removed and crystal violet solution (0.5% crystal violet, 20% methanol) was added. After 5 min of incubation the staining solution was removed and

the cell culture plates were washed with tap water. After drying, sodium citrate (0.1 M sodium citrate, 50% ethanol) was added, and absorbance was measured at 560 nm using a Multiscan ELISA reader.

2.2.5 MTT assay

Mitochondrial activity, correlating to cell viability, was measured using the thiazolyl blue tetrazolium bromide (MTT) assay. Soluble MTT is converted into insoluble formazan by intracellular NAD(P)H-dependent oxidoreductases in viable cells. For this, MTT was added to the cell culture medium at a final concentration of 500 µg/ml. Upon the formation of blue formazan crystals (after ~ 0.5-2 h incubation at 37°C) the medium was removed, DMSO was added to solve the formazan crystals, and absorbance was measured at 570 nm using a Multiscan ELISA reader.

2.2.6 Propidium iodide staining of murine hippocampal slice cultures

Murine hippocampal slice cultures were cultured at saturated humidity in 5% CO_2 at 37°C. The culture medium was changed three times per week.

Propidium iodide (PI) is a fluorescent molecule that is only able to enter cells if cell membranes are damaged. Intracellular PI intercalates into DNA and RNA. This leads to a fluorescence excitation maximum at 535 nm and an emission maximum at 617 nm, which makes PI suitable for the detection of dying cells using fluorescent microscopy. PI was added to the medium of murine hippocampal slice cultures at a final concentration of 2.5 µg/ml. After incubation (1 h, 37°C), photographs were taken and PI positive cells were counted using Image J.

Slice culture medium	
MEM	80%
Heat inactivated horse serum	20%
L-glutamine	1 mM
Ascorbic acid	0.00125%
Insulin	0.001 mg/ml

Calcium chloride	1 mM
Magnesium sulfate	2 mM
D-glucose	13 mM

2.2.7 RNA isolation

The NucleoSpin RNA isolation kit (Macherey-Nagel, Düren, Germany) was used to isolate RNA from cells according to the manufacturer's instructions. RNA concentration and purity was determined by measurement at 230, 260, and 280 nm using a NanoDrop spectrophotometer. RNA was stored at -80°C.

2.2.8 cDNA synthesis

RNA was reverse transcribed into complementary DNA (cDNA) using MMV reverse transcriptase (Superscript II). In a final volume of 20 µl, 5 µg RNA was incubated with 1 µl oligo-dT_{20}-primer (100 µM) and 1 µl dNTP mix (20 mM) for 10 min at 70°C. After short centrifugation, 4 µl 5x First Strand Buffer was added and the sample was incubated for 2 min at 42°C. Subsequently, 1 µl Superscript II enzyme was added, followed by a one hour incubation period (42°C). The enzyme was inactivated (10 min, 70°C), 30 µl RNase free water was added, and the samples were stored at -20°C.

2.2.9 Quantitative real time PCR (RT-qPCR)

To quantify differences in the amount of target mRNA in variable samples, RT-qPCR was used. Target gene specific primers were designed for amplification using the software available at the NCBI nucleotide database. For normalisation, a primer pair targeting the housekeeping gene glycerinealdehyde-3-phosphate dehydrogenase (GAPDH) was used.

cDNAs were diluted 1:7 in water and 5 µl of pre-diluted cDNA was pipetted into qPCR plates in duplicates. Water was used as a negative control. 10 µl of TaqMan RT-qPCR mix was added to each well, the RT-qPCR plate was sealed with RT-qPCR adhesive film and centrifuged shortly at 1200 rpm.

Mix per Well	[µl]
Millipore water	1.9
Primer fwd (5 µM)	0.3
Primer rev (5 µM)	0.3
2x RT-qPCR Mastermix	7.5
Total	10

RT-qPCR was performed on a 7500 Fast Real time PCR cycler using the following settings:

- Quantification Comparative
- 96 Well-Plate (Thermo Fast)
- 2 hours (Standard)
- SYBR Green
- Cycles: 45

The resulting cycle threshold (Ct) values were analyzed using Excel. The Ct value is specified as the first cycle with a fluorescent signal clearly above the threshold. The target values were normalized to the housekeeping value (ΔCt) and then related to the control value (ΔΔCt). The final value is depicted as n-fold expression to the control.

1. Calculation ΔCt

   $\Delta Ct1 = Ct(Sample1; Target1) - Ct(Sample1; Target\ Housekeeping)$

2. Calculation ΔΔCt

   $$\Delta\Delta Ct = \Delta Ct\ 1 - Mean\ \Delta Ct(Control1)$$

3. Calculation n-fold expression

   $$n\text{-}fold\ expression = 2^{-\Delta\Delta Ct}$$

2.2.10 Gene expression microarray

TaqMan gene expression microarrays to detect differentially regulated genes were performed according to the manufacturer's instructions. In brief, for each sample 10 µg RNA was reverse transcribed, water was added to obtain a final volume of 1080 µl,

and 1080 µl of TaqMan gene expression master mix was added. 20 µl of the mix was added to each well of the TaqMan array plate. The plate was sealed and centrifuged shortly at 1200 rpm. Microarrays were performed using a 7500 ABI real time PCR cycler. The resulting Ct values were analyzed as described in 2.2.9.

2.2.11 Transwell migration assay

The Transwell migration assay allows the quantification of migrated cells. Transwell migration chambers consist of a 24 well plate filled with a chemoattractant and inserts that separate the lower chamber containing the chemoattractant from the upper chamber containing the cells by a membrane with 8 µm pores. Cells are seeded in the upper chamber and actively migrate towards the chemoattractant. Conditioned medium (CM) from NIH/3T3 mouse fibroblasts (700 µl/well) was used as chemoattractant. The CM was obtained 48 h after seeding $10x10^6$ NIH/3T3 mouse fibroblasts in 20 ml of complete culture medium, clarified from cell debris by centrifugation (1200 rpm, 5 min), and stored at -80°C. 20000 LNT-229 or SMA-560 cells (200 µl/well) were seeded into the upper chamber. In parallel, 10000 cells were seeded in a 96-well plate to determine proliferation (measured by crystal violet staining). After 16-20 h of incubation at 37°C, cells in the upper chamber were removed using a cotton bud. Migrated cells on the lower side of the insert membrane were fixed for 10 min in methanol, stained for 10 min with haematoxylin and washed with water. The membranes were cut using a scalpel and embedded into Mowiol on a microscopic slide covered with a glass slip. Migrated cells were counted manually at 10-fold magnification (7 visual fields per membrane). To avoid false results evoking from enhanced or decreased cell proliferation, migrated cell values were normalized to cell proliferation.

2.2.12 Immunoblot

2.2.12.1 Generation of protein lysates and cell culture supernatants

Cells were collected using a cell scraper for the generation of protein lysates. The cells were centrifuged (1200 rpm, 5 min), the supernatant was removed, and the cell pellet

was resuspended in 100 µl lysis buffer. After 15 min incubation on ice, lysed cells were centrifuged (13000 rpm, 15 min) to remove insoluble material and the soluble protein containing supernatant was collected and stored at -20°C.

Lysis buffer	
Tris HCl pH 8	50 mM
Sodium chloride	120 mM
EDTA	5 mM
NP-40	0.5 %
Millipore water	
Proteinase inhibitor cocktail	10 µl in 2 ml lysis buffer short before usage

For the production of cell culture supernatants, cells were incubated for 48 h in serum free culture medium (SFM). After collection, supernatants were centrifuged (1200 rpm, 5 min) to remove dead cells and cell debris and stored at -80°C. Proteins from cell supernatants that are used for immunoblots were concentrated by acetone precipitation after determination of the protein concentration using the Bradford protein assay (see next chapter). For precipitation 20 µl of supernatant protein was mixed with three volumes of ice cold acetone and centrifuged (4000 rpm, 20 min). Protein pellets were air dried and resuspended in Laemmli buffer.

Laemmli buffer	
0.5 M Tris HCl pH 6.8	2 ml
SDS	400 mg
Bromophenol blue	2 mg
Glycerol	2 ml
Millipore water	to 10 ml

2.2.12.2 Bradford protein assay

To determine protein concentrations in lysates or supernatants the Bradford protein assay was used. As calibration curve a BSA solution (0, 1, 2, 4, 6, 8, 10, and 12 µg)

was diluted in water or serum free medium (50 µl/well). For cell lysates 1 µl of sample in 50 µl water or for supernatants 50 µl of the original sample were used. 150 µl/well of 1:5 pre-diluted Bradford reagent was added and absorbance was measured at 595 nm. The assay was performed in triplicates and the mean was used to calculate the protein concentration on basis of the standard curve.

2.2.12.3 SDS polyacrylamide gel electrophoresis (SDS-PAGE)

SDS-PAGE is a method to separate proteins according to their size. Proteins were denatured in Laemmli buffer (composition see 2.2.12.1) supplemented with 10% β-mercaptoethanol (10 min, 96°C). Equal amounts of protein (20 up to 40 µg of protein) were loaded on 10% polyacrylamide gels. Electrophoresis was performed at 200 V for 45-60 min in running buffer.

Polyacrylamide gel		
10% gel	Separating gel [ml]	Stacking gel [ml]
Millipore water	2	1.15
30% acrylamide	1.7	0.33
1.5 M Tris HCl	1.3 pH 8.8	0.5 pH 6.8
10% SDS	0.05	0.02
10% Ammonium persulfate	0.05	0.02
TEMED	0.002	0.002
Total	5	2

10x Running buffer	[g]
Tris	30
Glycine	144
SDS	10
Millipore water	to 1 l

2.2.12.4 Protein transfer to polyvinylidene fluoride membrane

To transfer separated proteins from the acrylamide gel to a polyvinylidene fluoride (PVDF) transfer membrane, the membrane was activated in methanol for one minute, washed in water for one minute, and stored in 1x transfer buffer (100 ml 10x transfer buffer, 700 ml water and 200 ml methanol) until usage. The transfer was performed at 100 V for one hour in 1x transfer buffer.

10x Transfer buffer	[g]
Tris	30
Glycine	144
Millipore water	to 1 l

2.2.12.5 Immunoblot antibody incubation and detection

After transfer the PVDF membrane was blocked in blocking solution (1 h, RT) followed by incubation with the primary antibody in TS-TMBSA (o/n, 4°C). Antibodies were diluted as recommended by the manufacturer. The membrane was washed three times in TBST, incubated with a HRP-conjugated secondary antibody diluted 1:10000 in blocking solution (1 h, RT), washed three times in TBST and the chemiluminescence signal was detected using the WesternBright ECL HRP substrate. For cellular proteins a housekeeping protein was used for normalisation. For supernatants, the membranes were stained with Ponceau S (5 min, RT), destained by three washes in water, and photographs were taken. All membranes were detected using the ChemiDoc™ Imaging System and analyzed using Image Lab (V 6.0).

Blocking solution	
Skim milk powder	10 g
TBST	200 ml

10x TBS	[g/l]
Tris HCl pH8.0	24.2
Sodium chloride	80

TBST	
1x TBS	
Tween-20	0.05 %

TS-TMBSA	
Tris HCl pH 7,5	10 mM
Sodium chloride	150 mM
Tween-20	1%
Skim milk powder	5%
BSA	2%
NaN_3	0.01%

Ponceau S staining solution	[g]
Ponceau S	0.2
5-Sulfosalicylacid	3
Trichloroacetic acid	3
Millipore water	to 100 ml

2.2.13 Zymography

For the detection of matrix metalloproteinase activity zymogram gelatine gels were used. Supernatants were generated as described in chapter 2.2.12.1 but were concentrated using 3 kD Amicon centrifugal filter units according to the manufacturer's instructions. Protein concentrations were determined by the Bradford assay (chapter 2.2.12.2). Samples were diluted 3:2 in Laemmli buffer (composition see 2.2.12.1). 20 µg of protein/lane were loaded on ready-made 10% gelatine zymogram gels. Electrophoresis was performed in running buffer (composition see 2.2.12.3) at

150 V for 1-2 h. Gels were washed twice (30 min) in washing buffer and incubated in developing buffer (o/n, 37°C). Subsequently, gels were stained (15-30 min) using Coomassie blue and destained by several washes in destaining solution. To sharpen the bands, gels were incubated in Millipore water (o/n, 4°C). Zymograms were analyzed using the ChemiDoc™ Imaging System and Image Lab (V 6.0).

Washing buffer	
Tris HCl pH 7.5	50 mM
Triton X-100	2.5%

Developing buffer	
Tris HCl pH 7.5	50 mM
Calcium chloride	10 mM
Sodium chloride	150 mM
NaN_3	0.05%

Staining solution (filtrated)	
Coomassie brilliant blue	0.2 g
Methanol	45 ml
Millipore water	45 ml
Acetic acid	10 ml

Destaining solution	[%]
Methanol	45
Millipore water	45
Acetic acid	10

2.2.14 ELISA

ELISAs were performed and evaluated according to the manufacturer's instructions (RayBiotech, Norcross, GA, USA). Freshly prepared as well as frozen (-80°C) cell

culture supernatants were produced as described in chapter 2.2.12.1. If necessary, supernatant proteins were concentrated using 3 kD Amicon centrifugal filter units. Protein concentrations were determined using the Bradford array (chapter 2.2.12.2) and were used for normalization.

2.2.15 Immunofluorescence of viscumin treated cells

To visualize the uptake of viscumins by glioma cells, $1x10^5$ GBM cells were seeded on poly-L-lysine covered glass slips coated (19 µg/cm^2) placed in 12-well plates. The next day, the cells were treated with ISCADOR Qu, Aviscumine, or native ML-1 (8 ng/ml ML) for different time periods or were left untreated. The cells were fixed (4% paraformaldehyde, 10 min, RT), washed three times with PBS, and blocked (10% goat serum, 0.3% Triton X-100, PBS, 1 h) followed by incubation using a polyclonal rabbit anti-ML antibody (IgG, 2 µg/ml) or normal rabbit IgG (o/n, 4°C). For visualization of viscumin uptake, an Alexa Fluor 488 coupled goat anti-rabbit IgG antibody was used (1 h, RT). The secondary antibody was diluted as recommended by the manufacturer. The glass slips were mounted in VECTASHIELD Antifade mounting medium containing DAPI and were examined by confocal microscopy using a Zeiss LSM 510. Images were analyzed using the software ImageJ.

2.2.16 Immunofluorescence detection of CD75s expression

To determine the expression of the ML-1 binding ganglioside CD75s, 50000 glioma cells were seeded on poly-L-lysine coated glass cover slips (19 µg/cm^2) placed in 12-well plates. After 48 h, the cells were fixed (4% paraformaldehyde, 10 min), washed three times with PBS, and blocked (10% goat serum, 0.3% Triton X-100, PBS, 1 h) followed by incubation (o/n, 4°C) using a monoclonal mouse anti-CD75s antibody (IgM, 4 µg/ml) or normal mouse IgM. To visualize CD75s, the cells were stained using a TexasRed coupled goat anti-mouse IgM antibody (1 h, RT) and mounted using VECTASHIELD hard set mounting medium with DAPI. Human GBM cryosections of seven patients were provided by the Biobank of the Institute for Pathology (University of Tübingen, ethical approval 475/2016BO2). The samples were fixed and stained for

CD75s expression as described above. A FITC labelled goat anti-mouse IgM antibody was used (1 h, RT). Secondary antibodies were diluted as recommended by the manufacturer. CD75s staining was examined by microscopy using a Zeiss Imager.Z1 and images were analyzed using ImageJ. All stainings and analyses of CD75s expression were performed under my supervision by Jennifer Theresia Miemietz as part of her bachelor thesis.

2.2.17 Flow cytometry

Adherent cells were detached using Accutase. Cells were washed once with flow cytometry buffer (0.5% BSA, 2 mM EDTA, 0.02% NaN3, PBS) and saturated to avoid background signals using Gamunex (human IgG, 0.5%, 20 min) on ice. Cell surface stainings were performed by incubation of the cells with fluorophore coupled primary antibodies in the dark (30 min, ice). Antibodies were diluted as recommended by the manufacturer. The cells were washed twice with flow cytometry buffer and analyzed using a CyAn ADP flow cytometer.

2.2.18 Cell cycle analysis by BrdU incorporation

To determine the amount of cells in each phase of the cell cycle (G_1, S, or G_2-M) $1x10^5$ glioma cells were seeded in 12-well plates, treated for 24 h with different concentrations of ISCADOR Qu, Aviscumine, or native ML-1, or were left untreated. To neutralize viscumin-mediated effects, a polyclonal rabbit anti-ML antibody (4.8 µg/ml) was added to the viscumin-containing medium 30 minutes before treatment. 5-Bromo-2-deoxyuridine (BrdU, 10 µM), incorporating into newly synthesized DNA of proliferating cells (S phase), was added to the cells. After 30 min cells were washed once using PBS, detached with Accutase, and washed again with PBS. The cells were fixed in 70 % ice-cold ethanol (30 min, ice) and washed twice with PBS. To denature the DNA, the cells were incubated in 2 M HCl (30 min, RT), neutralized by addition of sodium tetraborate (0.1 M, pH 8.5), washed once with flow cytometry buffer, and stained in the dark using a FITC coupled anti-BrdU antibody (30 min, ice). The secondary antibody was diluted as recommended by the manufacturer. To stain DNA the cells were washed twice with flow cytometry buffer and incubated in the dark

using PI/RNase A buffer (50 µg/ml PI, 100 µg/ml RNase A in flow cytometry buffer; 20 min). The cells were analyzed using a CyAn ADP flow cytometer.

2.2.19 Immunological studies

2.2.19.1 Isolation of PBMCs from whole blood

Human peripheral blood mononuclear cells (PBMCs) were isolated from whole blood via density centrifugation using Bicoll. Blood was diluted 1:3 in PBS and carefully layered on Bicoll. After centrifugation (2000 rpm, 30 min) the PBMC containing fraction was collected and washed twice (PBS, 2 mM EDTA). Remaining erythrocytes were lysed using ACK lysis buffer. PBMCs were washed once with PBS and were either stored frozen at -150°C or were directly used for further experiments.

2.2.19.2 NK cell expansion and isolation

For expansion of NK cells, PBMCs were incubated with irradiated RPMI8866 feeder cells (30 Gy) in a 4:1 ratio for 10 days. IL-2 (50 IU/ml) was added every second to third day. NK cells were isolated using the NK cell isolation kit (Miltenyi, Bergisch Gladbach, Germany). Purity of NK cells was determined by flow cytometry using anti-human CD56 and CD3 antibodies.

2.2.19.3 T cell expansion and activation

For expansion and activation of T cells, PBMCs were incubated for 3-5 weeks with irradiated and either ISCADOR Qu, Aviscumine, or native ML-1 (8 ng/ml ML, 24 h) treated, or untreated, LNT-229 cells in a ratio of 15:1. LNT-229 cells were irradiated (30 Gy) prior to co-culture. IL-2 (50 IU/ml) was added to the co-culture every second to third day. Every week expanding non-adherent PBMCs were harvested and transferred to fresh, irradiated (30 Gy) and either viscumin-treated or untreated, irradiated LNT-229 cells. Additionally and as a source for growth factor production necessary for the expansion of T cells, irradiated PBMCs (30 Gy) that origin from a different donor were added in a ratio of 1:4. Expanded T cells from these co-cultures were isolated using a T cell isolation kit (Miltenyi, Bergisch Gladbach, Germany).

Purity and activation status of T cells was determined by flow cytometry using anti-human CD3, CD4, CD8, CD69, and CD56 antibodies.

2.2.19.4 Immune cell lysis assay

LNT-229 Luc cells were seeded in 96-well plates (10000 cells/well) and allowed to attach. The cells were treated with ISCADOR Qu, Aviscumine, native ML-1 (8 ng/ml ML, 24 h), or were left untreated. After washing the cells to remove residual viscumins, NK or activated T cells were added at variable effector to target cell ratios and were co-cultured with the glioma cells for 4 h. As control, viscumin-treated or untreated LNT-229 Luc cells were cultured in the absence of immune cells (spontaneous lysis), or LNT-229 Luc cells were lysed by addition of 1% SDS (complete lysis). To determine luciferase activity the medium was removed, the cells were washed once with PBS, and 50 µl Luciferase lysis buffer was added to each well. The plates were frozen to additionally and mechanically destroy cell membranes. After thawing, 40 µl cell lysate/well was transferred to 96-well white plates and luciferase activity was measured by adding 100 µl luciferin containing buffer using a Mithras LB940 Fluorimeter. The amount of lysis was calculated by:

Lysis in percent = 100-((experimental lysis/spontaneous lysis)x100)

Lysis buffer 5x	
Tricine pH 7.8	40 mM
Sodium chloride	50 mM
EDTA	2 mM
EGTA	1 mM
DTT	5 mM
Triton X-100	1 %

Luciferin containing buffer pH 8	[mM]
Gly-Gly	25
K_2HPO_4 pH 8	15
EGTA	4
ATP	2
DTT	1
Magnesium sulfate	15
Coenzyme A	0.1
D-Luciferin	0.075

2.2.20 Mouse experiments

Athymic four week old female Rj:NMRI-Foxn1^{nu}/Foxn1^{nu} mice were purchased from Janvier (Le Genest-Saint-Isle, France). Immunocompetent VM/Dk mice were bred in-house [195, 196]. The experiments were performed according to the German law (approval N6/16, FK/K5112). 75000 human LNT-229 or 5000 murine SMA-560 GBM cells were stereotactically implanted in the right striatum of the mice (volume: 2 µl; injection rate: 1 µl/min) using the following coordinates: 2 mm right, 1 mm frontal of the bregma, 3 mm depth.

Rj:NMRI-Foxn1^{nu}/Foxn1^{nu} mice bearing LNT-229 tumors were intratumorally injected with ISCADOR Qu, Aviscumine (3 µl, 240 ng/ml ML), or PBS 7 days after tumor cell implantation. Additionally, mice were treated by i.p. injections of TMZ (1.5 mg/kg or 2.5 mg/kg, depending on the experiment) or PBS at day 7, 14, and 21 after tumor cell implantation. For triple therapy the mice were focally tumor irradiated (3 Gy) using a six megavoltage photon linear accelerator (LINAC 6C) at day 8 after the tumor cell implantation.

VM/Dk mice bearing SMA-560 tumors were treated every third day with ISCADOR Qu or PBS starting from day 8 after the tumor cell implantation by s.c. injections of 100 µl PBS containing increasing ML concentrations (6 injections: 2 x 0.8 ng/ml of ML, 2 x 8 ng/ml of ML, 2 x 80 ng/ml of ML). The mice were focally tumor irradiated

as described above at day 7. Additionally, triple treatment mice were injected i.p. with TMZ (2.5 mg/kg) or PBS at day 8, 14, and 20 after the tumor cell implantation.
If observing pain, weight loss, neurological or tumor associated symptoms the mice were sacrificed, brains were isolated, and fixed in 4% paraformaldehyde for histological evaluation.

2.2.21 Mouse inflammation antibody array

To determine changes of cytokine levels induced by viscumin-treatment, VM/Dk mice were injected (s.c.) with ISCADOR Qu or PBS at increasing concentrations every third day for three weeks (8 injections with 100 µl; 2 x 0.8 ng/ml, 2 x 8 ng/ml, 4 x 80 ng/ml of ML ISCADOR Qu). The mice were sacrificed and blood was collected. After clotting (30 min, RT) blood serum was collected by centrifugation (2000 rpm, 10 min). Using these sera, a mouse inflammation antibody-array was performed according to the manufacturer's protocol (RayBiotech, Norcross, GA, USA). For detection the array scan service (Tebu-Bio, Offenbach am Main, Germany) was utilized. Data were analyzed using Image Lab (V 6.0).

2.2.22 Statistical analysis

For *in vitro* assays, results were calculated as means ± standard deviation (SD) and compared using the two-tailed Student's t-test using Excel (*$p<0.05$, **$p<0.01$, ***$p<0.001$). All data result from at least three independent experiments (*n*). For *in vivo* assays, survival and median survival times were analyzed using the Kaplan-Meier method and compared using the log-rank test with JMP 13 (*$p<0.05$, **$p<0.01$, ***$p<0.001$).

3. Results

3.1 Cytotoxic effects of viscumins

Cytotoxic effects of ML-rich *Viscum album* extracts have previously been described by our group [118]. In the first part of the project, toxic effects of ISCADOR Qu, Aviscumine, and native ML-1 were determined in several glioma cell lines but also in non-neoplastic cell lines, in primary non-neoplastic cells, as well as in murine hippocampal slice cultures. Data received from ISCADOR treatments have already been shown in previous experiments [118]. In the present study, the existing data for ISCADOR Qu were verified and compared to newly collected data received from Aviscumine and native ML-1 treatments. Furthermore, the uptake of viscumins by LNT-229 cells as well as the expression of the viscumin receptor CD75s in several cell lines and primary tissue were determined to evaluate whether the uptake of viscumins or CD75s expression correlate with viscumin-cytotoxicity and predict viscumin-sensitivity of non-neoplastic and cancer cells. These data are essential to determine viscumin treatment concentrations for further experiments and to estimate possible toxic side effects.

3.1.1 IC_{50} values

A common way to compare the toxicity of substances is to determine IC_{50} values, which indicate the concentration that is necessary to inhibit 50% of cell growth compared to untreated controls. To determine IC_{50} values of viscumins, glioma and non-neoplastic cells were treated with increasing concentrations (0.8-240 ng/ml ML) of ISCADOR Qu, Aviscumine, or native ML-1 for 24 and 48 h. Cell density was measured by crystal violet staining. The viability of the non-adherent PBMCs were measured using the MTT assay. Using the software OriginPro 8, the Hill equation ($y = START + (END - START)\ x^n / (k^n+x^n)$) was utilized as interpolation function and to calculate IC_{50} values.

Table 1: IC_{50} values (24 h and 48 h) of viscumins in the treatment of glioma and non-neoplastic cells. ISCADOR Qu (ISC Qu), Aviscumine (Avi), native ML-1 (ML-1).

Cell	IC_{50} 24 h			IC_{50} 48 h		
	ISC Qu [ng/ml ML]	Avi [ng/ml]	ML-1 [ng/ml]	ISC Qu [ng/ml ML]	Avi [ng/ml]	ML-1 [ng/ml]
Glioma cells						
LNT-229	37.09	95.60	>240	10.50	17.78	29.73
LN-308	139.72	>240	>240	83.13	>240	>240
LN-319	71.36	>240	>240	24.64	18.23	27.95
U87MG	140.60	>240	>240	81.03	>240	>240
T98G	101.19	>240	>240	51.24	158.81	113.11
MZ-18	35.45	>240	>240	11.56	10.94	9.97
SMA-560	35.70	10.23	19.25	17.31	2.69	8.25
Non-neoplastic cells						
SVGA	65.95	>240	>240	2.36	1.37	1.02
HBVP	28.86	>240	58.37	4.85	23.59	5.01
hCMEC/D3	>240	>240	>240	27.92	105.12	42.02
PBMCs (MTT)	26.45	171.35	144.22	6.50	18.81	23.74

In general, ISCADOR Qu held lowest IC_{50} values (24 h), except for murine SMA-560 glioma cells that are highly sensitive towards Aviscumine treatment. Viscumin-mediated toxicity after 48 h of treatment varied. LNT-229, SMA-560, LN-319, and MZ-18 glioma cells were viscumin-sensitive, whilst LN-308, U87MG, and T98G cells were less vulnerable. All non-neoplastic cell lines and primary cells tested so far showed sensitivity towards viscumins. In the cohort of non-neoplastic cells, hCMEC/D3 human endothelial cells provided highest and immortalized astrocytic SVGA cells lowest IC_{50} values (Table 1).

For further experiments non-toxic concentrations (all below the determined IC_{50} values) were chosen. To treat LNT-229 glioma cells, a final concentration of 2.4 up to 16 ng/ml of ML was used. To treat LN-308 glioma cells a concentration of 16 ng/ml of ML and to treat SMA-560 glioma cells a concentration of 2.4 up to 16 ng/ml of ML ISCADOR Qu, 0.8 to 4.8 ng/ml Aviscumine, or 2.4 up to 16 ng/ml native ML-1 was chosen. IC_{50} values in the cohort of tumor cell lines and non-neoplastic cells varied between different cell lines, ranging from low to high values but were comparable. Therefore, viscumin-mediated toxic side effects on non-tumor cells or tissue could not be excluded by these experiments.

Furthermore, a viscumin-neutralizing antibody was used to block viscumin-mediated toxicity in LNT-229 cells (Figure 3). Cell death induced by Aviscumine treatment for 48 h was completely prevented even at high concentrations that were far above the IC_{50} (17.78 ng/ml). Even at a concentration of 80 ng/ml of Aviscumine, no cell death was observed in LNT-229 cells (Figure 3A). On the contrary, cell death induced by the *Viscum album* extract ISCADOR Qu was only blocked at low concentrations (below 8 ng/ml ML). Partial cell death inhibition was achieved at a concentration between 20 and 40 ng/ml ML, and no protecting effect was detectable anymore at a concentration of 80 ng/ml ML indicating that cell death induced by ML present in ISCADOR Qu can be blocked by the addition of the antibody, whilst cell death induced by additional compounds present in the extract could not be inhibited by addition of the antibody (Figure 3B).

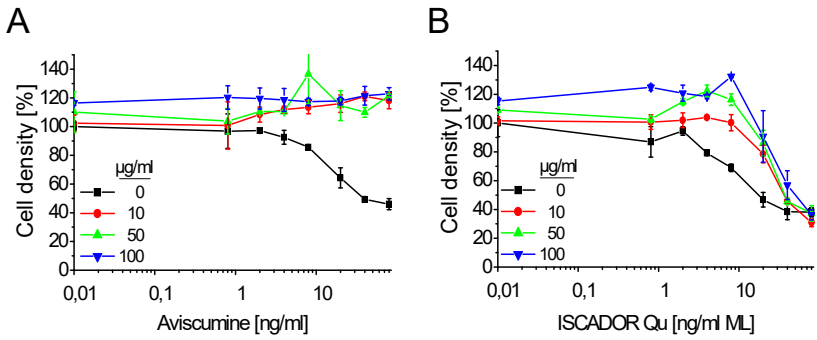

Figure 3: A viscumin-neutralizing antibody blocked cell death induction. LNT-229 cells were treated with Aviscumine (A) or ISCADOR Qu (B) at increasing concentrations in the absence or presence of a viscumin-neutralizing antibody (0, 10, 50, or 100 µg/ml). Cell density was measured 48 h later by crystal violet staining (n=1, mean ± SD).

3.1.2 Toxicity of viscumin-based drugs in murine hippocampal slice cultures

To further address the possibility of toxic side effects in healthy brain tissue, viscumin-mediated toxicity was also tested in organotypic human brain and murine hippocampal organotypic cultures. The cultures were treated for 24 or 48 h with increasing concentrations of ISCADOR Qu, ISCADOR P, Aviscumine, or native ML-1 and were stained with PI to measure the amount of dead cells. Data collected from human brain tissue could not be evaluated due to very high basal levels of cell death. In mouse brain cultures, ISCADOR Qu and ISCADOR P induced cell death, putatively an effect of viscotoxins (VT) that are present in these ME. For ISCADOR Qu, 24 h and 48 h after treatment cell death was detectable at ML concentrations of > 24 ng/ml, which corresponds to 1.03 µg/ml VT. For ISCADOR P > 10 mg/ml of the extract had to be used to induce cell death. This counts for less than 0.25 ng/ml of viscumins but for 3.76 µg/ml of VT. These data suggest that cytotoxic effects of ISCADOR preparations were a result of VT or other agents that are components of ME. No significant toxic effects were observed after treating mouse brain cultures with Aviscumine or native ML-1 (Figure 4).

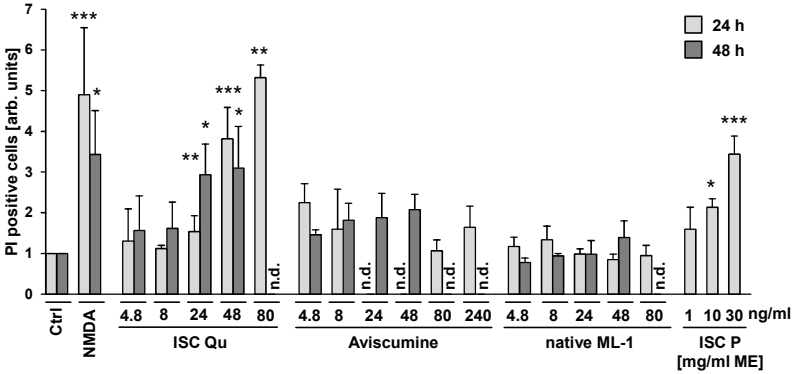

Figure 4: Induction of cell death in murine hippocampal slice cultures. Organotypic cultures were treated for 24 h or 48 h with ISCADOR Qu (ISC Qu), ISCADOR P (ISC P), Aviscumine, or native ML-1 at increasing concentrations. Four photographs per slice were taken and PI positive cells were counted. Incubation with NMDA (10 µM, 30 min) 24 h prior to PI staining served as a positive control for cell death induction (n=3-4, mean ± SD, Student's t-test *P < 0.05, **P < 0.01, ***P < 0.001).

3.1.3 Viscumin uptake and CD75s expression

Differences in the vulnerability towards viscumin-induced cell death might be a result of a variable uptake of viscumins by tumor cells. ISCADOR Qu contains, besides ML-1, also ML-2 and -3, whereas native ML-1 or Aviscumine are not. In contrast to ISCADOR Qu and native ML-1, Aviscumine presents a non-glycosylated form of ML-1. This might also influence the uptake of viscumins by cells. Furthermore, vulnerability towards viscumins might depend on the expression of the viscumin receptor CD75s on the cell surface.

Firstly, the uptake of viscumins was tested in LNT-229 cells treated with ISCADOR Qu, Aviscumine, or native ML-1 (8 ng/ml ML) for 1 or 6 h using immunofluorescence and confocal microscopy (data published in Schötterl et al. Int. J. Oncology 2017 [197]). Viscumins were detected equally in the cytoplasm of LNT-229 cells (Figure 5) after 6 h, indicating a fast uptake of viscumins by tumor cells.

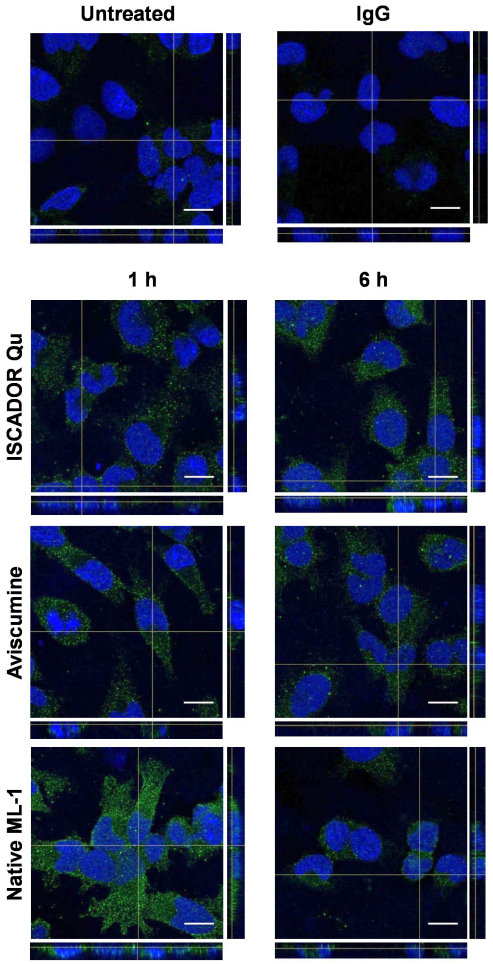

Figure 5: Viscumin uptake by LNT-229 glioma cells. LNT-229 cells were incubated for 1 or 6 h with ISCADOR Qu, Aviscumine, or native ML-1 (8 ng/ml ML). Z-stack confocal images were taken (40x magnification). Viscumins were stained using a ML-specific antibody (green), nuclei were stained using DAPI (blue). Viscumin localized in the cytoplasm is visible in the YZ (right) and XZ (bottom) boxes next to each photograph. As controls for specific viscumin staining, untreated or native ML-1 treated LNT-229 cells, followed by incubation with isotype IgG, were used. Scale bars: 15 µm. Representative photographs of three independent experiments are shown. Modified from Schötterl et al. Int. J. Oncology 2017 [197].

Besides, glycosylation of ML-1 or the presence of other components that are part of the ME ISCADOR Qu did not influence the uptake. Therefore, differences in cell death induction by ISCADOR Qu, Aviscumine, or native ML-1 were not an effect of differences in the uptake of viscumins.

Next, the expression of CD75s on glioma cells, on primary human microvascular pericytes (HBVPs), on human GBM tissue, and on human and murine normal brain was analyzed. These experiments were performed under my supervision and guidance by Jennifer T. Miemietz during her Bachelor thesis. Six glioma cell lines, HBVPs, seven human GBM biopsy samples, human and murine healthy brain, and murine spleen were analyzed for CD75s expression. All tested cell lines as well as 6/7 GBM specimens showed CD75s expression, even to a different extent (Table 2 and Figure 6A, B). Human and murine healthy brains were CD75s negative. Murine spleen was used as a positive control for CD75s expression since immune cells have been described to express CD75s [198]. Quantification of CD75s expression using Image J followed by correlation analyses demonstrated a strong correlation of viscumin-induced cell death (IC_{50} 48 h; Table 1) and CD75s staining (Figure 6C, D) for all glioma cell lines. The relation coefficients (R) were similar for ISCADOR Qu (R = -0.74), Aviscumine (R = -0.75), and native ML-1 (R = -0.77). The data fortify the equal amount of viscumin uptake detected in LNT-229 glioma cells for all viscumin preparations (Figure 5). Therefore, CD75s might be a biomarker that could be used to predict the efficiency of a viscumin-based therapy in GBM.

Table 2: CD75s expression of human GBM specimen. Specific CD75s expression was determined by comparing the staining intensity using the ML-specific antibody to that of the IgM isotype control. Experiments were performed under my supervision and guidance by Jennifer T. Miemietz during her Bachelor thesis. Specific CD75s expression was categorized as negative (-), positive (+), or strongly positive (++) according to the staining intensity.

GBM	primary/ secondary	IDH^{R132H} mutation	IDH sequence	MGMT status	CD75s expression
N28615	pGBM	negative	n.d.	unmethylated	+
N70315	pGBM	negative	n.d.	unmethylated	++
N156714	pGBM	negative	n.d.	unmethylated	-
N125014	pGBM	negative	n.d.	unmethylated	-/+
N152509	sGBM	positive	n.d.	methylated	++
N25914	sGBM	negative	R132G	methylated	++
N165014	sGBM	negative	R132G	methylated	+

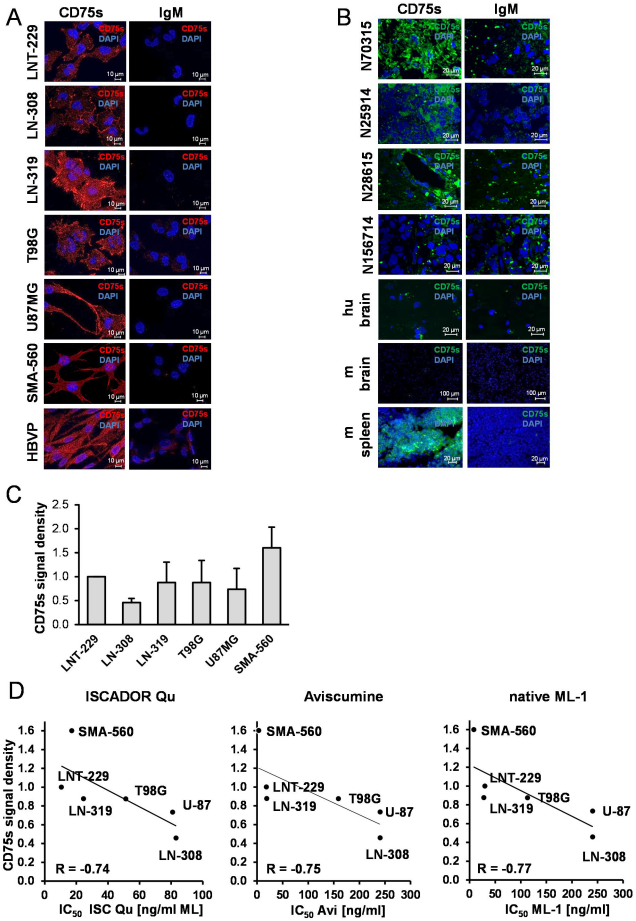

Figure 6: CD75s expression in GBM cells and tissue and correlation analysis of CD75s expression and viscumin-mediated cytotoxicity (IC_{50}, 48 h). Experiments were performed under my supervision and guidance by Jennifer T. Miemietz during her Bachelor thesis. A/B, CD75s expression in glioma cell lines (A) and healthy brain or human glioma specimen (B). Nuclei were stained with DAPI. As a control, cells or glioma specimen were stained using an isotype IgM. Photographs were taken at 63x magnification. Representative pictures of three independent experiments are shown. C, Relative CD75s signal density normalized to the signal determined for LNT-229 (n=3, mean ± SD, minimum of 4 photographs). D, Correlation analyses of CD75s signal density and viscumin-induced cell death (IC_{50}, 48 h, R relation coefficient).

3.2 Viscumins modify proliferation and cell cycle distribution

In tumor cells viscumins have been described to influence proliferation as well as cell cycle distribution [122, 124, 199, 200]. Here cell growth of glioma cells after viscumin treatment was determined and changes in cell cycle distribution were analyzed by flow cytometry using BrdU incorporation and quantification of the DNA content by PI. Furthermore, changes in the expression of cell cycle associated genes by viscumins were examined. These experiments help to understand the versatile actions of viscumins in glioma.

3.2.1 Viscumin mediated changes in the growth of GBM cells

To test the impact of viscumins on glioma cell proliferation, LNT-229 or SMA-560 glioma cells were treated with several concentrations of ISCADOR Qu, Aviscumine, or native ML-1 (0-16 ng/ml ML). After 24 h, viscumins were removed and cell density was measured at different time periods. There was a clear reduction in cell growth detectable upon viscumin treatment (Figure 7). Interestingly, no effect for native ML-1 on cell growth was detectable in LNT-229 and SMA-560 cells at any concentration tested. Growth reduction was similar for ISCADOR Qu and Aviscumine in LNT-229 cells. As SMA-560 cells are highly sensitive to Aviscumine, very low concentrations were sufficient to inhibit cell growth.

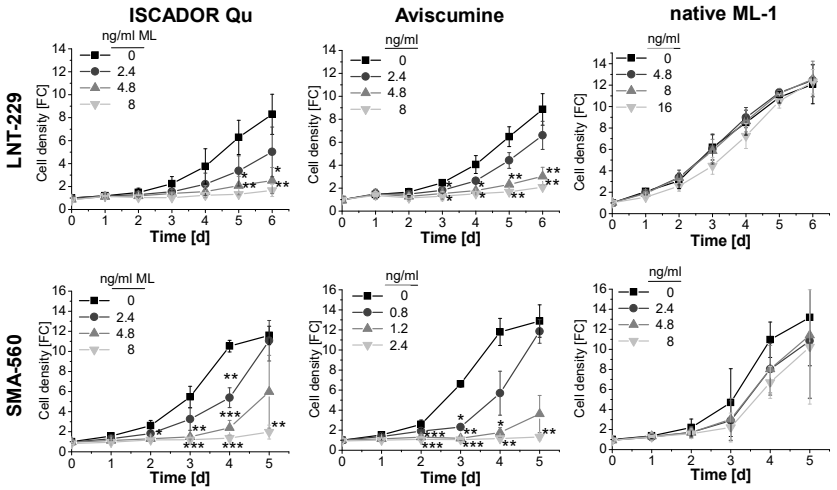

Figure 7: Reduced proliferation of LNT-229 and SMA-560 glioma cells upon viscumin treatment. Cells were treated with increasing concentrations of ISCADOR Qu, Aviscumine, or native ML-1 for 24 h. After removal of viscumins cells were stained with crystal violet every 24 h to determine cell density (FC fold change, d days, *n*=3, mean ± SD, Student's t-test *P < 0.05, **P < 0.01, ***P < 0.001).

3.2.2 Cell cycle distribution

To determine whether viscumin-mediated growth reduction is an effect of alterations of glioma cells in different phases of the cell cycle or whether glioma cells might arrest in a certain cell cycle phase, LNT-229 and SMA-560 glioma cells were treated with ISCADOR Qu, Aviscumine, or native ML-1 (0-16 ng/ml ML, 24 or 48 h). Cell cycle distribution was analyzed by BrdU incorporation and by measuring the cell's DNA content. BrdU is a synthetic thymidine analogue that is incorporated into the DNA during the S phase of the cell cycle. Incorporated BrdU was detected by flow cytometry using a FITC-coupled BrdU antibody. PI staining reveals the DNA content of a cell (2N, 4N). In Figure 8 an example for the flow cytometric analysis of the cell cycle is depicted. BrdU negative cells with low DNA content were gated as G_1 cells,

cells with high DNA content as G_2-M cells. BrdU positive cells were divided in an S phase ^{high} and an S phase ^{low} according to the level of incorporated BrdU.

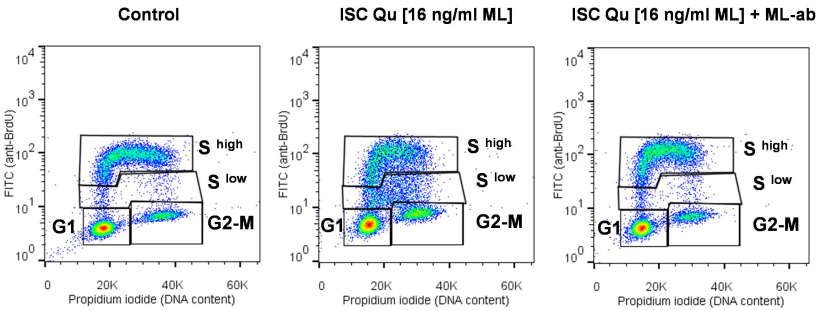

Figure 8: Gating example for flow cytometric cell cycle analysis. LNT-229 cells were treated with ISCADOR Qu (16 ng/ml ML, 24 h) in the presence or absence of a ML-specific antibody (4.8 µg/ml) that functionally neutralized viscumin effects. Afterwards, BrdU was added (30 min). Cells were fixed and BrdU incorporation was quantified using a FITC-coupled BrdU antibody. In parallel, DNA was stained using PI. The population of cells in the S phase was separated in two fractions (high and a low) dependent on the amount of incorporated BrdU. G_1 and G_2-M phase cells were defined by the total DNA content as measured by PI staining. Representative pictures of three independent experiments are shown.

After 24 h of ISCADOR Qu, Aviscumine, or native ML-1 treatment, only small alterations in the cell cycle distribution of LNT-229 cells became visible (Figure 9A). The amount of S phase ^{high} cells decreased by viscumin treatment (16 ng/ml ML), while the amount of S phase ^{low} and G_2-M phase cells increased. Treatment of LNT-229 cells with ISCADOR Qu or Aviscumine for 48 h strengthened these effects. Surprisingly, native ML-1 did not induce alterations in cell cycle distribution (Figure 9B). The effects of ISCADOR Qu or Aviscumine (48 h) were similar and included a strong accumulation of G_2-M phase cells, while the amount of S phase cells decreased. The amount of G_1 phase cells stayed constant.

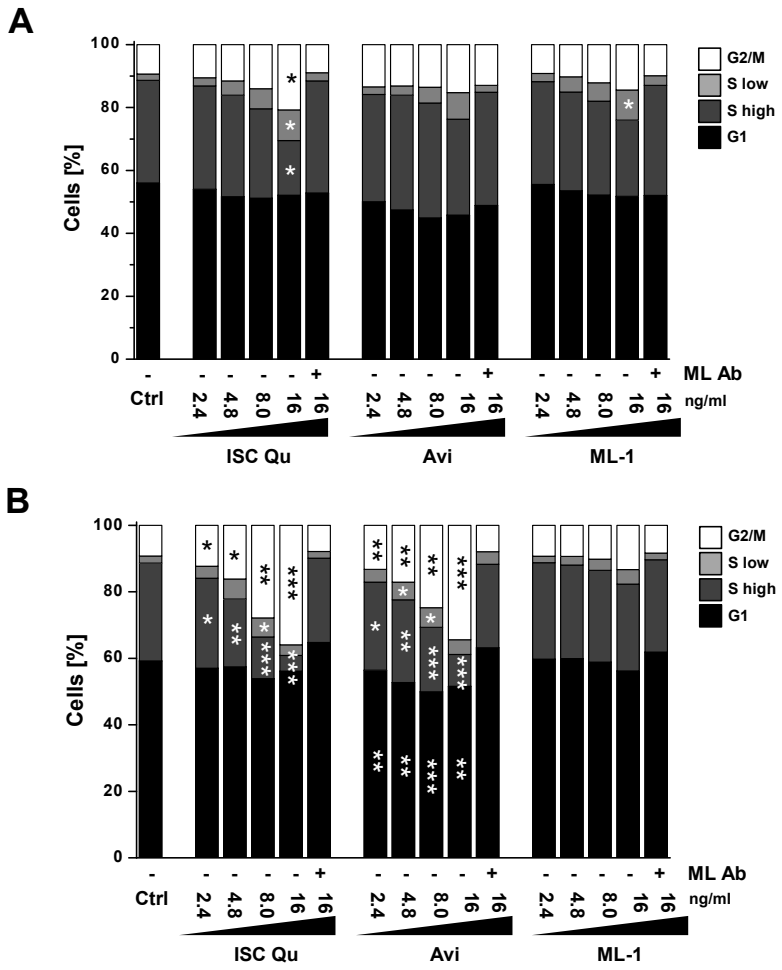

Figure 9: Cell cycle distribution of ISCADOR Qu (ISC Qu), Aviscumine (Avi), or native ML-1 (ML-1) treated LNT-229 glioma cells. Cells were treated for 24 h (A) or 48 h (B) with increasing viscumin concentrations in the absence or presence of a ML-specific antibody (4.8 µg/ml) to neutralize viscumin specific effects. DNA synthesis was determined by BrdU incorporation (30 min). Cells were fixed and BrdU stained using a FITC-coupled BrdU antibody. After RNAse digest total DNA content was determined by PI staining. Cell cycle phases (G_1, S ^{high}, S ^{low} and G_2-M) were gated as shown in Figure 8 (n=3, mean, Student's t-test *P < 0.05, **P < 0.01, ***P < 0.001).

In murine SMA-560 glioma cells the effect of both ISCADOR Qu and native ML-1 on cell cycle distribution was minor after 24 h (Figure 10A) and 48 h (Figure 10B). No accumulation of G_2-M phase cells was visible. Instead, SMA-560 cells showed a trend to accumulate in the G_1 phase. Nevertheless, the effect of Aviscumine on cell cycle distribution in SMA-560 cells was prominent. A massive reduction of S phase cells and accumulation of G_1 phase cells was detectable at 24 h. In SMA-560 cells, Aviscumine effects were strongest after 24 h and did not further increase. This might be due to the fact that SMA-560 cells proliferate faster than LNT-229 cells.

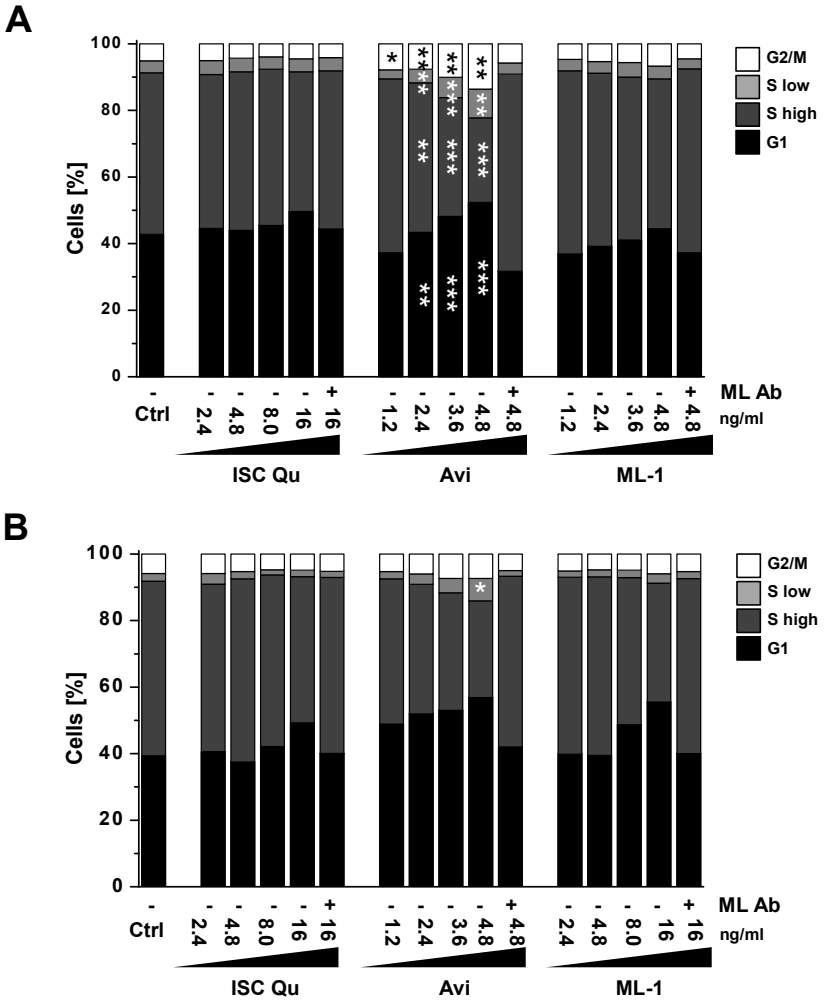

Figure 10: Cell cycle distribution of ISCADOR Qu, Aviscumine, or native ML-1 treated SMA-560 glioma cells. Cells were treated in the absence or presence of a ML-specific antibody (4.8 µg/ml) for 24 h (A) or 48 h (B). Newly synthesized DNA was measured by BrdU incorporation (30 min). Cells were fixed and BrdU stained using a FITC-coupled BrdU antibody. After RNAse digest, total DNA content was determined by PI staining. Cell cycle phases (G_1, S^{high}, S^{low} and G_2-M) were gated as shown in Figure 8 (n=3, mean, Student's t-test *P < 0.05, **P < 0.01, ***P < 0.001).

3.2.3 Modulation of cell cycle associated gene expression by viscumins

To identify underlying mechanisms how viscumins might reduce proliferation, the expression of cell cycle associated genes was analyzed in LNT-229 glioma cells using a RT-qPCR-based microarray that allows to determine the expression of 44 genes involved in the regulation of proliferation. 35/44 genes were differentially expressed in viscumin-treated compared to untreated cells. The expression of 21/35 differentially expressed genes found in the microarray were validated by RT-qPCR. 13 genes were found to be false positives. Regulated genes (microarray and RT-qPCR) are depicted in Figure 11A. In the panel of cyclins, cyclin A1, A2, B1, B2, B3, E1, and E2 were not regulated by viscumins (data not shown). Cyclin D1, D2, and D3 were differentially expressed in viscumin-treated cells (Figure 11B). Cyclin D1 was upregulated, whilst cyclin D2 and D3 were downregulated. The cyclin dependent kinase inhibitors CDKN1A (p21) and CDKN1B (p27) were not regulated at all (data not shown). In the panel of histone deacetylases (HDACs), five HDACs were not regulated (HDAC2, HDAC3, HDAC5, HDAC7, and HDAC9), and only HDAC6 was downregulated (Figure 11B and data not shown). Furthermore, E2F transcription factor 1 and 2 (E2F1, E2F2), ataxia telangiectasia and Rad3-related protein (ATR), and retinoblastoma protein (RB1) were not regulated, whilst ataxia telangiectasia mutated (ATM), TGFB1, and TGFB2 were downregulated, and protein phosphatase 2 catalytic subunit alpha (PPP2CA) was upregulated (Figure 11B, Figure 12B, and data not shown). It is remarkable, that native ML-1 led to changes in the expression of cell cycle regulating genes, although there was no noticeable effect of native ML-1 on cell growth and cell cycle distribution.

In conclusion, viscumin treatment of LNT-229 and SMA-560 glioma cells induced a reduction in proliferation as well as alterations in cell cycle distribution. Effects of ISCADOR Qu and Aviscumine were comparable, while the effects of native ML-1 were minor.

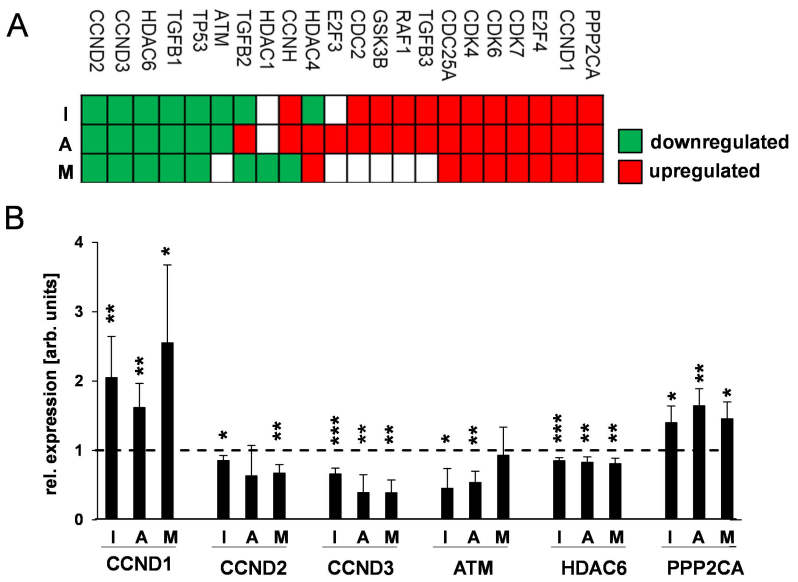

Figure 11: Viscumins caused changes in the expression of cell cycle associated genes. A, Gene expression heat map depicting changes in viscumin treated LNT-229 glioma cells (24 h, 8 ng/ml ML) based on a RT-qPCR microarray analysis (red = upregulated, green = downregulated, white = no change). B, RT-qPCR of assorted genes in viscumin-treated LNT-229 cells. Cells were treated as in A (n=3, mean ± SD, Student's t-test *P < 0.05, **P < 0.01, ***P < 0.001, ISCADOR Qu (I), Aviscumine (A), native ML-1 (M)).

3.3 Influence of viscumins on glioma cell migration

As previously described by our group, ISCADOR Qu provides anti-migratory effects linked to changes in gene expression of motility associated genes [118]. In the present study, effects of ISCADOR Qu, Aviscumine, and native ML-1 were compared and novel viscumin-regulated, motility-associated genes were identified by RT-qPCR based gene expression microarray analysis, followed by RT-qPCR validation. MMP and TGF-β expression and activation status were tested by immunoblot, ELISA, and

zymography. Viscumin-based anti-migratory effects were analyzed using a transwell migration assay (data published in Schötterl et al. Int. J. Oncology 2017 [197]).

3.3.1 Gene expression

In 2012 our group demonstrated that in GBM cells ISCADOR Qu reduced the expression of genes that are mainly upregulated in glioma but induced expression of genes that are often downregulated in glioma [118]. In the present study these analyses were expanded to determine whether Aviscumine or native ML-1 show comparable effects. For this, LNT-229 cells were treated with ISCADOR Qu, Aviscumine, native ML-1, or the cells were left untreated (24 h, 8 ng/ml ML). RNA was isolated and transcribed into cDNA. Using a RT-qPCR based microarray that allows determining the expression of 92 metastasis and motility associated genes, 49 differentially regulated genes were detected. RT-qPCR based validation identified 10/49 genes to be false positive. The remaining 39 genes are depicted in Figure 12A. 19 genes were found to be down- and 20 genes to be upregulated by viscumins. In the ISCADOR Qu group 16 mRNAs were down- and 9 upregulated. In the Aviscumine group 8 mRNAs were down- and 19 up-, and in the native ML-1 group 7 mRNAs were down- and 14 upregulated. Nevertheless, the panel of regulated genes varied between the different treatment groups.

Most of the 19 genes found to be downregulated harbour pro-migratory or pro-invasive properties. Two genes were of pro-tumorigenic nature: HRAS is an oncogene, and VEGFA is involved in angiogenesis. The function of 4 genes regarding their involvement in cancer generation and progression is discussed in the literature (TNFSF10, KISS1R, RBL1, and RBL2). The 20 upregulated genes showed functional diversity: 4 upregulated genes reduce cell migration (BRMS1, FGF2, NME, and SERPINB5), whilst 9 harbour pro-migratory properties (FAT1, IL18, KRAS, LYPD3, MMP1, MMP10, PTGS2, S1004A, and SERPIN1). 4 genes have been described to be either pro- or anti-migratory dependent on the surrounding micro-milieu (HGF, IL1B, MET, and MYC). 3/20 genes were not directly connected to cell motility but provide pro-angiogenic (PECAM1 and VEGFA) or oncogenic function (ERBB2).

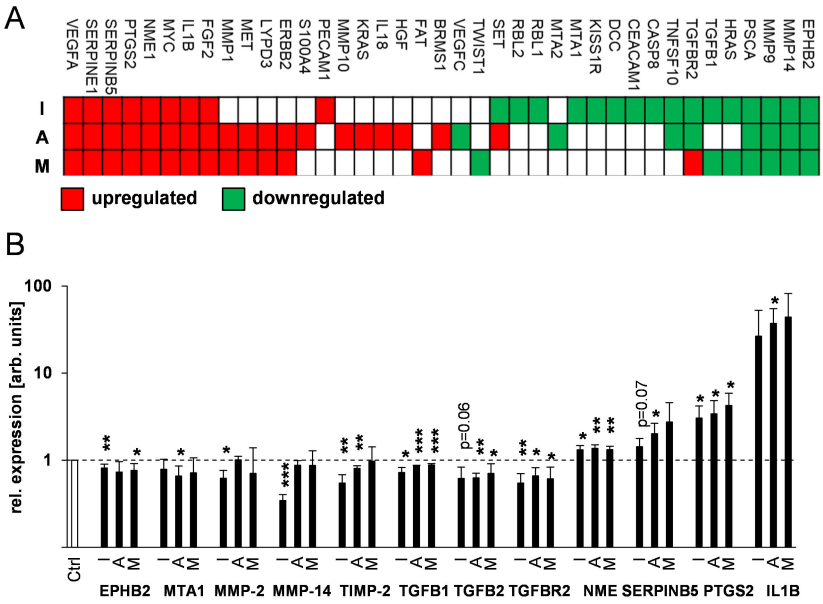

Figure 12: In LNT-229 glioma cells viscumins modulated the expression of motility-regulating genes. A, Gene expression heat map depicting changes in viscumin treated LNT-229 glioma cells (24 h, 8 ng/ml ML) based on a RT-qPCR microarray analysis (red = upregulated, green = downregulated, white = no change). B, RT-qPCR analysis of genes identified in A. Cells were treated as in A (n=3, mean ± SD, Student's t-test *P < 0.05, **P < 0.01, ***P < 0.001; ISCADOR Qu (I), Aviscumine (A), native ML-1 (M)). Modified from Schötterl et al. Int. J. Oncology 2017 [197].

Viscumin-mediated modulation of EPHB2, MTA1, MMP-14, TGFB1, TGFBR2, NME, SERPINB5, PTGS2, and IL1B expression was also validated by RT-qPCR (Figure 12B). By microarray, MTA1 was only found to be downregulated by ISCADOR Qu. Nevertheless, the more sensitive RT-qPCR analysis showed that MTA1 expression was also reduced by Aviscumine and native ML-1. Similar results were generated for TGFB1 and TGBR2. Vice versa, MMP-14 that showed reduced expression in the microarray was only downregulated by ISCADOR Qu. Some differences in gene expression using the RT-qPCR based microarray and RT-qPCR

were also found for MMP-2. Since important regulators of cell migration like TGFB2 and tissue inhibitor of metalloproteinase (TIMP)-2 were not included in the microarray panel, the expression of these genes were also tested by RT-qPCR. TIMP-2 was downregulated by ISCADOR Qu and Aviscumine, whereas TGFB2 was downregulated by all viscumins.

3.3.2 TGF-β

In GBM TGF-β is an essential tumor promoting cytokine that induces the suppression of anti-tumoral immune attacks but also pushes glioma cell migration and invasion [201]. Previously, our group showed that in glioma cells TGF-β expression was reduced by ISCADOR Qu [118]. Here we demonstrate that this is also true for Aviscumine and native ML-1. Downregulation of TGF-β could be abrogated by the addition of a ML-neutralizing antibody (Figure 13A). In addition to TGF-β, also the mRNA levels of the TGF-β receptor 2 (TGFBR2) were reduced upon viscumin treatment (Figure 12B). Viscumin-mediated changes in the expression of TGF-β were also determined for secreted TGF-β protein. These analyses were partially done by Vivien Veninga during her bachelor thesis under my supervision and guidance. Not only TGF-β mRNA but also the level of secreted TGF-β protein was reduced by viscumins, an effect that was also abrogated by the addition of a ML-neutralizing antibody (Figure 13B).

SMAD2 is an important intracellular TGF-β signal transducer. No viscumin-modulating effects on SMAD2 mRNA expression had been found by the RT-qPCR based analyses. Nevertheless, SMAD2 protein was reduced after viscumin treatment, but again, this effect was abrogated by the addition of the ML antibody (Figure 13C, D). Summing up, the study demonstrated that TGF-β expression, the expression of genes and proteins involved in TGF-β signalling like TGFBR2 or SMAD2, and TGF-β-regulated genes were negatively regulated by viscumins.

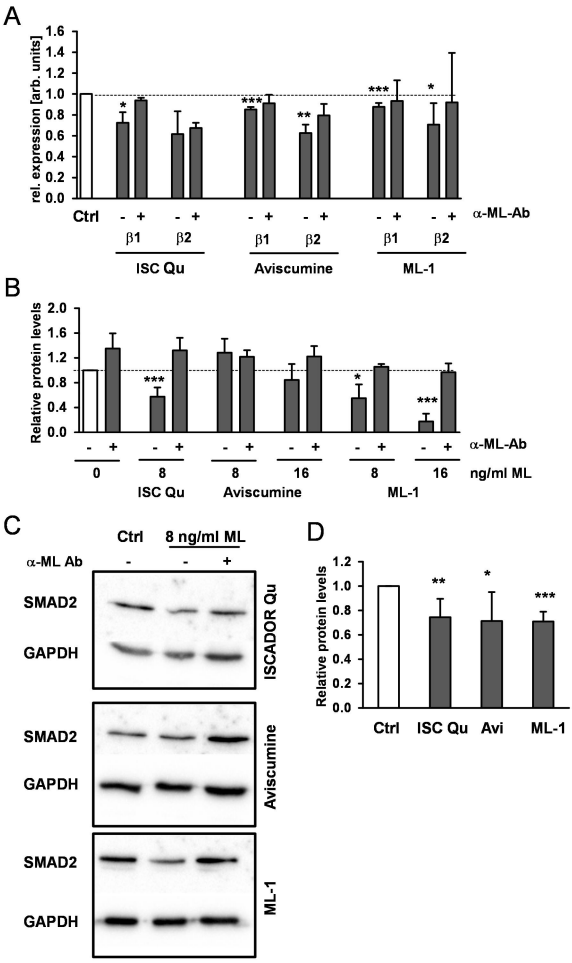

Figure 13: Viscumins modulated the expression of TGF-β and SMAD2. A, RT-qPCR analysis of LNT-229 cells treated with viscumins (8 ng/ml ML, 24 h) in the absence or presence of a ML-neutralizing antibody (4.8 µg/ml). B, TGF-β 1 was quantified in medium of viscumin treated LNT-229 cells by ELISA. Parts of the ELISA analyses were performed by Vivien Veninga during her bachelor thesis under my supervision and guidance. C, Representative western blots showing SMAD2 expression in viscumin treated LNT-229 cells. GAPDH was used as loading control. Cells were treated as in A. D, Quantification of SMAD2 protein levels relative to GAPDH (A/B/D, *n*=3, mean ± SD, Student's t-test *P < 0.05, **P < 0.01, ***P < 0.001). Modified from Schötterl et al. Int. J. Oncology 2017 [197].

3.3.3 Matrix metalloproteinases

Matrix metalloproteinases (MMPs) are responsible for the degradation of the extracellular matrix (ECM), one important process that finally facilitates the invasion of GBM cells into the healthy brain. It is known for long that in glioma TGF-β influences the expression and activity of MMPs and also of MMP inhibitors or activators [30, 202]. Our group has shown that ISCADOR Qu reduced the expression of MMPs [118]. The present study broadens these analyses to evaluate if Aviscumine and native ML-1 provide similar effects. Using the RT-qPCR based microarray, we found MMP-9 and -14 to be downregulated by all three viscumin-based drugs, whilst MMP-1 and -10 were upregulated by Aviscumine, and MMP-1 was upregulated by native ML-1 (Figure 12A). Further RT-qPCR analyses revealed that MMP-2 and -14 were significantly downregulated by ISCADOR Qu, whilst the expression of TIMP-2 was downregulated by ISCADOR Qu and Aviscumine (Figure 12B).

Interestingly, viscumin-mediated differences in MMP-2, MMP-14, and TIMP-2 mRNA did not directly reflect to protein levels. On the protein level a more general downregulation of MMP-2, MMP-14, and TIMP-2 was detectable. ISCADOR Qu (8 ng/ml ML) or native ML-1 (16 ng/ml), reduced MMP-2 and TIMP-2 protein levels, whilst these effects were lesser for Aviscumine (8 ng/ml). The viscumin-mediated downregulation to the above mentioned proteins was abrogated by the addition of a ML-neutralizing antibody (Figure 14A).

Measuring MMP-2 activity by gelatinase-based zymography showed that only ISCADOR Qu but not Aviscumine or native ML-1 reduced both MMP-2 and -9 activities (Figure 14C) suggesting that viscumins mainly influence the expression but not the activation of MMPs and that additional compounds, which are present in MEs like ISCADOR Qu, might be necessary to mitigate MMP activity.

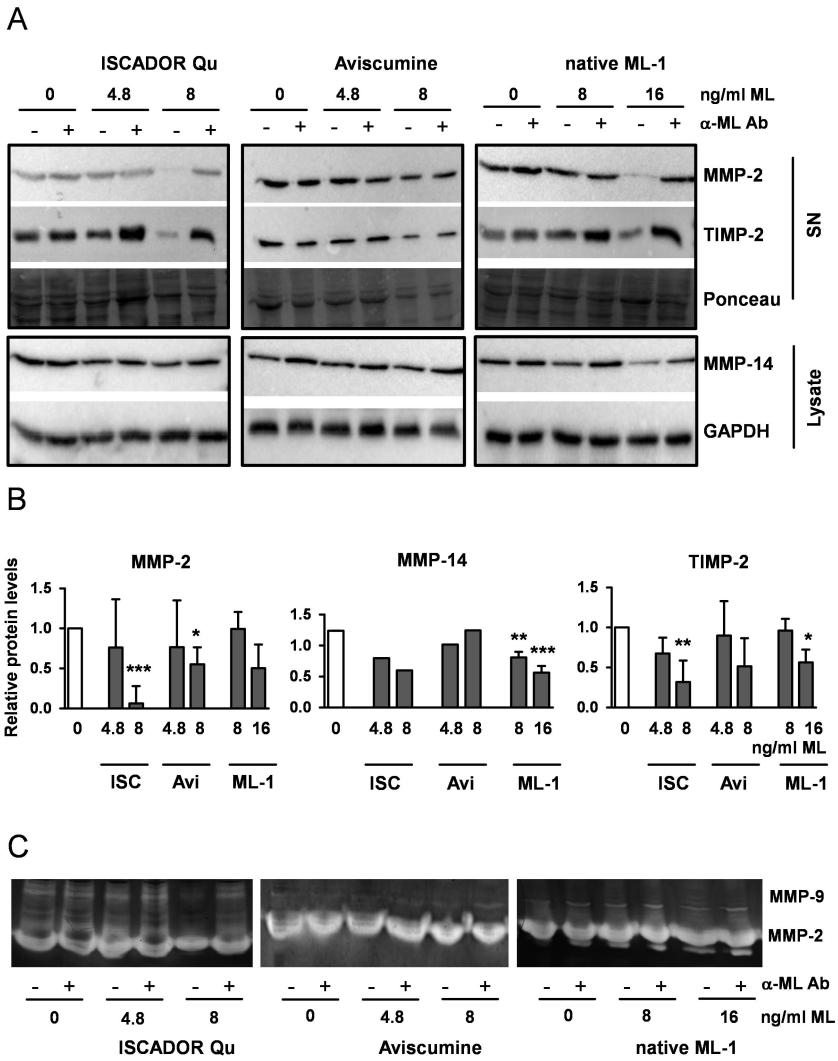

Figure 14: In LNT-229 cells viscumins modulated the expression of MMPs and TIMP-2. A, LNT-229 cells were treated with viscumins (24 h) in the presence or absence of a ML-neutralizing antibody. MMP expression was analyzed in supernatants (SN) or lysates as indicated. B, Quantification of MMP-2 and TIMP-2 protein. C, LNT-229 cells were treated as in A. MMP activity was analyzed in supernatants by zymography (n=3, mean ± SD, Student's t-test *P < 0.05, **P < 0.01, ***P < 0.001). Modified from Schötterl et al. Int. J. Oncology 2017 [197].

3.3.4 Cell motility

As shown above, treatment of LNT-229 cells with viscumins led to changes in the expression of motility associated genes. Our group has shown that cell migration was reduced in ISCADOR Qu treated glioma cells [118]. The present study enlarges these analyses to determine whether Aviscumine or native ML-1 provide similar anti-migratory capacity. Indeed, all viscumin-based drugs reduced the migration of both human LNT-229 and murine SMA-560 glioma cells (Figure 15).

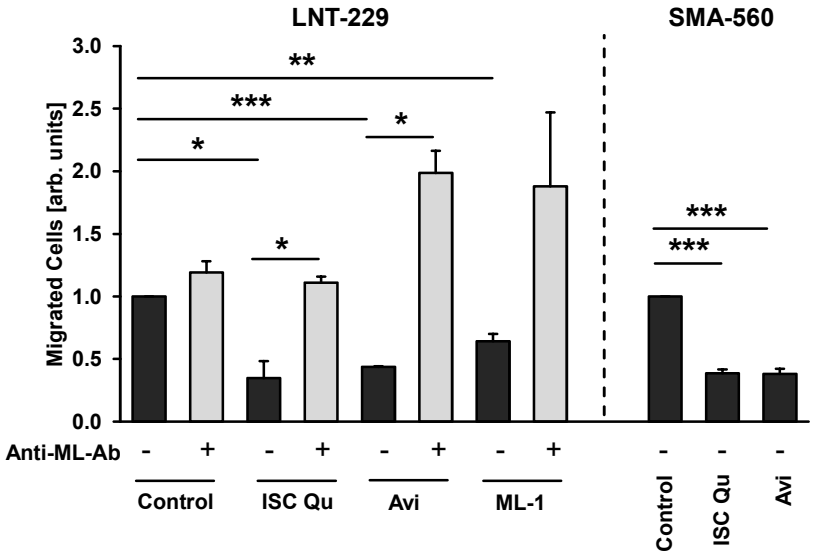

Figure 15: Viscumins reduced glioma cell migration. The cells were treated with ISCADOR Qu, Aviscumine, or native ML-1 (24 h, 8 ng/ml of each ML, except SMA-560 cells: 0.8 ng/ml Aviscumine) or were left untreated in the absence or presence of a ML-neutralizing antibody. For migration $2x10^4$ cells were seeded in transwell chambers. After 24 h migrated cells were counted. Values were normalized to proliferation controls to avoid effects resulting from viscumin-based changes in proliferation (n=3, mean ± SD, Student's t-test *P < 0.05, **P < 0.01, ***P < 0.001). Modified from Schötterl et al. Int. J. Oncology 2017 [197].

3.4 Immune-modulating effects of viscumins

It is known for decades that viscumins are able to stimulate cells of both the adaptive (e.g. T cells) and the innate (e.g. NK cells) immune system [138, 143, 149, 203-205]. One mode how viscumins act is by induction of pro-inflammatory interleukins and interferon-γ [130, 206, 207]. Additionally, in glioma cells viscumins reduce the secretion of TGF-β (see chapter 3.3). Nevertheless, the mechanisms how viscumins lead to a stimulation of immune cells, and how they might help to induce an anti-tumor cell response have not been elucidated in detail. In the present study effects of ISCADOR Qu, Aviscumine, and native ML-1 on the NK and T cell mediated killing of glioma cells were analyzed.

3.4.1 Viscumins enhance the NK cells mediated lysis of LNT-229 glioma cells

Our group demonstrated in a former study that viscumin-rich ISCADOR Qu but not viscumin-poor ISCADOR P enhanced the NK cell mediated cell killing of LNT-229 cells [118]. In the current study we additionally analyzed the effects of Aviscumine and native ML-1 in NK cells from three different healthy human donors. LNT-229 Luc cells were treated with ISCADOR Qu, Aviscumine, native ML-1 (24 h, 8 ng/ml ML), with ISCADOR P (24 h, 1 mg/ml ME), or were left untreated. After intense washing to remove residual viscumins, NK cells were added at increasing effector to target ratios for 4 h. Luciferase activity was measured to determine NK cell mediated glioma cell lysis. As shown in Figure 16A/B, both ISCADOR Qu and Aviscumine enhanced the NK cell mediated lysis of glioma cells, whilst ISCADOR P and native ML-1 did not (n=1, data not shown).

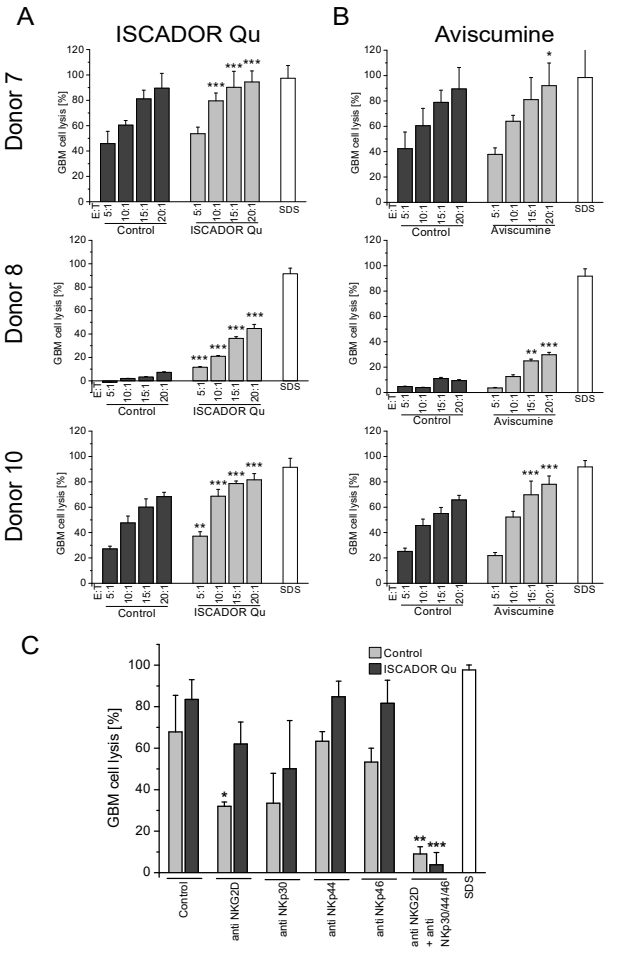

Figure 16: Viscumins enhanced the NK cell mediated glioma cell killing. A/B, LNT-229-Luc cells were treated ISCADOR Qu (A), Aviscumine (B), or were left untreated (24 h, 8 ng/ml ML). NK cells were added at increasing effector (E) to target (T) ratios and luciferase activity was measured. Experiments were carried out in 6 replicates. C, LNT-229 Luc cells were treated as in A, but prior to the addition of NK cells at a ratio of E/T = 20:1, NK cells were incubated with neutralizing antibodies for either NKG2D, NKp30, NKp40, NKp46, or all (each 10 µg/ml, 30 min, *n*=3, mean ± SD, Student's t-test *P < 0.05, **P < 0.01, ***P < 0.001). Modified from Schötterl et al., KVC, 2016 [208].

To identify if viscumins were bound on target cells and compete for the binding of NK cells to the target cell by specific NK cell surface molecules, the function of the activating NK cell receptors NKp30, NKp44, NKp46, and NKG2D on NK cells was blocked by addition of neutralizing antibodies prior to co-cultivation of NK and target cells. Neutralizing NKp30, NKp44, NKp46, or NKG2D resulted in a reduction of target cell lysis but did not influence the viscumin-mediated enhancement of glioma cell lysis. The blockade of all NK cell surface binding proteins, by this inhibiting the binding of NK cells to their targets, abrogated the NK cell mediated lysis of both, viscumin-treated and untreated target cells (Figure 16C). Data shown in this chapter are partially published (Schötterl et al., KVC, 2016 [208]).

3.4.2 Viscumins enhance the T cell mediated lysis of LNT-229 glioma cells

It has been described in the literature that viscumins influence the activity and motility of T cells [142, 149, 209]. Therefore, we analyzed whether viscumins are able to enhance the T cell mediated killing of glioma cells. For this we chose an allogenic approach. T cells from PBMCs of three healthy human donors (D15, 17, 18) were expanded in the presence of irradiated human LNT-229 cells as described in the methods part. T cells were purified from co-cultures using a T cell isolation kit. Purity and activity were determined by flow cytometry (FACS) using anti-human CD3, CD4, CD8, CD69, and CD56 antibodies. On average > 95% of cells were $CD3^+$, and in this population > 50% of cells were $CD69^+$. There was a slight but significant enhancement of glioma cell lysis if target LNT-229 cells were pre-treated with viscumins prior to the addition of T cells (Figure 17, 1st to 6th bar of each graph). Nonetheless, the increase of glioma cell lysis was variable and dependent on the T cell donor as well as on the viscumin preparation.

To determine whether viscumin treatment of glioma cells enhances the expansion of naïve T cells, LNT-229 cells used for co-cultures during the T cell expansion period were pre-treated with ISCADOR Qu, Aviscumine, or native ML-1 (8 ng/ml ML, 24 h) prior to co-cultures. Residual non-bound viscumins were removed by intensive

washing steps prior to the addition of PBMCs. T cells generated by this approach showed enhanced glioma cell lytic activity compared to T cells generated by co-culturing PBMCs with non-treated glioma cells (Figure 17, 7^{th} to 12^{th} bar of each graph). Even glioma cells which have never been treated with viscumins were killed more efficiently. In this approach, native ML-1 showed only minor effects and only in T cells of one donor. Aviscumine showed enhancing activity in 2/3 T cell donors and ISCADOR Qu in T cells of all donors tested so far.

To determine direct effects of viscumins on immune cells, PBMCs were cultured for 24 h and 48 h in the presence or absence of increasing concentrations of ISCADOR Qu, Aviscumine, or native ML-1. Viscumins induced cell death in PBMCs (IC_{50} 24 h: 26.45 ng/ml ML ISCADOR Qu, 171.35 ng/ml Aviscumine, 144.22 ng/ml native ML-1; IC_{50} 48 h: 6.50 ng/ml ML ISCADOR Qu, 18.81 ng/ml Aviscumine, 23.74 ng/ml native ML-1) demonstrating that PBMCs, compared to glioma cells, were highly vulnerable towards viscumin treatment (Table 1, Figure 18A).

Additionally, we analyzed effects of viscumins on T cell viability and activity using flow cytometry-based detection of cell death (PI and annexin V) and of activation surface proteins like CD69, CD25, and HLA-DR. For this, expanded T cells were cultivated in the absence or presence of ISCADOR Qu or Aviscumine (0-8 ng/ml ML, 24 h or 48 h). In accordance to the data observed for PBMCs, also T cell viability was reduced by both ISCADOR Qu and Aviscumine (Figure 18D, E). Although CD69 expression was not modulated by viscumins (data not shown), CD25 and HLA-DR surface expression was significantly reduced after 48 h of viscumin treatment (Figure 18B, C) indicating that viscumins, even if used in concentrations that do not influence glioma cells, mitigate immune cell activity. The viscumin-mediated downregulation of immune cell activation markers on expanded T cells was paralleled by the reduction of their lytic activity on glioma cells (Figure 18F, G).

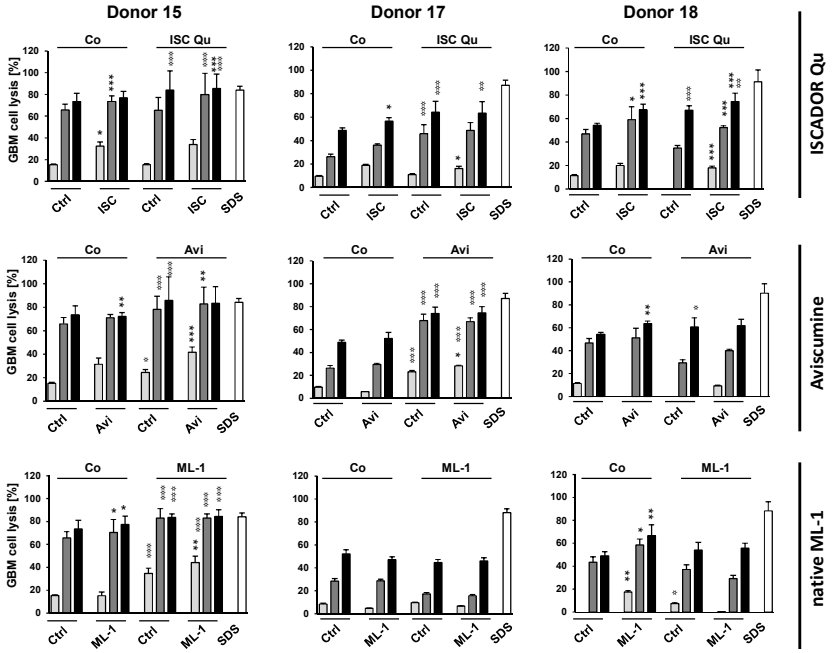

Figure 17: T cell mediated killing of glioma cells was enhanced by viscumins. Results for three individual donors (D15, 17, 18) are depicted. PBMCs were co-cultured with untreated (Co, label on top of bars) or ISCADOR Qu (ISC Qu), Aviscumine (Avi), or native ML-1 (ML-1) pretreated LNT-229 glioma cells for 3-5 weeks to achieve allogenic T cell activation. Activated T cells were added in different effector to target (E:T) ratios (as indicated by light grey 5:1, dark grey 10:1 and black color 20:1, respectively) to untreated (Ctrl, x-axis) or viscumin-treated (ISC, Avi, ML-1; 8 ng/ml ML; x-axis) LNT-229 Luc cells for 4 h. Luciferase activity was measured and used to calculate the amount of glioma cell lysis. (Mean ± SD of 6-8 replicates; Student's t-test compared to the Ctrl (*) or the Co (°) */°P < 0.05, **/°°P < 0.01, ***/°°°P < 0.001).

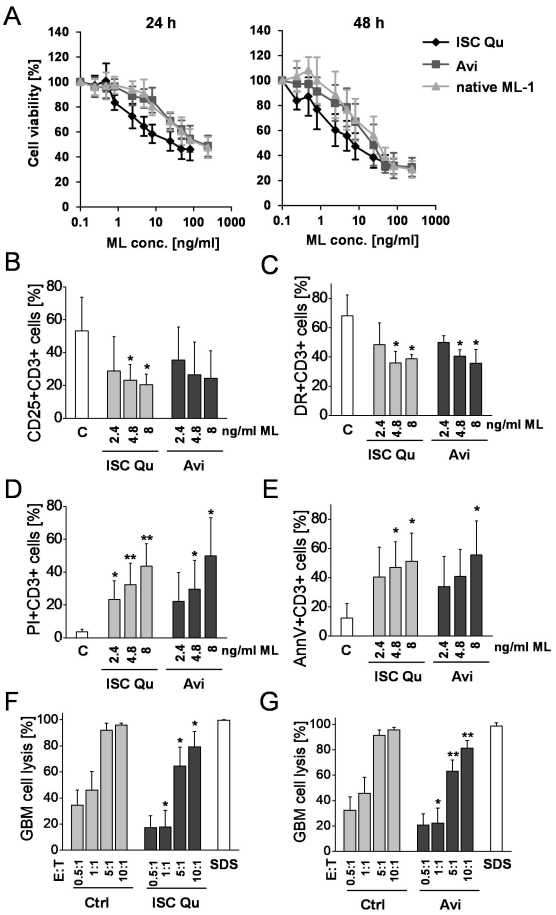

Figure 18: Viscumins induced cell death in PBMCs and reduced T cell lytic activity. A, PBMC viability measured by MTT. PBMCs were treated with increasing concentrations of ISCADOR Qu (ISC Qu), Aviscumine (Avi), or native ML-1 (24 or 48 h). B-E. Flow cytometric analysis of T cells treated for 48 h with increasing concentrations of ISCADOR Qu (ISC Qu) or Aviscumine (Avi). CD25 (B) and HLA-DR (C) surface expression, PI (D) and Annexin V (E) staining. F-G. LNT-229 lysis assay. T cells were left untreated (Ctrl) or were treated with ISCADOR Qu (F) or Aviscumine (G) (2.4 ng/ml ML, 24 h). Afterwards, these cells were co-cultured for 4 h at different effector to target (E:T) ratios with LNT-229 Luc cells. The remaining luciferase activity was measured and used to calculate the amount of glioma cell lysis. (n=3; mean ± SD; Student's t-test compared to control *P < 0.05, **P < 0.01, ***P < 0.001)

3.4.3 Viscumin mediated changes of immune response associated gene expression

To identify the underlying mechanisms how viscumins might induce the immune cell mediated killing of glioma cells, LNT-229 glioma cells were treated with ISCADOR Qu, Aviscumine, or native ML-1 (24 h, 8 ng/ml ML), and viscumin-based changes in the expression of immune response related genes were analyzed using a RT-qPCR based microarray that allows the detection of 92 genes, followed by RT-qPCR validation.

After removal of targets that are not expressed in glioma, 42 differentially regulated genes were identified by the use of the microarray (Figure 19A). ISCADOR Qu treatment of LNT-229 cells downregulated 15 and upregulated 21 mRNAs. Aviscumine downregulated 4 and upregulated 24 mRNAs, whilst native ML-1 downregulated 15 and upregulated 18 mRNAs. In total, 23 mRNAs were upregulated, 15 were downregulated, and 4 were either up- or downregulated dependent on the used viscumin. 17/23 genes are known to provide pro-inflammatory functions (IL1A, IL1B, IL6, IL8, IL12A, IL15, IKBKB, CCL2, CSF1, CSF2, CSF3, CD86, PTGS2, TNF, SELE, C3, VEGFA), 3 are described to be anti-inflammatory (IL10, LIF, SMAD3), 2 are known to be anti-apoptotic (BCL2, BCL2L1), and 1 is described to provide pro-apoptotic features (FAS). The 4 either up- or downregulated genes are pro-inflammatory (NFKB2, ICAM1, EDN1, LY96). In the panel of downregulated mRNAs, 13 mRNAs are described to provide pro-inflammatory activity (STAT3, HLADR, NOS2, SKI, LRP2, SMAD7, FN1, LTA, NFATC3, NFATC4, CXCL11, ACE, CD34), whereas 2 mRNAs are known to hold anti-inflammatory capacity (TGFB1, HMOX1).

The expression of 8 differentially expressed genes identified by microarray analysis was further determined by RT-qPCR. By this the microarray data were validated (Figure 19B). These data demonstrated that treatment of LNT-229 cells with viscumins enhanced the expression of many pro-inflammatory genes and might explain the enhanced immune cell mediated killing of glioma cells after viscumin treatment. Additionally, this more “pro-inflammatory phenotype” of glioma cells might support immune cell attraction to the tumor and might boost an anti-tumor immune response.

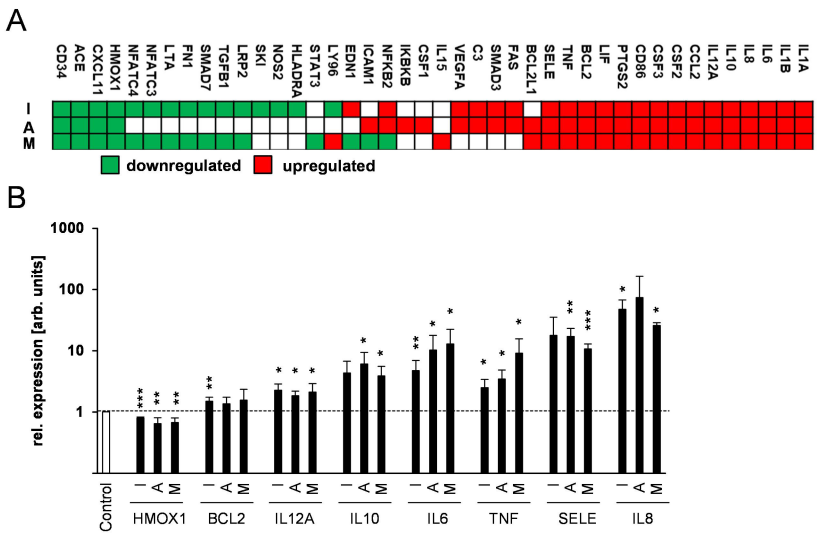

Figure 19: Viscumins modulated the expression of inflammation associated genes. A, Gene expression heat map depicting changes in viscumin treated LNT-229 glioma cells (24 h, 8 ng/ml ML) based on a RT-qPCR microarray analysis (red = upregulated, green = downregulated, white = no change). B, RT-qPCR analysis of genes identified in A. Cells were treated as in A (n=3; mean ± SD; Student's t-test compared to control *P < 0.05, **P < 0.01, ***P < 0.001, ISCADOR Qu (I), Aviscumine (A), native ML-1 (M)).

3.5 Viscumins as adjuvant cancer therapeutics *in vitro*

Viscumins are generally used as adjuvant cancer therapeutics in the clinic, which are administered in parallel to standard cancer treatment (tumor irradiation and TMZ-based chemotherapy). In our study we were interested whether viscumins might support the effects of standard glioma therapy or might even synergize with tumor irradiation and/or chemotherapy.

In a first approach we measured clonogenic survival of human (LNT-229, LN-308) and murine (SMA-560) glioma cells as described in the methods part. For this human GBM cells were treated with viscumins in combination with TMZ as indicated in

Figure 20. Concentrations for single treatments were adapted to every cell line in a way that single treatments never reached a therapeutic effect of > 40% of clonogenic survival reduction. After 24 h, specific treatment groups were additionally irradiated. The medium was changed to remove residual viscumins and TMZ. Since SMA-560 cells do not form colonies, a similar approach was used, but cells were seeded in microtiter plates and the assay was stopped if control groups have grown to confluency. Additive effects of the three single treatments were calculated using the Webb method [210]. Therapeutic effects were defined to be synergistic if values determined for triple treatment were lower than calculated additive effects.

In LNT-229 cells adjuvant viscumin therapy yields synergistic effects for ISCADOR Qu and Aviscumine and an additive effect for native ML-1 (Figure 20A). In LN-308 cells adjuvant viscumin treatment showed additive effects (Figure 20B), and in SMA-560 cells adjuvant viscumin treatment showed synergy (Figure 20C). In total, adjuvant viscumin therapy in parallel to irradiation and TMZ showed additive to synergistic effects regarding clonogenic survival in all tested glioma cell lines. These supporting effects seemed to be independent on the cell susceptibility towards viscumins, TMZ, or irradiation.

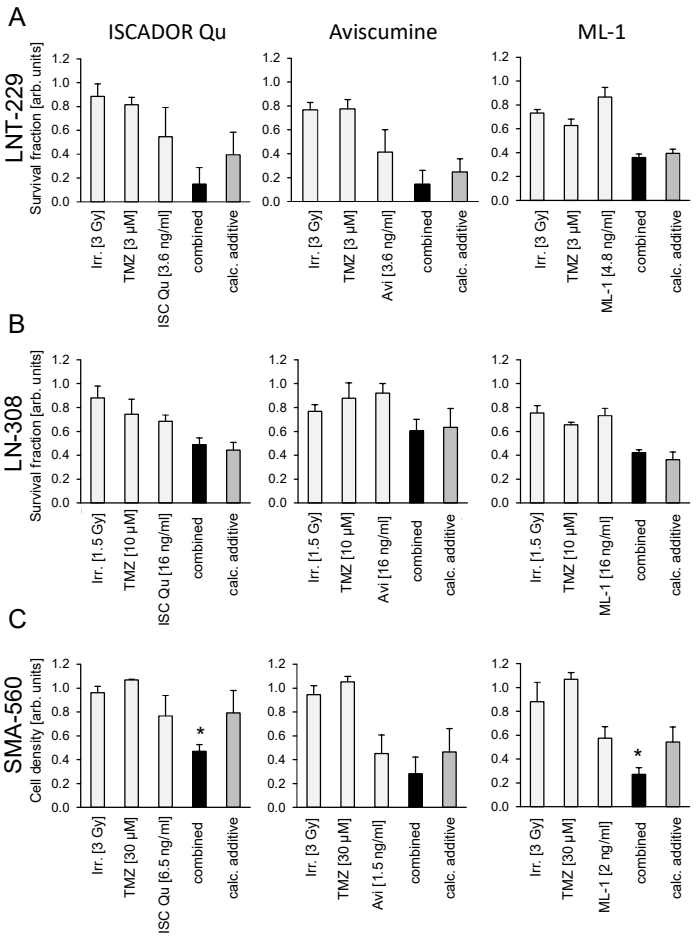

Figure 20: Additive and synergistic effects of viscumins regarding clonogenic survival of glioma cells. LNT-229 (A), LN-308 (B), and SMA-560 (C) cells were exposed to irradiation, TMZ, or viscumin (light grey bars) or were exposed to radio-chemotherapy in combination with ISCADOR Qu (ISC Qu), Aviscumine (Avi), or native ML-1 (combined, black bars). Dark grey bars indicate the predicted effect of combined treatment calculated using the Webb method [211]. The following conditions were chosen: LNT-229: 3 Gy, 3 µM TMZ, 3.6 ng/ml ML ISCADOR Qu or Aviscumine, 4.8 ng/ml native ML-1; LN-308: 1.5 Gy, 10 µM TMZ, 16 ng/ml of each viscumin; SMA-560: 3 Gy, 30 µM TMZ, 6.5 ng/ml ML ISCADOR Qu, 1.5 ng/ml Aviscumine or 2 ng/ml native ML-1. (n=3, mean ± SD, Student's t-test *P < 0.05, **P < 0.01, ***P < 0.001).

3.6 Viscumins as adjuvant cancer therapeutics *in vivo*

The promising *in vitro* data we observed using adjuvant viscumin treatment of glioma cells prompted us to test whether this is also true *in vivo*. We used two different mouse GBM-models: Rj:NMRI-Foxn1^{nu}/Foxn1^{nu} (NMRI) mice bearing orthotopically growing human LNT-229 tumors provide a model that allows to analyze direct effects of viscumins on tumor growth, but it has the disadvantage that determination of anti-tumoral immune responses are not possible in these immunocompromised mice. To determine putative viscumin-mediated immune-stimulating effects, we used an immunocompetent syngeneic mouse glioma model (SMA-560 cells orthotopically growing in VM/Dk mice). In a preliminary dose-escalation study executed in collaboration with the group of M. Mittelbronn (Neurological Institute, Edinger Institute, Frankfurt/Main), we determined the highest well tolerated doses of ISCADOR Qu and Aviscumine when injected in brains of NMRI mice and found them to be approximately > 0.7 ng of ML. We did not use native ML-1 in these experiments since *in vitro* native ML-1 showed only minor therapeutic immune-stimulatory effects compared to ISCADOR Qu and Aviscumine. In a first experiment using the LNT-229-NMRI nude mouse model, we performed single or double treatments. Single treatment mice received a single intra-tumoral injection of Aviscumine or ISACDOR (0.7 ng of ML) nine days after tumor implantation, or received TMZ (2.5 mg/kg i.p.) at day 9, 16, and 23. Double treatment mice received viscumins and TMZ. Survival was determined by the preparation of Kaplan-Meyer survival curves.

Only TMZ showed a significant benefit in the median survival compared to the control treatment. Aviscumine single treatment mice showed a trend towards prolonged survival, whereas animals of the ISCADOR Qu treatment group lived even shorter than control animals (Figure 21 and Table 3). Post mortem, mouse brains were pathologically examined by our collaborator Naita M. Wirsik (Group Mittelbronn, Neurological Institute, Edinger Institute, Frankfurt/Main). All tumors showed necrosis (data not shown), but the differences in proliferation, invasion, and apoptosis rate of control and treatment groups were variable and differences were negligible in total (Figure 21C).

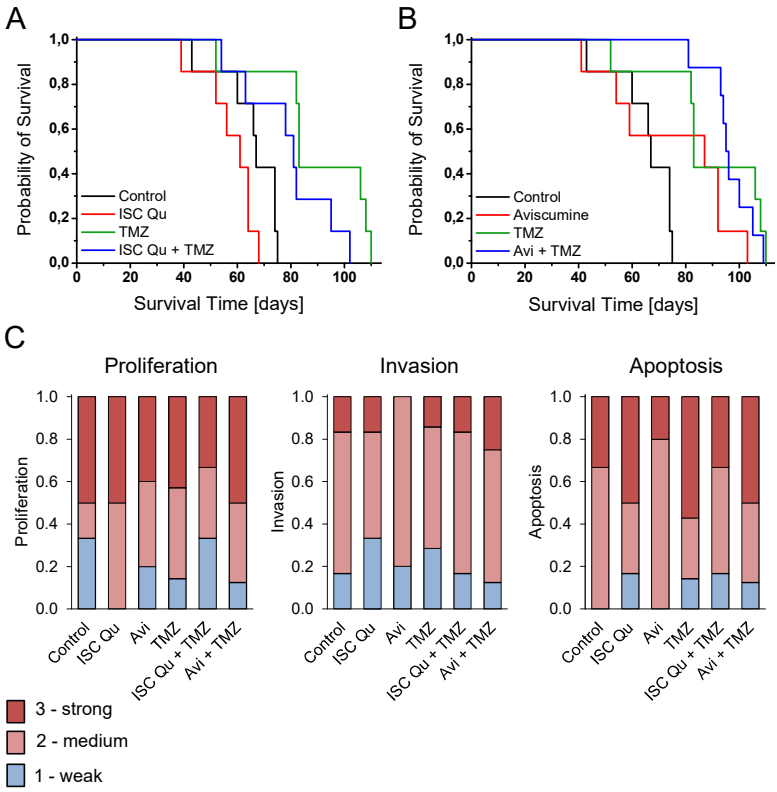

Figure 21: Combinational treatment of LNT-229 tumors with viscumins and TMZ (Kaplan Meyer survival curves). A, Mice were intratumorally injected with either PBS or ISCADOR Qu (ISC Qu, 0.7 ng ML in total) at day 9 after tumor cell implantation. At day 7, 14, and 21 mice received i.p injections with PBS or TMZ (2.5 mg/kg). B, Mice were treated as in A, but Aviscumine (Avi, 0.7 ng) was used instead of ISCDOR Qu (*n*=7-8). C, Post mortem pathological evaluation of proliferation (left), tumor cell invasion (middle), and apoptosis (right) performed by our collaborator Naita M. Wirsik (Group Mittelbronn, Neurological Institute, Edinger Institute, Frankfurt/Main).

Table 3: Combination treatment of LNT-229 tumors with viscumins and TMZ (median survival). Mice were treated as indicated in Figure 21 and median survival was determined.

Group	Control	ISC Qu	Avi	TMZ	ISC Qu + TMZ	Avi + TMZ
Median survival (days)	67	61	87	83	81	95.5
p-value log-rank (Ctrl)	-	0.06	0.15	0.0034	0.02	0.0001
p-value log-rank (TMZ)	-	-	-	-	0.0788	0.7209

The observation that there were only minor effects of double treatment using viscumins and TMZ prompted us to perform an adjuvant viscumin treatment study, meaning that viscumins were used in combination with standard glioma radio-chemotherapy using the LNT-229 NMRI mouse glioma model and intra-tumoral viscumin injections. Due to the shortened survival of intratumorally ISCADOR Qu treated glioma mice we observed in our former experiment we skipped ISCADOR Qu in this experiment. Ten days after LNT-229 cell implantation, NMRI mice received an intra-tumoral injection of Aviscumine (0.7 ng) as well as a first injection (i.p.) of TMZ (1.5 mg/kg). The TMZ concentration was further reduced due to the fact that LNT-229 cells are highly TMZ-sensitive [212] and due to its strong pro-survival effect in the previous experiment. The next day (day 11 post tumor cell implantation), some treatment groups additionally received a focal tumor irradiation of 3 Gy. The TMZ treatment was repeated at day 18 and 25 (Figure 22A).

Aviscumine led to a trend for prolonged survival compared to the control group (Aviscumine 62 d, control 46.5 d, p=0.0803) as already shown in the first experiment

but was even more effective than irradiation alone (Aviscumine 62 d, irradiation 57 d, p=0.1222). Also the lower TMZ concentration led to a strong survival benefit. Nevertheless, even if not significant, Aviscumine, if used in combination with irradiation and TMZ, further prolonged the median survival of glioma-bearing mice (TMZ + irradiation 84 d, Aviscumine + TMZ + irradiation 90.5 d, p=0.1704, Figure 22 B/C).

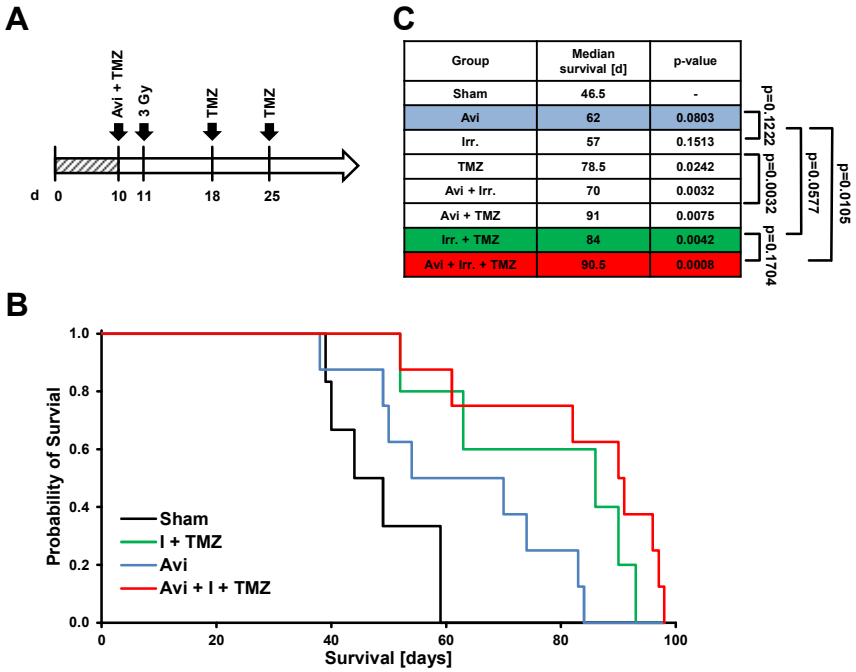

Figure 22: Adjuvant Aviscumine treatment of LNT-229 glioma bearing NMRI mice. A, Treatment pattern. B, Kaplan Mayer survival curves. Mice were intratumorally sham-injected with PBS or with Aviscumine (Avi, 0.7 ng) at day 10. Focal tumor irradiation (3 Gy) was performed 24 h later followed by weekly intraperitoneal TMZ injections (1.5 mg/kg) for three weeks. C, Median survival (*n*=6-8 animals, p-values, Log-rank test).

To analyze putative anti-tumoral effects of viscumins that might be associated to its immune-stimulatory properties we used the immunocompetent SMA-560 VM/Dk

mouse model. Since ISACDOR Qu showed the best immune-stimulatory effects of all viscumins tested so far (chapter 3.4), subcutaneous repeating ISCADOR Qu injection at increasing concentration analogous to the human clinical treatment pattern were used. Some treatment groups received focal tumor irradiation (3 Gy and/or weekly TMZ i.p. injections, 2.5 mg/kg). The detailed treatment scheme is depicted in Figure 23A. Combined radio-chemotherapy showed nearly equal effects on survival as ISCADOR Qu monotherapy did. Adjuvant viscumin treatment further and significantly prolonged the survival of glioma bearing mice. Kaplan Meyer survival curves and median survival times are shown in Figure 23B/C.

To determine immune-stimulating effects of an ISCADOR Qu treatment, healthy VM/Dk mice were treated with ISCADOR Qu the same mode that was used to treat glioma mice (Figure 23A). After finishing the treatment, cytokine levels were determined in the serum of mice as described in the methods part. 10/40 cytokines that can be detected by this approach were found to be upregulated (IL-6, BLC, TIMP1, CCL24, CXCL9, CCL25, CXCL5, MIP-1α, CX3CL1, and CSF3) and only one showed a reduced serum level (Leptin) (Figure 23D). All upregulated cytokines provide pro-inflammatory functions indicating that the superior effect of ISCADOR Qu might result from an immune-stimulatory effect that works in combination to the additional anti-tumoral effects of viscumins.

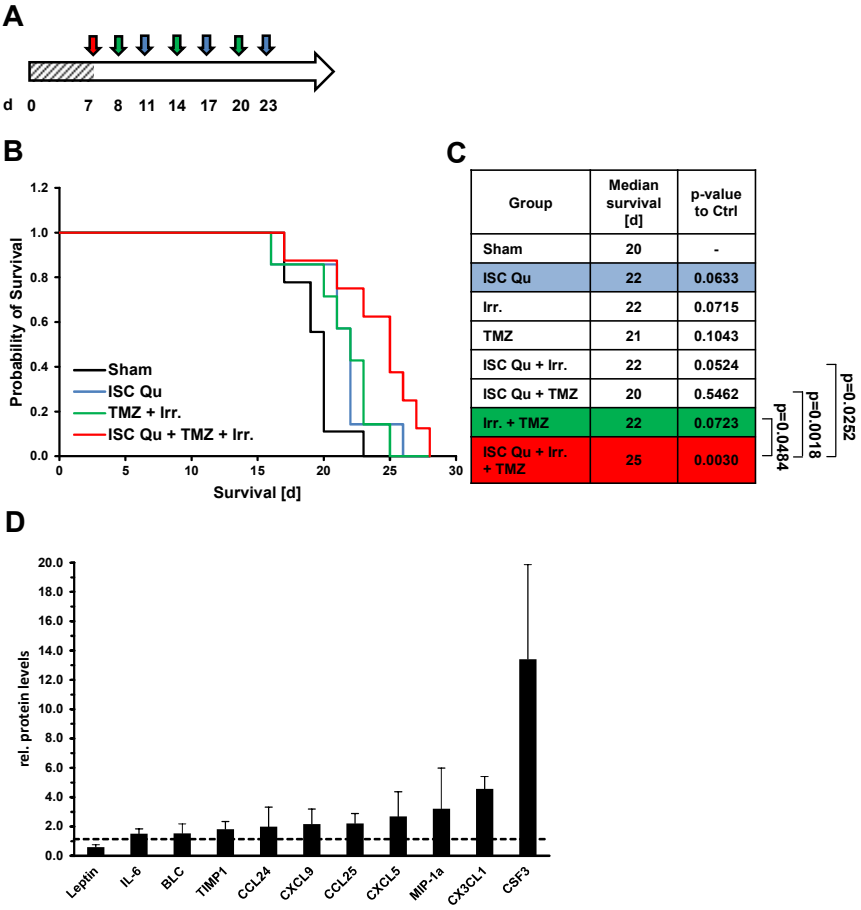

Figure 23: Adjuvant ISCADOR Qu therapy prolonged the survival of SMA-560 glioma bearing VM/Dk mice. A, Treatment pattern: Irradiation (red arrow), ISCADOR Qu (blue arrow), ISCADOR Qu + TMZ (green arrow). B, Kaplan Mayer survival curves of the sham, ISCADOR Qu, TMZ + irradiation and combined treatment groups. C, Median survival of treatment groups (*n*=7-8 animals; p-values, Log-rank test). D, Differential expression of cytokines in the serum of VM/Dk mice injected with ISCADOR Qu or PBS (*n*=4 animals; mean ± SD).

4. Discussion

The aim of this thesis encompassed the evaluation of effects of viscumin-based drugs as adjuvant therapeutics in the treatment of experimental GBM and to identify the putative mechanisms the anti-tumoral effects of these agents rely on.

4.1 Cytotoxicity of viscumins in tumor and non-neoplastic cells correlates to the expression of the ML receptor CD75s

The fact that viscumins induce cell death has been shown by several groups and for different cancer entities like leukemia, breast cancer, colon cancer, melanoma, and hepatocarcinoma. In a previous study our group has shown that viscumin-rich *Viscum album* L extracts (ISCADOR Qu, ISCADOR M) induced cell death in glioma cells, whereas a viscumin-poor extract (ISCADOR P) did not [110-116, 118]. To determine cancer cell specific cytotoxic effects, several GBM but also non-neoplastic either primary or immortalized cell lines as well as human and mouse brain organotypic cultures were treated with ISCADOR Qu, ISCADOR P, Aviscumine, or native ML-1. Additionally, we performed a dose escalation study in healthy NMRI mice to determine the highest well-tolerated dose of ISCADOR Qu and Aviscumine. In the panel of GBM cell lines, the sensitivity towards viscumin-induced cell death and growth inhibition varied. Two cell lines (LN-308, U87MG) were highly resistant, whilst others were more sensitive (LNT-229, MZ-18). Nevertheless, *in vitro* most tumor cell lines showed higher resistance towards viscumin induced cell death than non-neoplastic cells (Table 1). These results are in accordance with published data that demonstrated that high viscumin concentrations induce cell death also in immune and endothelial cells [120, 123, 131, 147]. Nonetheless, the results collected from *in vitro* experiments did not reflect to the data we observed *in situ* or even *in vivo* since in organotypic mouse brain cultures only very high concentrations of ISCADOR Qu, but not Aviscumine, nor native ML-1, induced cell death (Figure 4). Similar results were collected from mice that received intracerebral viscumin injections. We hypothesized

that different vulnerabilities towards viscumin induced cell death or different cytotoxicity levels of ISCADOR Qu, Aviscumine, or native ML-1 might be due to the different uptake of these drugs. This is not the case since all drugs were equally taken up by glioma cells (Figure 5). We further analysed whether the different vulnerability of cancer and non-transformed cells was an effect of expression of the viscumin receptor CD75s on target cells. Indeed, we found CD75s to be expressed on all GBM cell lines tested so far. The level of CD75s surface expression correlated well with the cell lines susceptibility towards viscumin induced cell death (Figure 6). In tissue samples we found CD75s to be expressed in 6/7 GBM specimen but not in the surrounding non-neoplastic tissue nor in healthy human or mouse brains (Table 2, Figure 6). This and the short half-life of ML-1 (< 15 min; [169]) might explain the insensitiveness of mouse brain tissue towards the viscumin-mediated cytotoxic effect and might also explain that in mice even intracerebral injection of 0.7 ng of viscumin did not induce adverse unwanted effects. Finally, our observations fit well to the observation that in cancer patients high doses of viscumins, applied either as extracts like ISCADOR or as single substances like Aviscumine, have been described to be well tolerated [191]. In contrast to brain tissue, CD75s was detected in the spleen, the organ where immune cells, known to express CD75s, are highly prominent (Figure 6) [198, 213, 214]. The high expression of CD75s in immune cells might also explain the observation that these cells are highly vulnerable to viscumin induced cell death (Table 1 and Figure 18).

To determine whether the cytotoxic effects of viscumin-based drugs we observed at high concentrations were an effect of viscumins or of additional components present in the extract (ISCADOR Qu), we added a viscumin-neutralizing antibody and measured cell death induction in cell culture (Figure 3). For Aviscumine, cell death induction could be completely blocked by addition of the antibody, whilst this was only partially the case for ISCADOR Qu. This indicates that cytotoxic effects achieved from a high dose treatment of glioma cells with ISCADOR Qu were not only produced by viscumins but also by additional compounds present in this extract like viscotoxins that are able to disrupt cell membranes and by this mechanism induce cell death [178, 179]. The data collected in this study constrain that the use of viscumin containing extracts,

or even better, viscotoxin-reduced *Viscum album* extracts or purified recombinant viscumins is safe and well tolerated.

4.2 Viscumins inhibit glioma cell proliferation and alter the cell cycle distribution

It has been described in the past that viscumins are able to inhibit the proliferation of tumor cells by inducing a cell cycle arrest either in the G_1 or the G_2-M phase, dependent on the cell line [121, 122, 124]. Our group has previously shown that ISCADOR Qu inhibits the growth of LNT-229 and SMA-560 glioma cells and of subcutaneously growing LNT-229 and SMA-560 tumors [118]. In line with these findings, ISCADOR Qu and Aviscumine, even at low concentrations far below IC_{50} values, reduced proliferation and induced a cell cycle arrest (Figure 7, Figure 9, and Figure 10). Unexpectedly, native ML-1 did not show these effects at any tested concentration. This might be explained by our findings that in our portfolio of viscumin-based drugs, native ML-1 was the agent with lowest toxicity but also lowest efficacy. One could speculate that a further increase of the concentration of native ML-1 might also inhibit proliferation (Table 1). On the other hand, it might be possible that during the purification process the protein loses parts of its activity.

Alterations in cell growth and cell cycle distribution were accompanied by changes in the expression of cell cycle regulators. Cyclin D1 was upregulated by viscumins, whilst Cyclin D2 and D3 were reduced (Figure 11). Furthermore, the tumor suppressor PPP2CA was upregulated in viscumin treated cells (Figure 11). PPP2CA negatively regulates cell cycle progression by dephosphorylation of several cell cycle regulators [215, 216]. Proliferation is also regulated by epigenetic modifications and it has previously been published that HDACs are able to modulate the function of cell cycle regulators and of cellular skeleton proteins, by this attenuating tumor cell growth. Inhibition of HDACs can induce a G_2-M arrest and finally mitotic catastrophe [217-219]. We found HDAC6 to be downregulated in viscumin treated LNT-229 glioma cells. This viscumin mediated downregulation of HDAC6 might explain the G_2-M arrest (Figure 9). The kinase ATM was also downregulated after viscumin treatment.

ATM is involved in the cell cycle regulation if cells harbour double strand breaks [220]. Interestingly, ATM, PPP2CA, and HDAC6 enhance the vulnerability of tumor cells towards chemotherapy and irradiation in glioma and other tumors [221-225]. This might be of importance if viscumin therapy will be combined with glioma therapy. This item will be discussed in detail in chapter 4.4.

Interestingly, the above mentioned genes were also regulated in glioma cells treated with native ML-1 although native ML-1 did not induce a cell cycle arrest in LNT-229 cells (Figure 9 and Figure 11). Therefore, cell cycle inhibitory effects of viscumins are obscure and further investigations are necessary to explain in detail how viscumins attenuate tumor cell proliferation. One could also speculate that the accumulation of LNT-229 cells in G_2-M after viscumin treatment might be unrelated to a cell cycle arrest but might be caused by a disturbance of mitosis. Actually, it has been shown that some herbal compounds induce an arrest in G_2-M. Curcumin, a diarylheptanoid, disrupts mitotic spindle structures thereby inducing a G_2-M arrest [226]. Besides, a polyphenol molecule isolated from licorice roots leads to a stop in G_2-M by microtubule disruption [227]. In total, viscumins attenuate glioma cell proliferation, putatively by the retention of glioma cells in either G_1 or G_2-M. Nevertheless, the underlying mechanisms how viscumins influence cell cycle progression of glioma cells remain elusive.

4.3 Viscumins reduce the motility of GBM cells

Our group has previously shown that ISCADOR Qu mitigates glioma cell motility [118]. With a few exceptions, ISCADOR Qu, Aviscumine, and native ML-1 modify the expression of migration and invasion associated genes in glioma cells. Pro-migratory genes like the EPH receptor B2 (EPHB2), metastasis-associated protein 1 (MTA1), TGF-β1, TGF-β2, and TGFBR2 were downregulated in viscumin treated LNT-229 cells (Figure 12). In glioma, TGF-β is an important pro-tumorigenic cytokine and, apart from its immunosuppressive effects, it induces glioma invasion and migration by enhancing the expression of MMPs [30, 201]. TGF-β as wells as

SMAD2, a central TGF-β signal transducer protein whose activity is regulated by phosphorylation, were downregulated after viscumin treatment (Figure 13) [228]. Whether TGF-β target genes like EPHB2, MTA1, or MMP-2 are directly regulated by viscumins or whether their downregulation is an effect of lower TGF-β expression or lesser activation of the TGF-β signalling pathway needs further investigation. EPHB2 overexpression reduces cell adhesion and increases migration of glioma cells, while EPHB2 silencing reduces migration and is linked to Ras, a proto-oncogene that we found downregulated by native ML-1 and ISCADOR Qu (Figure 12A) [229, 230]. MTA1 enhances the invasiveness of pancreas carcinoma cells and is amplified in invasive cells from recurrent GBM [231, 232].

Downregulation of motility associated genes was more prominent in ISCADOR Qu treated cells compared to Aviscumine or native ML-1. This might be due to several other components present in *Viscum album* extracts that are absent in purified or recombinant ML and that might potentiate the effects of ML. Nevertheless, even if minor components like flavonoids or triterpenes can modulate mRNA expression (for review see [233, 234]), viscumins seemed to be the main inducers of altered gene expression in LNT-229 cells since addition of a viscumin specific antibody that neutralized their function abrogates the viscumin mediated differential expression of motility associated factors (Figure 13 and Figure 14). In the category of genes that were exclusively regulated by ISCADOR Qu several pro-migratory factors were downregulated: Lowering caspase-8 (CASP8) expression reduces migration of glioma cells [235]. CEACAM1, an adhesion molecule, promotes migration and invasion in cancer [236, 237]. The netrin-1 receptor DCC enhances cell migration by activating CDC42, Rac1, and by filopodia formation [238]. MMP-2, MMP-14, and TIMP-2 are responsible for the degradation of the ECM during glioma cell invasion and migration [239]. The nuclear proto-oncogene SET1 is associated with the invasion of breast cancer and knocking down SET1 blocks migration and invasion of breast cancer cells [240]. The KISS1 receptor (KISS1R) function is still under discussion in the context of cancer, but it was recently published that KISS1R stimulates invadopodia formation and invasion of cancer cells [241]. The function of the retinoblastoma like protein (RBL1) in regard to glioma cell motility is controversially discussed as it is

overexpressed in GBM and colon cancer. Nonetheless, its expression decreases during invasion [242].

In the cohort of mRNAs that were upregulated upon viscumin treatment 4 genes provide anti-migratory functions (BRMS1, FGF2, NME, and SERPINB5), 9 have been published to be pro-migratory (FAT1, IL-18, KRAS, LYPD3, MMP1, MMP10, PTGS2, S1004A, and SERPIN1), whereas 4 genes could be either pro- or anti-migratory depending on the circumstances of their expression (HGF, IL1B, MET, and MYC). The breast cancer metastasis suppressor 1 (BRMS1) inhibits glioma progression via modulating invasion, migration, and adhesion [243]. Fibroblast growth factor 2 (FGF2) is upregulated in the less invasive pro-neural GBM subtype in comparison to the more invasive mesenchymal subtype. Patients with low FGF2-dependent PDGF receptor A (PDGFRA) expression have a better prognosis compared to patients with high PDGFRA levels [244, 245]. The NME/NM23 nucleoside diphosphate kinase 1 (NME) is suggested to play a role in glioma invasion and migration [246, 247]. Serpin family B member 5 (SERPINB5), which is often silence in GBM due to promoter methylation, effectively suppresses migration and invasion of cancer cells [248, 249]. Even if we found some pro-migratory genes being upregulated by viscumins there seemed to be no functional consequence since ISCADOR Qu, Aviscumine, and native ML-1 significantly reduced GBM motility (Figure 15). Not all genes we found by gene expression array analysis were validated by RT-qPCR, so there is still the possibility that differentially expressed factors have to be graded as false positives. This might explain some of the discrepancies. Nevertheless, patients carrying invasively growing tumors might benefit from adjuvant viscumins therapy.

4.4 Viscumins support anti-tumoral immune effects

In the past years several *in vivo* and *in vitro* studies have shown that viscumins boost the immune system and promote anti-tumoral activity [168, 172, 189, 250-253]. In our lab it was shown that ISCADOR Qu enhances NK cell mediated killing of glioma cells [118]. Here we firstly extended these investigations related to immune-supporting

effects of Aviscumine and native ML-1. Secondly, we measured the effect of these three viscumin-based drugs in the context of anti-glioma T cell activity.

Anti-glioma NK cell activity was not only supported by the treatment of glioma cells with ISCADOR Qu but also by using Aviscumine (Figure 16A, B). Native M-1 war not tested. The enhanced killing we observed seemed not to be mediated by a specific surface protein of NK cells but is probably a more general effect that needs further investigation. NK cells are activated by binding of the activating NK receptors like NKG2D to their corresponding ligands, which are up-regulated on the cell surface of dangerous cells but often downregulated on tumor cells. Additionally, NK cells transmit their cytotoxicity by a set of activating natural cytotoxicity receptors like NKp30, NKp44, and NKp46, which recognize their ligands on tumor cells. Inhibition of each of these interacting proteins reduced the killing of glioma cells but did not significantly influenced supporting effects of viscumins (Figure 16 C). Only the inhibition of all receptor-ligand interactions between NK and glioma cells abrogated the NK cell mediated killing of glioma cells in both, viscumin treated and control glioma cells, indicating that the viscumin-mediated enhancement of the NK cell mediated killing of glioma cells was not dependent on a single receptor-ligand interaction. The stimulating viscumin effect seemed to be a more general feature. The mechanism how viscumins stimulate NK cells to kill their glioma targets still remains elusive. One could hypothesize that viscumins might stick on target cells and act like a glue to strengthen the interaction between NK and cancer cells. Nonetheless, we did not block the interaction of every known, rare NK cell surface interacting protein. Therefore, we could not exclude that one of these proteins or its interaction partners on glioma cells might be the target of viscumins.

Besides stimulation of the NK cell mediated killing of glioma cell, viscumins also supported the T cell mediated killing of glioma cells and enhanced the generation of activated, tumor- specific T cells. Nevertheless, these activating effects of viscumins varied between the preparations we used but also in the cohort of donors the T cells were isolated from. ISCADOR Qu was the most competent booster among the three tested drugs. This superior effect might rest on additional compounds like triterpenes, flavonoids, oligo- and polysaccharides, or triterpenes that are present in the extract but

not in Aviscumine or native ML-1. Most of these additional compounds have been described to influence immune cell functions [254-256].

Activation of T cells, and especially the expansion of activated and target specific T cells is dependent on the presence of several immuno-stimulating or pro-inflammatory cyto- and chemokines. We therefore tested whether viscumins modulate the expression of cytokines in glioma cells as well as in mice (see also chapter 4.6.). Viscumin treatment of glioma cells led to an increased expression of immune-modulating and pro-inflammatory genes like IL-1A, IL-1β, IL-6, IL-8, IL-12A, IL-15, IKBKB, BCL2L1, CCL-2, CSF-1, -2, -3, CD86, PTGS2, TNF, CD62/SELE, C3, and VEGFA (Figure 12, 19). IL-1 β is an important mediator of the immune response and induces the expression of IL-6, IL-8, and PTGS2/COX2, the latter being the most important prostanoid source in inflammatory processes [257-260]. The release of the pro-inflammatory cytokine IL-6 is induced by TNF, a cytokine that is known to enhance macrophage recruitment to brain tumors and thereby reduces tumor growth [261]. Several studies have already shown enhanced TNF levels in the blood of cancer patients upon viscumin therapy, and even elevated IL-6 levels have been found upon viscumin treatment [126-128, 131]. The anti-apoptotic factor BCL2L1 is essential for the immune system as it promotes the survival of T cells, whereas IL-12A activates the innate and adaptive immune system and pushes the immune response against tumor cells, also in glioma [262-264]. CD62/SELE is mainly expressed by endothelial cells. It is an adhesion molecule that recruits leukocytes to the site of inflammation [265]. Additionally, we found immune-suppressive IL-10 to be upregulated by viscumins. Viscumin mediated induction of IL-10 has already been described in PBMCs, but viscumin mediated downregulation of IL-10 was also reported [126, 131]. The anti-inflammatory, cytoprotective, and antioxidant factor HMOX1 we found to be downregulated in viscumin-treated glioma cells promotes the termination of inflammation and modulates glioma cell proliferation [266, 267]. HMOX1 expression is linked to a poor prognosis of GBM patients [268]. TGF-β is a major immunosuppressive cytokine in glioma [269]. Both TGF-β mRNA as well as protein was reduced in viscumin treated glioma cells (Figures 12, 13). We suggest that the enhancement of the T cell mediated killing of glioma cells relies on multiple

processes: (i) Induction of the expression of pro-inflammatory and immune-stimulating cytokines, (ii) reduction of the expression of immune-suppressive factors, (iii) enhancement of the tumor-specific T cell activity, and (iv) elevation of the production and expansion of tumor specific T cells (Figure 17). In this context, one could suggest that viscumin treatment of glioma cells that are used to prime naïve T cells induced cell death in glioma cells and by this led to the presentation of neo-antigens by the dying tumor cells. These neo-antigens might be taken up by antigen presenting cells that are present in the co-cultures during the T cell priming period and that will help to expand the population of anti-tumor specific T cells. Additionally, damage-associated molecular patterns (DAMPs) might be released by viscumin treated glioma cells. DAMPs boost the immune response by binding to DAMP receptors, thus enhancing the secretion of pro-inflammatory cytokines and attracting immune cells to the tumor [270]. Nevertheless, we did not examine this issue, therefore further investigation will be necessary to clarify the detailed mechanism how viscumins support an anti-cancer T cell response.

Despite the viscumin mediated immune-stimulating effects we observe in glioma cells upon viscumin treatment, a direct treatment of PBMC and T cells with viscumins induced death in these cells, reduced the expression of T cell activity marker proteins, and decreased the killing of glioma cells by T cells (Figure 18, Table 1). Besides us, other groups also demonstrated viscumin mediated toxicity in human immune cells [149, 271, 272]. The vulnerability of immune cells towards viscumins could be explained by the elevated expression of CD75s on these cells [214, 273, 274]. The viscumin concentration we used to treat PBMCs or T cells was rather high and is above the concentration that is achieved in the serum of cancer patients [275]. Other groups have shown a viscumin mediated increase of HLA-DQ and IL-2 receptor expression in human lymphocytes both *in vitro* and *in vivo*. Additionally, elevated levels of the complement factor C3 (being upregulated in glioma cells upon viscumin treatment, Figure 19A) as well as elevated numbers of activated innate and adaptive immune cells were found in the blood of cancer patients during viscumin therapy [146, 276-278].

4.5 Viscumins enhance cytostatic effects if used as adjuvant therapeutics

A natural compound that is well tolerated by cancer patients and that can be used as adjuvants to optimize the impact of a standard therapy might provide benefit for cancer patients and also for GBM patients. Viscumins are mainly used in combination with standard cancer treatment in the clinic. Best results in treating glioma should be achieved if viscumins are applied in combination with TMZ and/or tumor irradiation. *In vitro* we identified at least additive effects of viscumins in the reduction of the clonal survival of glioma cells. In viscumin sensitive human and murine glioma cells (LNT-229, SMA-560) combined viscumin-radiochemotherapy accomplished the level of a superadditive/synergistic effect for all three tested viscumin-based drugs (Figure 20), which might be explained by viscumin mediated changes in the expression of cell cycle regulators like PPP2CA, ATM, or HDAC6 (Figure 11), finally leading to a cell cycle arrest of glioma cells in G_1 or G_2-M. ATM, which is downregulated in ISCADOR Qu and Aviscumine treated LNT-229 cells, has been described to be upregulated in glioma tissue. Inhibition of ATM reduces glioma growth, and additionally glioma cells were sensitized for irradiation and TMZ-based chemotherapy [221, 222, 279-281]. PPP2CA showed elevated expression in viscumin treated LNT-229 cells and is able to interact with ATM [225]. Therefore, besides its function as a phosphatase of cell cycle regulating proteins, PPP2CA might modulate proliferation also via ATM. HDAC6 promotes cell proliferation and confers resistance to temozolomide in glioblastoma [223, 224]. Therefore, the viscumin mediated reduction of HDAC6 expression in glioma cells might also be responsible for the synergistic effect of an adjuvant viscumin therapy, at least *in vitro*. The G_1/S-specific cyclin D1 (CCND1), being upregulated during viscumin treatment, is a regulatory component of the cyclin D1-CDK4 complex and controls the cell cycle during the G_1/S transition. Cyclin D1 overexpression perturbs DNA replication and induces DNA double-strand breaks in irradiation resistant cells [282]. In combination with ATM, viscumin mediated disturbed expression of CCND1 might violate the DSB repair machinery thereby enhancing the effects of irradiation in glioma cells. Our data should be kept in

mind in the clinic since TMZ application and irradiation doses might need to be adapted if patients receive an adjuvant viscumin therapy.

4.6 Adjuvant viscumin therapy prolongs the survival of glioma-bearing mice

To unravel both, immuno-supporting as well as cancer-suppressive impacts like cytotoxic or cytostatic effects or even reduction of glioma cell invasion of an adjuvant viscumin therapy, two different mouse glioma models were used. Using a xenograft model (orthotopically growing LNT-229 tumors in NMRI nude mice), we analyzed the effect of a single, high dose intratumoral viscumin injection in combination with local tumor irradiation and/or TMZ-based chemotherapy. Intratumoral viscumin injections were used in the first approaches since we observed in our *in vitro* experiments that a direct treatment of glioma cells with viscumins provided the anti-cancer effects mentioned above. Besides, this route of administration is lately used to treat solid tumors [162, 163]. As demonstrated in Figure 21 A, the injection of ISCADOR Qu *per se*, or in combination with TMZ, was not successful and even shortened the survival of tumor mice indicating that intra-tumoral high dose ISCADOR Qu injections were highly irksome and did not provide benefit. In contrast, Aviscumine monotherapy provided some benefit but was not better than TMZ (Figure 21 B). This might be due to the fact that LNT-229 cells that were used to develop tumors in the mice are highly TMZ sensitive. Therefore, TMZ alone provided a superior therapeutic impact. Post mortem histological analyses did not show significant differences in tumor size, proliferation, invasion, or apoptosis in the different treatment groups. Nonetheless, these post mortem analyses only reflect the situation just prior to tumor associated death since the mice were sacrificed when developing neurological symptoms. Effects were therefore measured in those tumor cells that survived all therapy approaches and these data might not be representative to demonstrate effects of a viscumin-based cancer treatment. In a second approach, based on the unwanted adverse effects of intratumoral ISADOR Qu injections we observed and based on our *in vitro* data where we demonstrated synergy if Aviscumine was adjuvantly used in combination with

irradiation and TMZ, we started a therapy of LNT-229 glioma bearing NMRI nude mice using an intratumoral injection of Aviscumine in combination with local tumor irradiation and intraperitoneal TMZ injections. Again, we observed a therapeutic impact if animals were solely treated with Aviscumine (Figure 22), but the therapeutic impact of Aviscumine did not reach the effect of tumor irradiation in combination with TMZ. Nevertheless, if Aviscumine was used in combination with irradiation and TMZ, this treatment, even being not significant, prolonged the median survival of glioma mice for further six days.

To determine immune-supporting anti-cancer effects of viscumins, we used a syngeneic mouse glioma model (SMA-560 tumors in VM/Dk mouse brains) and did serial subcutaneous injections with increasing concentrations of ISCADOR Qu since this route of application is routinely used in tumor patients. Due to the short half-life of viscumins and due to the knowledge that viscumins hardly pass the blood-brain barrier, mainly immune-supporting effects will be determined in this mouse model. We did not use Aviscumine in this approach since in our *in vitro* analyses it provided lesser immune-stimulating effects than ISCADOR Qu. In contrast to LNT-229 cells, SMA-560 cells are mainly resistant to TMZ [283] so the therapeutic impact of TMZ was small in the group of mice receiving irradiation and TMZ. Interestingly, ISCADOR Qu monotherapy provided a similar period of prolonged survival as glioma standard therapy did. If ISCADOR Qu was applied adjuvantly in parallel to TMZ and irradiation, a significant further prolongation of survival was observed (Figure 23). We postulate that the therapeutic impact of an adjuvant ISCADOR Qu treatment was mainly based on anti-tumor immune effects. This was supported by the observation that mainly pro-inflammatory cytokines like BLC, CCL24, CXCL9, CCL25, CCL3/MIP-1α, CX3CL1, and CSF3 were detected in the serum of VM/Dk mice treated with ISCADOR Qu (Figure 23 D). Besides, TIMP1 and MMPs, factors mainly known to push tumor cell invasion, were upregulated upon ISCADOR Qu injections. Nevertheless, enhanced levels of TIMPs and MMPs are in accordance with the immune-supporting impact of viscumins since these proteins have been described to be involved in a general activation of the immune system. MMPs provide both, pro-inflammatory and anti-inflammatory features. MMPs cleave pro-IL-1β into the active

form but also degrade IL-1β [284, 285]. TIMP-1 can bind to CD63 and like a cytokine promotes the growth and survival of B cells and granulocytes [286].

To sum up, the results of the *in vivo* experiments indicate that s.c. viscumin therapy with increasing doses as it is currently used for many kinds of tumors as well as intratumoral viscumin application is working positively together with glioma standard therapy in the tested murine models and its application might be beneficial for glioma patients.

5. Conclusion

In the present study we demonstrate that viscumins provide therapeutic impact in the treatment of GBM, especially if used as adjuvant therapeutics. Viscumins provide both cytotoxic and cytostatic functions, they mitigate glioma cell motility, lead to the downregulation of factors involved in the TGF-ß signalling pathway, and boost NK cell as well as T cell mediated glioma cell killing. Nevertheless, different viscumin-based drugs possess diverse advantages and disadvantages. While *Viscum album* extracts like ISCADOR Qu provide superior anti-cancer and immune-supporting effects, maybe due to several additional compounds present in the extracts that enhance the function of viscumins, they also provide enhanced toxicity in non-neoplastic cells as well as in the brain. For this multi-compound *Viscum album* extracts should not be used to treat brain tumors by intratumoral injections. On the other hand, a profound prolongation of survival was observed if ISCADOR Qu was subcutaneously administered in parallel to glioma standard therapy. Aviscumine also showed anti-cancer therapeutic effects, however its grade of action was lower than that of ISCADOR Qu. Nonetheless, intracerebral injections of Aviscumine seemed to be save, at least in mice and even if not significant, adjuvant Aviscumine therapy further prolonged the survival of glioma mice.

In total, our data demonstrate that viscumins are feasible adjuvant therapeutics, at least to treat experimental glioma. Nevertheless, the route of administration as well as the concentration and preparation of viscumin-based drugs will be of importance in the treatment of glioma and should be kept in mind. Only future high-quality clinical trials can provide final evidence whether an adjuvant viscumin therapy will be beneficial in the treatment of glioma patients.

6. Literature

1. Ostrom, Q.T., et al., *CBTRUS statistical report: Primary brain and central nervous system tumors diagnosed in the United States in 2006-2010.* Neuro Oncol, 2013. 15 Suppl 2: p. ii1-56.
2. Ostrom, Q.T., et al., *CBTRUS Statistical Report: Primary Brain and Central Nervous System Tumors Diagnosed in the United States in 2008-2012.* Neuro Oncol, 2015. 17 Suppl 4: p. iv1-iv62.
3. Stupp, R., et al., *Effects of radiotherapy with concomitant and adjuvant temozolomide versus radiotherapy alone on survival in glioblastoma in a randomised phase III study: 5-year analysis of the EORTC-NCIC trial.* Lancet Oncol, 2009. 10(5): p. 459-66.
4. Marosi, C. and M. Preusser, *Milestones of the last 10 years: CNS cancer.* Memo, 2017. 10(1): p. 18-21.
5. Lawrence, Y.R., et al., *Improving prognosis of glioblastoma in the 21st century: who has benefited most?* Cancer, 2012. 118(17): p. 4228-34.
6. Behin, A., et al., *Primary brain tumours in adults.* Lancet, 2003. 361(9354): p. 323-31.
7. Louis, D.N., et al., *WHO Classification of Tumours of the Central Nervous System*. Vol. 1. 2016, France: International Agency for Research on Cancer.
8. Ohgaki, H. and P. Kleihues, *The definition of primary and secondary glioblastoma.* Clin Cancer Res, 2013. 19(4): p. 764-72.
9. Louis, D.N., et al., *The 2016 World Health Organization Classification of Tumors of the Central Nervous System: a summary.* Acta Neuropathol, 2016. 131(6): p. 803-20.
10. de Vries, N.A., et al., *Restricted brain penetration of the tyrosine kinase inhibitor erlotinib due to the drug transporters P-gp and BCRP.* Invest New Drugs, 2012. 30(2): p. 443-9.
11. Zhao, P., Y.Z. Zhang, and M.Z. Sun, *[Regulatory effect of small interfering RNA targeting multidrug resistant protein 1 on chemosensitivity of human multiforme glioblastoma cell line BT325].* Ai Zheng, 2005. 24(12): p. 1436-41.
12. Happold, C., et al., *Distinct molecular mechanisms of acquired resistance to temozolomide in glioblastoma cells.* J Neurochem, 2012. 122(2): p. 444-55.
13. Hegi, M.E., et al., *MGMT gene silencing and benefit from temozolomide in glioblastoma.* N Engl J Med, 2005. 352(10): p. 997-1003.
14. Liang, B.C., *Effects of hypoxia on drug resistance phenotype and genotype in human glioma cell lines.* J Neurooncol, 1996. 29(2): p. 149-55.
15. Haar, C.P., et al., *Drug Resistance in Glioblastoma: A Mini Review.* Neurochemical research, 2012. 37(6): p. 1192-1200.
16. Amberger-Murphy, V., *Hypoxia helps glioma to fight therapy.* Curr Cancer Drug Targets, 2009. 9(3): p. 381-90.
17. Abou-Antoun, T.J., et al., *Brain Cancer Stem Cells in Adults and Children: Cell Biology and Therapeutic Implications.* Neurotherapeutics, 2017.

18. De Bacco, F., et al., *MET inhibition overcomes radiation resistance of glioblastoma stem-like cells.* EMBO Mol Med, 2016. 8(5): p. 550-68.
19. Eramo, A., et al., *Chemotherapy resistance of glioblastoma stem cells.* Cell Death Differ, 2006. 13(7): p. 1238-41.
20. Shi, L., et al., *MiR-21 protected human glioblastoma U87MG cells from chemotherapeutic drug temozolomide induced apoptosis by decreasing Bax/Bcl-2 ratio and caspase-3 activity.* Brain Res, 2010. 1352: p. 255-64.
21. Ujifuku, K., et al., *miR-195, miR-455-3p and miR-10a(*) are implicated in acquired temozolomide resistance in glioblastoma multiforme cells.* Cancer Lett, 2010. 296(2): p. 241-8.
22. Berthois, Y., et al., *Differential expression of miR200a-3p and miR21 in grade II-III and grade IV gliomas: evidence that miR200a-3p is regulated by O(6)-methylguanine methyltransferase and promotes temozolomide responsiveness.* Cancer Biol Ther, 2014. 15(7): p. 938-50.
23. Zhang, W., et al., *miR-181d: a predictive glioblastoma biomarker that downregulates MGMT expression.* Neuro Oncol, 2012. 14(6): p. 712-9.
24. Asuthkar, S., et al., *Epigenetic regulation of miRNA-211 by MMP-9 governs glioma cell apoptosis, chemosensitivity and radiosensitivity.* Oncotarget, 2012. 3(11): p. 1439-54.
25. Chen, H., et al., *miR-130a can predict response to temozolomide in patients with glioblastoma multiforme, independently of O6-methylguanine-DNA methyltransferase.* J Transl Med, 2015. 13: p. 69.
26. Armento, A., et al., *Molecular Mechanisms of Glioma Cell Motility*, in *Glioblastoma*, S. De Vleeschouwer, Editor. 2017: Brisbane (AU).
27. Konnecke, H. and I. Bechmann, *The role of microglia and matrix metalloproteinases involvement in neuroinflammation and gliomas.* Clin Dev Immunol, 2013. 2013: p. 914104.
28. Forsyth, P.A., et al., *Gelatinase-A (MMP-2), gelatinase-B (MMP-9) and membrane type matrix metalloproteinase-1 (MT1-MMP) are involved in different aspects of the pathophysiology of malignant gliomas.* Br J Cancer, 1999. 79(11-12): p. 1828-35.
29. Wang, M., et al., *The expression of matrix metalloproteinase-2 and -9 in human gliomas of different pathological grades.* Brain Tumor Pathol, 2003. 20(2): p. 65-72.
30. Wick, W., M. Platten, and M. Weller, *Glioma cell invasion: regulation of metalloproteinase activity by TGF-beta.* J Neurooncol, 2001. 53(2): p. 177-85.
31. Imai, K., et al., *Degradation of decorin by matrix metalloproteinases: identification of the cleavage sites, kinetic analyses and transforming growth factor-beta1 release.* Biochem J, 1997. 322 (Pt 3): p. 809-14.
32. Yu, Q. and I. Stamenkovic, *Cell surface-localized matrix metalloproteinase-9 proteolytically activates TGF-beta and promotes tumor invasion and angiogenesis.* Genes Dev, 2000. 14(2): p. 163-76.
33. Markovic, D.S., et al., *Gliomas induce and exploit microglial MT1-MMP expression for tumor expansion.* Proc Natl Acad Sci U S A, 2009. 106(30): p. 12530-5.

34. Sato, H., et al., *A matrix metalloproteinase expressed on the surface of invasive tumour cells.* Nature, 1994. 370(6484): p. 61-5.
35. Murphy, G., et al., *Mechanisms for pro matrix metalloproteinase activation.* APMIS, 1999. 107(1): p. 38-44.
36. Sarkar, S., et al., *Tenascin-C stimulates glioma cell invasion through matrix metalloproteinase-12.* Cancer Res, 2006. 66(24): p. 11771-80.
37. Wang, J., et al., *Increased expression of matrix metalloproteinase-13 in glioma is associated with poor overall survival of patients.* Med Oncol, 2012. 29(4): p. 2432-7.
38. Yeh, W.L., et al., *Leptin induces migration and invasion of glioma cells through MMP-13 production.* Glia, 2009. 57(4): p. 454-64.
39. Wang, H., et al., *miR-132 can inhibit glioma cells invasion and migration by target MMP16 in vitro.* Onco Targets Ther, 2015. 8: p. 3211-8.
40. Laurent, M., et al., *NOVH increases MMP3 expression and cell migration in glioblastoma cells via a PDGFR-alpha-dependent mechanism.* FASEB J, 2003. 17(13): p. 1919-21.
41. Deng, Y., et al., *Expression of Matrix Metalloproteinase-26 promotes human glioma U251 cell invasion in vitro and in vivo.* Oncol Rep, 2010. 23(1): p. 69-78.
42. Rome, C., et al., *MMP-7 (matrilysin) expression in human brain tumors.* Mol Carcinog, 2007. 46(6): p. 446-52.
43. Lettau, I., et al., *Matrix metalloproteinase-19 is highly expressed in astroglial tumors and promotes invasion of glioma cells.* J Neuropathol Exp Neurol, 2010. 69(3): p. 215-23.
44. Jackson, H.W., et al., *TIMPs: versatile extracellular regulators in cancer.* Nat Rev Cancer, 2017. 17(1): p. 38-53.
45. Joseph, J.V., et al., *TGF-beta is an inducer of ZEB1-dependent mesenchymal transdifferentiation in glioblastoma that is associated with tumor invasion.* Cell Death Dis, 2014. 5: p. e1443.
46. Massague, J., *TGF-beta signaling in development and disease.* FEBS Lett, 2012. 586(14): p. 1833.
47. Massaous, J. and A. Hata, *TGF-beta signalling through the Smad pathway.* Trends Cell Biol, 1997. 7(5): p. 187-92.
48. Platten, M., et al., *Transforming growth factors beta(1) (TGF-beta(1)) and TGF-beta(2) promote glioma cell migration via Up-regulation of alpha(V)beta(3) integrin expression.* Biochem Biophys Res Commun, 2000. 268(2): p. 607-11.
49. Onken, J., et al., *Versican isoform V1 regulates proliferation and migration in high-grade gliomas.* J Neurooncol, 2014. 120(1): p. 73-83.
50. Liu, S., J. Sun, and Q. Lan, *TGF-beta-induced miR10a/b expression promotes human glioma cell migration by targeting PTEN.* Mol Med Rep, 2013. 8(6): p. 1741-6.
51. Canazza, A., et al., *Increased migration of a human glioma cell line after in vitro CyberKnife irradiation.* Cancer Biol Ther, 2011. 12(7): p. 629-33.
52. Mangani, D., M. Weller, and P. Roth, *The network of immunosuppressive pathways in glioblastoma.* Biochem Pharmacol, 2017. 130: p. 1-9.

53. Claudio, L., *Ultrastructural features of the blood-brain barrier in biopsy tissue from Alzheimer's disease patients.* Acta Neuropathol, 1996. 91(1): p. 6-14.
54. Lou, J., et al., *Brain microvascular endothelial cells and leukocytes derived from patients with multiple sclerosis exhibit increased adhesion capacity.* Neuroreport, 1997. 8(3): p. 629-33.
55. Hickey, W.F., B.L. Hsu, and H. Kimura, *T-lymphocyte entry into the central nervous system.* J Neurosci Res, 1991. 28(2): p. 254-60.
56. Calzascia, T., et al., *Homing phenotypes of tumor-specific CD8 T cells are predetermined at the tumor site by crosspresenting APCs.* Immunity, 2005. 22(2): p. 175-84.
57. Baron, J.L., et al., *Surface expression of alpha 4 integrin by CD4 T cells is required for their entry into brain parenchyma.* J Exp Med, 1993. 177(1): p. 57-68.
58. Yednock, T.A., et al., *Prevention of experimental autoimmune encephalomyelitis by antibodies against alpha 4 beta 1 integrin.* Nature, 1992. 356(6364): p. 63-6.
59. El Andaloussi, A. and M.S. Lesniak, *CD4+ CD25+ FoxP3+ T-cell infiltration and heme oxygenase-1 expression correlate with tumor grade in human gliomas.* J Neurooncol, 2007. 83(2): p. 145-52.
60. Heimberger, A.B., et al., *Incidence and prognostic impact of FoxP3+ regulatory T cells in human gliomas.* Clin Cancer Res, 2008. 14(16): p. 5166-72.
61. Lohr, J., et al., *Effector T-cell infiltration positively impacts survival of glioblastoma patients and is impaired by tumor-derived TGF-beta.* Clin Cancer Res, 2011. 17(13): p. 4296-308.
62. Fu, S., et al., *TGF-beta induces Foxp3 + T-regulatory cells from CD4 + CD25 - precursors.* Am J Transplant, 2004. 4(10): p. 1614-27.
63. Chen, W., et al., *Conversion of peripheral CD4+CD25- naive T cells to CD4+CD25+ regulatory T cells by TGF-beta induction of transcription factor Foxp3.* J Exp Med, 2003. 198(12): p. 1875-86.
64. Thomas, D.A. and J. Massague, *TGF-beta directly targets cytotoxic T cell functions during tumor evasion of immune surveillance.* Cancer Cell, 2005. 8(5): p. 369-80.
65. Friese, M.A., et al., *RNA interference targeting transforming growth factor-beta enhances NKG2D-mediated antiglioma immune response, inhibits glioma cell migration and invasiveness, and abrogates tumorigenicity in vivo.* Cancer Res, 2004. 64(20): p. 7596-603.
66. Eisele, G., et al., *TGF-beta and metalloproteinases differentially suppress NKG2D ligand surface expression on malignant glioma cells.* Brain, 2006. 129(Pt 9): p. 2416-25.
67. Gabrilovich, D.I., et al., *Production of vascular endothelial growth factor by human tumors inhibits the functional maturation of dendritic cells.* Nat Med, 1996. 2(10): p. 1096-103.
68. Voron, T., et al., *VEGF-A modulates expression of inhibitory checkpoints on CD8+ T cells in tumors.* J Exp Med, 2015. 212(2): p. 139-48.

69. Bloch, O., et al., *Gliomas promote immunosuppression through induction of B7-H1 expression in tumor-associated macrophages.* Clin Cancer Res, 2013. 19(12): p. 3165-75.
70. Roth, P., et al., *Regeneration and tolerance factor: a novel mediator of glioblastoma-associated immunosuppression.* Cancer Res, 2006. 66(7): p. 3852-8.
71. Sippel, T.R., et al., *Neutrophil degranulation and immunosuppression in patients with GBM: restoration of cellular immune function by targeting arginase I.* Clin Cancer Res, 2011. 17(22): p. 6992-7002.
72. Wang, L., et al., *Neural stem/progenitor cells modulate immune responses by suppressing T lymphocytes with nitric oxide and prostaglandin E2.* Exp Neurol, 2009. 216(1): p. 177-83.
73. Badie, B. and J.M. Schartner, *Flow cytometric characterization of tumor-associated macrophages in experimental gliomas.* Neurosurgery, 2000. 46(4): p. 957-61; discussion 961-2.
74. Komohara, Y., et al., *Possible involvement of the M2 anti-inflammatory macrophage phenotype in growth of human gliomas.* J Pathol, 2008. 216(1): p. 15-24.
75. Coniglio, S.J., et al., *Microglial stimulation of glioblastoma invasion involves epidermal growth factor receptor (EGFR) and colony stimulating factor 1 receptor (CSF-1R) signaling.* Mol Med, 2012. 18: p. 519-27.
76. Wesolowska, A., et al., *Microglia-derived TGF-beta as an important regulator of glioblastoma invasion--an inhibition of TGF-beta-dependent effects by shRNA against human TGF-beta type II receptor.* Oncogene, 2008. 27(7): p. 918-30.
77. Markovic, D.S., et al., *Microglia stimulate the invasiveness of glioma cells by increasing the activity of metalloprotease-2.* J Neuropathol Exp Neurol, 2005. 64(9): p. 754-62.
78. Riabov, V., et al., *Role of tumor associated macrophages in tumor angiogenesis and lymphangiogenesis.* Front Physiol, 2014. 5: p. 75.
79. Jacobs, J.F., et al., *Regulatory T cells and the PD-L1/PD-1 pathway mediate immune suppression in malignant human brain tumors.* Neuro Oncol, 2009. 11(4): p. 394-402.
80. Berghoff, A.S., et al., *Programmed death ligand 1 expression and tumor-infiltrating lymphocytes in glioblastoma.* Neuro Oncol, 2015. 17(8): p. 1064-75.
81. Saas, P., et al., *Fas ligand expression by astrocytoma in vivo: maintaining immune privilege in the brain?* J Clin Invest, 1997. 99(6): p. 1173-8.
82. Weller, M., et al., *CD95-Dependent T-Cell Killing by Glioma Cells Expressing CD95 Ligand: More on Tumor Immune Escape, the CD95 Counterattack, and the Immune Privilege of the Brain.* Cellular Physiology and Biochemistry, 1997. 7(5): p. 282-288.
83. Wiendl, H., et al., *A functional role of HLA-G expression in human gliomas: an alternative strategy of immune escape.* J Immunol, 2002. 168(9): p. 4772-80.

84. Wischhusen, J., et al., *HLA-E protects glioma cells from NKG2D-mediated immune responses in vitro: implications for immune escape in vivo.* J Neuropathol Exp Neurol, 2005. 64(6): p. 523-8.
85. Fischer, K., et al., *Inhibitory effect of tumor cell-derived lactic acid on human T cells.* Blood, 2007. 109(9): p. 3812-9.
86. Crane, C.A., et al., *Immune evasion mediated by tumor-derived lactate dehydrogenase induction of NKG2D ligands on myeloid cells in glioblastoma patients.* Proc Natl Acad Sci U S A, 2014. 111(35): p. 12823-8.
87. Miyazaki, T., et al., *Indoleamine 2,3-dioxygenase as a new target for malignant glioma therapy. Laboratory investigation.* J Neurosurg, 2009. 111(2): p. 230-7.
88. Gilbert, M.R., et al., *Dose-dense temozolomide for newly diagnosed glioblastoma: a randomized phase III clinical trial.* J Clin Oncol, 2013. 31(32): p. 4085-91.
89. Stupp, R., et al., *Cilengitide combined with standard treatment for patients with newly diagnosed glioblastoma with methylated MGMT promoter (CENTRIC EORTC 26071-22072 study): a multicentre, randomised, open-label, phase 3 trial.* Lancet Oncol, 2014. 15(10): p. 1100-8.
90. Chinot, O.L., et al., *Bevacizumab plus radiotherapy-temozolomide for newly diagnosed glioblastoma.* N Engl J Med, 2014. 370(8): p. 709-22.
91. Gilbert, M.R., et al., *A randomized trial of bevacizumab for newly diagnosed glioblastoma.* N Engl J Med, 2014. 370(8): p. 699-708.
92. Stupp, R., et al., *Maintenance Therapy With Tumor-Treating Fields Plus Temozolomide vs Temozolomide Alone for Glioblastoma: A Randomized Clinical Trial.* JAMA, 2015. 314(23): p. 2535-43.
93. Malkki, H., *Trial Watch: Glioblastoma vaccine therapy disappointment in Phase III trial.* Nat Rev Neurol, 2016. 12(4): p. 190.
94. Schuessler, A., et al., *Autologous T-cell therapy for cytomegalovirus as a consolidative treatment for recurrent glioblastoma.* Cancer Res, 2014. 74(13): p. 3466-76.
95. Freeman, A.I., et al., *Phase I/II trial of intravenous NDV-HUJ oncolytic virus in recurrent glioblastoma multiforme.* Mol Ther, 2006. 13(1): p. 221-8.
96. Geletneky, K., et al., *Phase I/IIa study of intratumoral/intracerebral or intravenous/intracerebral administration of Parvovirus H-1 (ParvOryx) in patients with progressive primary or recurrent glioblastoma multiforme: ParvOryx01 protocol.* BMC Cancer, 2012. 12: p. 99.
97. Maier-Hauff, K., et al., *Efficacy and safety of intratumoral thermotherapy using magnetic iron-oxide nanoparticles combined with external beam radiotherapy on patients with recurrent glioblastoma multiforme.* J Neurooncol, 2011. 103(2): p. 317-24.
98. Shea, A., et al., *MicroRNAs in glioblastoma multiforme pathogenesis and therapeutics.* Cancer Med, 2016. 5(8): p. 1917-46.
99. Okubamichael, D.Y., M.E. Griffiths, and D. Ward, *Host specificity in parasitic plants - perspectives from mistletoes.* AoB Plants, 2016.

100. Zänker, K.S., ed. *Mistletoe From Mythology to Evidence-Based Medicine*. Translational Research in Biomedicine, ed. S.H.H. Chan. Vol. 4. 2015, Karger.
101. ISCADOR. *Präparate*. 2016 [cited 2016 06.11.2016]; Available from: https://www.iscador.com/de/mistelpraeparate/sortimentsuebersicht.html.
102. Kienle, G.S., *Die Mistel in der Onkologie: Fakten und konzeptionelle Grundlagen*. 2003: Schattauer.
103. Krauspenhaar, R., et al., *Crystal structure of mistletoe lectin I from Viscum album.* Biochem Biophys Res Commun, 1999. 257(2): p. 418-24.
104. Olsnes, S., et al., *Isolation and characterization of viscumin, a toxic lectin from Viscum album L. (mistletoe).* J Biol Chem, 1982. 257(22): p. 13263-70.
105. Endo, Y., K. Tsurugi, and J.M. Lambert, *The site of action of six different ribosome-inactivating proteins from plants on eukaryotic ribosomes: the RNA N-glycosidase activity of the proteins.* Biochem Biophys Res Commun, 1988. 150(3): p. 1032-6.
106. Müthing, J., et al., *Tumor-associated CD75s gangliosides and CD75s-bearing glycoproteins with Neu5Acalpha2-6Galbeta1-4GlcNAc-residues are receptors for the anticancer drug rViscumin.* The FASEB journal : official publication of the Federation of American Societies for Experimental Biology, 2005. 19(1): p. 103-105.
107. Muthing, J., et al., *Preferential binding of the anticancer drug rViscumin (recombinant mistletoe lectin) to terminally alpha2-6-sialylated neolacto-series gangliosides.* Glycobiology, 2002. 12(8): p. 485-97.
108. Hartley, M.R. and J.M. Lord, *Cytotoxic ribosome-inactivating lectins from plants.* Biochim Biophys Acta, 2004. 1701(1-2): p. 1-14.
109. Mengs, U., D. Gothel, and E. Leng-Peschlow, *Mistletoe extracts standardized to mistletoe lectins in oncology: review on current status of preclinical research.* Anticancer Res, 2002. 22(3): p. 1399-407.
110. Doser, C., et al., *Influence of carbohydrates on the cytotoxicity of an aqueous mistletoe drug and of purified mistletoe lectins tested on human T-leukemia cells.* Arzneimittelforschung, 1989. 39(6): p. 647-51.
111. Janssen, O., A. Scheffler, and D. Kabelitz, *In vitro effects of mistletoe extracts and mistletoe lectins. Cytotoxicity towards tumor cells due to the induction of programmed cell death (apoptosis).* Arzneimittelforschung, 1993. 43(11): p. 1221-7.
112. Schumacher, U., et al., *Biochemical, histochemical and cell biological investigations on the actions of mistletoe lectins I, II and III with human breast cancer cell lines.* Glycoconj J, 1995. 12(3): p. 250-7.
113. Burger, A.M., et al., *Antiproliferative activity of an aqueous mistletoe extract in human tumor cell lines and xenografts in vitro.* Arzneimittelforschung, 2001. 51(9): p. 748-57.
114. Valentiner, U., et al., *The cytotoxic effect of mistletoe lectins I, II and III on sensitive and multidrug resistant human colon cancer cell lines in vitro.* Toxicology, 2002. 171(2-3): p. 187-99.

115. Thies, A., et al., *Influence of mistletoe lectins and cytokines induced by them on cell proliferation of human melanoma cells in vitro.* Toxicology, 2005. 207(1): p. 105-16.
116. Pae, H.O., et al., *Mistletoe lectin synergizes with paclitaxel in human SK-hep1 hepatocarcinoma cells.* Immunopharmacol Immunotoxicol, 2001. 23(4): p. 531-40.
117. Lenartz, D., et al., *Efficiency of treatment with galactoside-specific lectin from mistletoe against rat glioma* Anticancer Research, 1998. 18: p. 1011-1014.
118. Podlech, O., et al., *Fermented mistletoe extract as a multimodal antitumoral agent in gliomas.* Evid Based Complement Alternat Med, 2012. 2012: p. 501796.
119. Pryme, I.F., et al., *Suppression of growth of tumour cell lines in vitro and tumours in vivo by mistletoe lectins.* Histol Histopathol, 2006. 21(3): p. 285-99.
120. Elluru, S.R., et al., *Antiangiogenic properties of viscum album extracts are associated with endothelial cytotoxicity.* Anticancer Res, 2009. 29(8): p. 2945-50.
121. Harmsma, M., et al., *Effects of mistletoe (Viscum album L.) extracts Iscador on cell cycle and survival of tumor cells.* Arzneimittelforschung, 2006. 56(6A): p. 474-82.
122. Harmsma, M., et al., *Differential effects of Viscum album extract IscadorQu on cell cycle progression and apoptosis in cancer cells.* Int J Oncol, 2004. 25(6): p. 1521-9.
123. Duong Van Huyen, J.P., et al., *Induction of apoptosis of endothelial cells by Viscum album: a role for anti-tumoral properties of mistletoe lectins.* Mol Med, 2002. 8(10): p. 600-6.
124. Weissenstein, U., et al., *Interaction of a standardized mistletoe (Viscum album) preparation with antitumor effects of Trastuzumab in vitro.* BMC Complement Altern Med, 2016. 16: p. 271.
125. Stirpe, F., et al., *Inhibition of protein synthesis by a toxic lectin from Viscum album L. (mistletoe).* Biochem J, 1980. 190(3): p. 843-5.
126. Boneberg, E.M. and T. Hartung, *Mistletoe lectin-1 increases tumor necrosis factor-alpha release in lipopolysaccharide-stimulated whole blood via inhibition of interleukin-10 production.* J Pharmacol Exp Ther, 2001. 298(3): p. 996-1000.
127. Hajto, T., et al., *Increased secretion of tumor necrosis factors alpha, interleukin 1, and interleukin 6 by human mononuclear cells exposed to beta-galactoside-specific lectin from clinically applied mistletoe extract.* Cancer Res, 1990. 50(11): p. 3322-6.
128. Joller, P.W., et al., *Stimulation of cytokine production via a special standardized mistletoe preparation in an in vitro human skin bioassay.* Arzneimittelforschung, 1996. 46(6): p. 649-53.
129. Hostanska, K., et al., *A plant lectin derived from Viscum album induces cytokine gene expression and protein production in cultures of human peripheral blood mononuclear cells.* Nat.Immun., 1995. 14(5-6): p. 295-304.

130. Huber, R., et al., *Mistletoe treatment induces GM-CSF- and IL-5 production by PBMC and increases blood granulocyte- and eosinophil counts: a placebo controlled randomized study in healthy subjects.* Eur J Med Res, 2005. 10(10): p. 411-8.
131. Elsasser-Beile, U., et al., *Biological effects of natural and recombinant mistletoe lectin and an aqueous mistletoe extract on human monocytes and lymphocytes in vitro.* J Clin Lab Anal, 2000. 14(6): p. 255-9.
132. Hostanska, K., et al., *A plant lectin derived from Viscum album induces cytokine gene expression and protein production in cultures of human peripheral blood mononuclear cells.* Nat Immun, 1995. 14(5-6): p. 295-304.
133. Mannel, D.N., et al., *Induction of tumor necrosis factor expression by a lectin from Viscum album.* Cancer Immunol Immunother, 1991. 33(3): p. 177-82.
134. Ribereau-Gayon, G., et al., *Mistletoe lectins I, II and III induce the production of cytokines by cultured human monocytes.* Cancer Lett, 1996. 109(1-2): p. 33-8.
135. Ribereau-Gayon, G., et al., *Modulation of cytotoxicity and enhancement of cytokine release induced by Viscum album L. extracts or mistletoe lectins.* Anticancer Drugs, 1997. 8 Suppl 1: p. S3-8.
136. Stein, G.M., et al., *Intracellular expression of IL-4 and inhibition of IFN-gamma by extracts from European mistletoe is related to induction of apoptosis.* Anticancer Res, 2000. 20(5A): p. 2987-94.
137. Stein, G.M., et al., *Toxic proteins from European mistletoe (Viscum album L.): increase of intracellular IL-4 but decrease of IFN-gamma in apoptotic cells.* Anticancer Res, 2000. 20(3A): p. 1673-8.
138. Stein, G.M., A. Bussing, and M. Schietzel, *Stimulation of the maturation of dendritic cells in vitro by a fermented mistletoe extract.* Anticancer Res, 2002. 22(6C): p. 4215-9.
139. Stein, G.M., A. Bussing, and M. Schietzel, *Activation of dendritic cells by an aqueous mistletoe extract and mistletoe lectin-3 in vitro.* Anticancer Res, 2002. 22(1A): p. 267-74.
140. Thies, A., et al., *Low-dose mistletoe lectin-I reduces melanoma growth and spread in a scid mouse xenograft model.* Br J Cancer, 2008. 98(1): p. 106-12.
141. Mossalayi, M.D., A. Alkharrat, and D. Malvy, *Nitric oxide involvement in the anti-tumor effect of mistletoe (Viscum album L.) extracts Iscador on human macrophages.* Arzneimittelforschung, 2006. 56(6A): p. 457-60.
142. Stein, G.M. and P.A. Berg, *Flow cytometric analyses of the specific activation of peripheral blood mononuclear cells from healthy donors after in vitro stimulation with a fermented mistletoe extract and mistletoe lectins.* Eur J Cancer, 1998. 34(7): p. 1105-10.
143. Lee, C.H., et al., *Immunomodulating effects of Korean mistletoe lectin in vitro and in vivo.* Int Immunopharmacol, 2009. 9(13-14): p. 1555-61.
144. Park, C.H., et al., *cDNA cloning and sequence analysis of the lectin genes of the Korean mistletoe (Viscum album coloratum).* Mol Cells, 2001. 12(2): p. 215-20.

145. Heiny, B.M., V. Albrecht, and J. Beuth, *Correlation of immune cell activities and beta-endorphin release in breast carcinoma patients treated with galactose-specific lectin standardized mistletoe extract.* Anticancer Res, 1998. 18(1B): p. 583-6.
146. Beuth, J., et al., *Thymocyte proliferation and maturation in response to galactoside-specific mistletoe lectin-1.* In Vivo, 1993. 7(5): p. 407-10.
147. Bussing, A., et al., *Induction of apoptosis in human lymphocytes treated with Viscum album L. is mediated by the mistletoe lectins.* Cancer Lett, 1996. 99(1): p. 59-72.
148. Bussing, A., et al., *Induction of Fas ligand (CD95L) by the toxic mistletoe lectins in human lymphocytes.* Anticancer Res, 1999. 19(3A): p. 1785-90.
149. Nikolai, G., et al., *Effect of a mistletoe extract (Iscador QuFrF) on viability and migratory behavior of human peripheral CD4+ and CD8+ T lymphocytes in three-dimensional collagen lattices.* In Vitro Cell Dev Biol Anim, 1997. 33(9): p. 710-6.
150. Hamprecht, K., et al., *Mediation of human NK-activity by components in extracts of Viscum album.* Int J Immunopharmacol, 1987. 9(2): p. 199-209.
151. Baxevanis, C.N., et al., *Mistletoe lectin I-induced effects on human cytotoxic lymphocytes. I. Synergism with IL-2 in the induction of enhanced LAK cytotoxicity.* Immunopharmacol Immunotoxicol, 1998. 20(3): p. 355-72.
152. Tabiasco, J., et al., *Mistletoe viscotoxins increase natural killer cell-mediated cytotoxicity.* Eur J Biochem, 2002. 269(10): p. 2591-600.
153. Steinmassl, M. and F.A. Anderer, *Enhancement of human NK and LAK cytotoxicity against HCMV-infected cells by rhamnogalacturonan: specificity of reaction.* Viral Immunol, 1996. 9(1): p. 27-34.
154. Mueller, E.A. and F.A. Anderer, *Chemical specificity of effector cell/tumor cell bridging by a Viscum album rhamnogalacturonan enhancing cytotoxicity of human NK cells.* Immunopharmacology, 1990. 19(1): p. 69-77.
155. Burger, A.M., et al., *Anticancer activity of an aqueous mistletoe extract (AME) in syngeneic murine tumor models.* Anticancer Res, 2001. 21(3B): p. 1965-8.
156. Zarkovic, N., et al., *The Viscum album preparation Isorel inhibits the growth of melanoma B16F10 by influencing the tumour-host relationship.* Anticancer Drugs, 1997. 8 Suppl 1: p. S17-22.
157. Schumacher, U., S. Feldhaus, and U. Mengs, *Recombinant mistletoe lectin (rML) is successful in treating human ovarian cancer cells transplanted into severe combined immunodeficient (SCID) mice.* Cancer Lett, 2000. 150(2): p. 171-5.
158. Mengs, U., et al., *Antitumoral effects of an intravesically applied aqueous mistletoe extract on urinary bladder carcinoma MB49 in mice.* Anticancer Res, 2000. 20(5B): p. 3565-8.
159. Kuttan, G., et al., *Anticarcinogenic and antimetastatic activity of Iscador.* Anticancer Drugs, 1997. 8 Suppl 1: p. S15-6.

160. Schaffrath, B., et al., *Anticancer activity of rViscumin (recombinant mistletoe lectin) in tumor colonization models with immunocompetent mice.* Anticancer Res, 2001. 21(6A): p. 3981-7.
161. Pryme, I.F., et al., *Dietary mistletoe lectin supplementation and reduced growth of a murine non-Hodgkin lymphoma.* Histol Histopathol, 2002. 17(1): p. 261-71.
162. Rostock, M., et al., *Anticancer activity of a lectin-rich mistletoe extract injected intratumorally into human pancreatic cancer xenografts.* Anticancer Res, 2005. 25(3B): p. 1969-75.
163. Beuth, J., et al., *Intratumoral application of standardized mistletoe extracts down regulates tumor weight via decreased cell proliferation, increased apoptosis and necrosis in a murine model.* Anticancer Res, 2006. 26(6B): p. 4451-6.
164. Seifert, G., et al., *Molecular mechanisms of mistletoe plant extract-induced apoptosis in acute lymphoblastic leukemia in vivo and in vitro.* Cancer Lett, 2008. 264(2): p. 218-28.
165. Cebovic, T., S. Spasic, and M. Popovic, *Cytotoxic effects of the Viscum album L. extract on Ehrlich tumour cells in vivo.* Phytother Res, 2008. 22(8): p. 1097-103.
166. Galm, O., et al., *Synergism between rViscumin and cisplatin is not dependent on ERCC-1 expression.* Cancer Lett, 2002. 187(1-2): p. 143-51.
167. Abuharbeid, S., et al., *Cytotoxicity of the novel anti-cancer drug rViscumin depends on HER-2 levels in SKOV-3 cells.* Biochem Biophys Res Commun, 2004. 321(2): p. 403-12.
168. Hostanska, K., et al., *Recombinant mistletoe lectin induces p53-independent apoptosis in tumour cells and cooperates with ionising radiation.* Br J Cancer, 2003. 88(11): p. 1785-92.
169. Schoffski, P., et al., *Phase I trial of intravenous aviscumine (rViscumin) in patients with solid tumors: a study of the European Organization for Research and Treatment of Cancer New Drug Development Group.* Ann Oncol, 2004. 15(12): p. 1816-24.
170. Schoffski, P., et al., *Weekly 24 h infusion of aviscumine (rViscumin): a phase I study in patients with solid tumours.* Eur J Cancer, 2005. 41(10): p. 1431-8.
171. Bergmann, L., et al., *Phase I trial of r viscumin (INN: aviscumine) given subcutaneously in patients with advanced cancer: a study of the European Organisation for Research and Treatment of Cancer (EORTC protocol number 13001).* Eur J Cancer, 2008. 44(12): p. 1657-62.
172. Trefzer, U., et al., *Treatment of unresectable stage IV metastatic melanoma with aviscumine after anti-neoplastic treatment failure: a phase II, multi-centre study.* J Immunother Cancer, 2014. 2: p. 27.
173. Eck, J., et al., *Characterization of recombinant and plant-derived mistletoe lectin and their B-chains.* Eur J Biochem, 1999. 265(2): p. 788-97.
174. Giudici, M., et al., *Antifungal effects and mechanism of action of viscotoxin A3.* FEBS J, 2006. 273(1): p. 72-83.

175. Orru, S., et al., *Amino acid sequence, S-S bridge arrangement and distribution in plant tissues of thionins from Viscum album.* Biol Chem, 1997. 378(9): p. 989-96.
176. Schaller, G., et al., *Viscotoxin composition of the three European subspecies of Viscum album.* Planta Med, 1998. 64(7): p. 677-8.
177. Romagnoli, S., et al., *NMR structural determination of viscotoxin A3 from Viscum album L.* Biochem J, 2000. 350 Pt 2: p. 569-77.
178. Coulon, A., et al., *Modes of membrane interaction of a natural cysteine-rich peptide: viscotoxin A3.* Biochim Biophys Acta, 2002. 1559(2): p. 145-59.
179. Giudici, M., et al., *Interaction of viscotoxins A3 and B with membrane model systems: implications to their mechanism of action.* Biophys J, 2003. 85(2): p. 971-81.
180. Coulon, A., et al., *Comparative membrane interaction study of viscotoxins A3, A2 and B from mistletoe (Viscum album) and connections with their structures.* Biochem J, 2003. 374(Pt 1): p. 71-8.
181. Klein, R., et al., *Induction of antibodies to viscotoxins A1, A2, A3, and B in tumour patients during therapy with an aqueous mistletoe extract.* Eur J Med Res, 2002. 7(8): p. 359-67.
182. Stein, G.M., et al., *Thionins from Viscum album L: influence of the viscotoxins on the activation of granulocytes.* Anticancer Res, 1999. 19(2A): p. 1037-42.
183. Stein, G.M., U. Pfuller, and M. Schietzel, *Viscotoxin-free aqueous extracts from European mistletoe (Viscum album L.) stimulate activity of human granulocytes.* Anticancer Res, 1999. 19(4B): p. 2925-8.
184. Horneber, M.A., et al., *Mistletoe therapy in oncology.* Cochrane Database Syst Rev, 2008(2): p. CD003297.
185. Ernst, E., K. Schmidt, and M.K. Steuer-Vogt, *Mistletoe for cancer? A systematic review of randomised clinical trials.* Int J Cancer, 2003. 107(2): p. 262-7.
186. Kienle, G.S. and H. Kiene, *Review article: Influence of Viscum album L (European mistletoe) extracts on quality of life in cancer patients: a systematic review of controlled clinical studies.* Integr Cancer Ther, 2010. 9(2): p. 142-57.
187. Kienle, G.S. and H. Kiene, *Complementary cancer therapy: a systematic review of prospective clinical trials on anthroposophic mistletoe extracts.* Eur J Med Res, 2007. 12(3): p. 103-19.
188. Kienle, G.S., et al., *Viscum album L. extracts in breast and gynaecological cancers: a systematic review of clinical and preclinical research.* J Exp Clin Cancer Res, 2009. 28: p. 79.
189. Ostermann, T., C. Raak, and A. Bussing, *Survival of cancer patients treated with mistletoe extract (Iscador): a systematic literature review.* BMC Cancer, 2009. 9: p. 451.
190. Lenartz, D., et al., *Survival of glioma patients after complementary treatment with galactoside-specific lectin from mistletoe.* Anticancer Research, 2000. 20(3B): p. 2073-2076.

191. Kienle, G.S., R. Grugel, and H. Kiene, *Safety of higher dosages of Viscum album L. in animals and humans--systematic review of immune changes and safety parameters.* BMC Complement Altern Med, 2011. 11: p. 72.
192. Kienle, G.S., et al., *Intravenous Mistletoe Treatment in Integrative Cancer Care: A Qualitative Study Exploring the Procedures, Concepts, and Observations of Expert Doctors.* Evid Based Complement Alternat Med, 2016. 2016: p. 4628287.
193. Steele, M.L., et al., *Use and safety of intratumoral application of European mistletoe (Viscum album L) preparations in Oncology.* Integr Cancer Ther, 2015. 14(2): p. 140-8.
194. Bosch, D., D. Asede, and I. Ehrlich, *Ex Vivo Optogenetic Dissection of Fear Circuits in Brain Slices.* J Vis Exp, 2016(110): p. e53628.
195. Pilkington, G.J., et al., *Cell lines (VMDk) derived from a spontaneous murine astrocytoma. Morphological and immunocytochemical characterization.* J Neurol Sci, 1983. 62(1-3): p. 115-39.
196. Pilkington, G.J., et al., *Tumorigenicity of cell lines (VMDk) derived from a spontaneous murine astrocytoma. Histology, fine structure and immunocytochemistry of tumours.* J Neurol Sci, 1985. 71(2-3): p. 145-64.
197. Schotterl, S., et al., *Viscumins functionally modulate cell motility-associated gene expression.* Int J Oncol, 2017. 50(2): p. 684-696.
198. Guy, K. and J.M. Andrew, *Expression of the CDw75 (beta-galactoside alpha 2,6-sialyltransferase) antigen on normal blood cells and in B-cell chronic lymphocytic leukaemia.* Immunology, 1991. 74(2): p. 206-14.
199. Han, S.Y., et al., *Anti-cancer effects of enteric-coated polymers containing mistletoe lectin in murine melanoma cells in vitro and in vivo.* Mol Cell Biochem, 2015. 408(1-2): p. 73-87.
200. Kovacs, E., *Investigation of the proliferation, apoptosis/necrosis, and cell cycle phases in several human multiple myeloma cell lines. Comparison of Viscum album QuFrF extract with vincristine in an in vitro model.* ScientificWorldJournal, 2010. 10: p. 311-20.
201. Platten, M., W. Wick, and M. Weller, *Malignant glioma biology: role for TGF-beta in growth, motility, angiogenesis, and immune escape.* Microsc Res Tech, 2001. 52(4): p. 401-10.
202. Nakano, A., et al., *Matrix metalloproteinases and tissue inhibitors of metalloproteinases in human gliomas.* J Neurosurg, 1995. 83(2): p. 298-307.
203. Braedel-Ruoff, S., *Immunomodulatory effects of Viscum album extracts on natural killer cells: review of clinical trials.* Forsch Komplementmed, 2010. 17(2): p. 63-73.
204. Gren, A., *Effects of Iscador preparations on the reactivity of mouse immune system.* Neuro Endocrinol Lett, 2009. 30(4): p. 530-4.
205. Park, H.J., et al., *TLR4-mediated activation of mouse macrophages by Korean mistletoe lectin-C (KML-C).* Biochem Biophys Res Commun, 2010. 396(3): p. 721-5.
206. Lyu, S.Y. and W.B. Park, *Mistletoe lectin (Viscum album coloratum) modulates proliferation and cytokine expressions in murine splenocytes.* J Biochem Mol Biol, 2006. 39(6): p. 662-70.

207. Kovacs, E., *Serum levels of IL-12 and the production of IFN-gamma, IL-2 and IL-4 by peripheral blood mononuclear cells (PBMC) in cancer patients treated with Viscum album extract.* Biomed Pharmacother, 2000. 54(6): p. 305-10.
208. Schötterl, S., et al., *Effects of mistletoe lectins on the natural killer (NK) cell activity against glioma cells.*, in *Die Mistel in der Tumortherapie - 4, aktueller Stand der Forschung und klinische Anwendung*, R. Scheer, Editor. 2016, KVC-Verlag: Essen.
209. Hajto, T., et al., *Effects of mistletoe extract on murine thymocytes in vivo and on glucocorticoid-induced cell count reduction.* Forsch Komplementmed, 2006. 13(1): p. 22-7.
210. Webb, J.L., *Effect of more than one inhibitor*, in *Enzymes and metabolic inhibitors*. 1961, Academic Press: New York.
211. Webb, J.L., *Effect of more than one inhibitor*, in *Enzymes and metabolic inhibitors*. 1961, Academic Press: New York, N.Y. p. 66, 488.
212. Hermisson, M., et al., *O6-methylguanine DNA methyltransferase and p53 status predict temozolomide sensitivity in human malignant glioma cells.* J Neurochem, 2006. 96(3): p. 766-76.
213. Eichler, W., *Characteristics of two CD75-related cell-surface expressed antigens of human lymphocytes.* Mol Immunol, 2007. 44(8): p. 2047-55.
214. Zimring, J.C., et al., *CD75s is a marker of murine CD8(+) suppressor T cells.* Int Immunol, 2003. 15(11): p. 1389-99.
215. Bononi, A., et al., *Protein kinases and phosphatases in the control of cell fate.* Enzyme Res, 2011. 2011: p. 329098.
216. Wlodarchak, N. and Y. Xing, *PP2A as a master regulator of the cell cycle.* Crit Rev Biochem Mol Biol, 2016. 51(3): p. 162-84.
217. Telles, E. and E. Seto, *Modulation of cell cycle regulators by HDACs.* Front Biosci (Schol Ed), 2012. 4: p. 831-9.
218. Li, Y., L. Peng, and E. Seto, *Histone Deacetylase 10 Regulates the Cell Cycle G2/M Phase Transition via a Novel Let-7-HMGA2-Cyclin A2 Pathway.* Mol Cell Biol, 2015. 35(20): p. 3547-65.
219. Lee, S.J., et al., *Curcumin-induced HDAC inhibition and attenuation of medulloblastoma growth in vitro and in vivo.* BMC Cancer, 2011. 11: p. 144.
220. Goodarzi, A.A., W.D. Block, and S.P. Lees-Miller, *The role of ATM and ATR in DNA damage-induced cell cycle control.* Prog Cell Cycle Res, 2003. 5: p. 393-411.
221. Biddlestone-Thorpe, L., et al., *ATM kinase inhibition preferentially sensitizes p53-mutant glioma to ionizing radiation.* Clin Cancer Res, 2013. 19(12): p. 3189-200.
222. Eich, M., et al., *Contribution of ATM and ATR to the resistance of glioblastoma and malignant melanoma cells to the methylating anticancer drug temozolomide.* Mol Cancer Ther, 2013. 12(11): p. 2529-40.
223. Marampon, F., et al., *HDAC4 and HDAC6 sustain DNA double strand break repair and stem-like phenotype by promoting radioresistance in glioblastoma cells.* Cancer Lett, 2017. 397: p. 1-11.

224. Wang, Z., et al., *HDAC6 promotes cell proliferation and confers resistance to temozolomide in glioblastoma.* Cancer Lett, 2016. 379(1): p. 134-42.
225. Goodarzi, A.A., et al., *Utilizing protein phosphatase inhibitors to define PP2A as a regulator of ataxia-telangiectasia mutated.* Methods Mol Biol, 2007. 365: p. 47-59.
226. Holy, J.M., *Curcumin disrupts mitotic spindle structure and induces micronucleation in MCF-7 breast cancer cells.* Mutat Res, 2002. 518(1): p. 71-84.
227. Rafi, M.M., et al., *Novel polyphenol molecule isolated from licorice root (Glycrrhiza glabra) induces apoptosis, G2/M cell cycle arrest, and Bcl-2 phosphorylation in tumor cell lines.* J Agric Food Chem, 2002. 50(4): p. 677-84.
228. Naumann, U., et al., *Glioma gene therapy with soluble transforming growth factor-beta receptors II and III.* Int J Oncol, 2008. 33(4): p. 759-65.
229. Nakada, M., et al., *The phosphorylation of EphB2 receptor regulates migration and invasion of human glioma cells.* Cancer Res, 2004. 64(9): p. 3179-85.
230. Wang, S.D., et al., *EphB2 receptor controls proliferation/migration dichotomy of glioblastoma by interacting with focal adhesion kinase.* Oncogene, 2012. 31(50): p. 5132-43.
231. Huang, Q., et al., *Glioma stem cells are more aggressive in recurrent tumors with malignant progression than in the primary tumor, and both can be maintained long-term in vitro.* BMC Cancer, 2008. 8: p. 304.
232. Hofer, M.D., et al., *Expression of MTA1 promotes motility and invasiveness of PANC-1 pancreatic carcinoma cells.* Br J Cancer, 2004. 90(2): p. 455-62.
233. Zhang, W., X. Men, and P. Lei, *Review on anti-tumor effect of triterpene acid compounds.* J Cancer Res Ther, 2014. 10 Suppl 1: p. 14-9.
234. Kandaswami, C., et al., *The antitumor activities of flavonoids.* In Vivo, 2005. 19(5): p. 895-909.
235. Gdynia, G., et al., *Basal caspase activity promotes migration and invasiveness in glioblastoma cells.* Mol Cancer Res, 2007. 5(12): p. 1232-40.
236. Liu, W., et al., *CEACAM1 impedes thyroid cancer growth but promotes invasiveness: a putative mechanism for early metastases.* Oncogene, 2007. 26(19): p. 2747-58.
237. Ebrahimnejad, A., et al., *CEACAM1 enhances invasion and migration of melanocytic and melanoma cells.* Am J Pathol, 2004. 165(5): p. 1781-7.
238. Shekarabi, M. and T.E. Kennedy, *The netrin-1 receptor DCC promotes filopodia formation and cell spreading by activating Cdc42 and Rac1.* Mol Cell Neurosci, 2002. 19(1): p. 1-17.
239. Nakada, M., et al., *Roles of membrane type 1 matrix metalloproteinase and tissue inhibitor of metalloproteinases 2 in invasion and dissemination of human malignant glioma.* J Neurosurg, 2001. 94(3): p. 464-73.
240. Lam, B.D., E.C. Anthony, and P.L. Hordijk, *Analysis of nucleo-cytoplasmic shuttling of the proto-oncogene SET/I2PP2A.* Cytometry A, 2012. 81(1): p. 81-9.

241. Goertzen, C.G., et al., *KISS1R signaling promotes invadopodia formation in human breast cancer cell via beta-arrestin2/ERK.* Cell Signal, 2016. 28(3): p. 165-76.
242. Wu, F., et al., *p107 Expression in colorectal tumours rises during carcinogenesis and falls during invasion.* Eur J Cancer, 2002. 38(14): p. 1838-48.
243. Mei, P., et al., *BRMS1 suppresses glioma progression by regulating invasion, migration and adhesion of glioma cells.* PLoS One, 2014. 9(5): p. e98544.
244. Sooman, L., et al., *FGF2 as a potential prognostic biomarker for proneural glioma patients.* Acta Oncol, 2015. 54(3): p. 385-94.
245. Chen, D., et al., *Better prognosis of patients with glioma expressing FGF2-dependent PDGFRA irrespective of morphological diagnosis.* PLoS One, 2013. 8(4): p. e61556.
246. Boissan, M., M.F. Poupon, and M.L. Lacombe, *[NM23 and metastasis suppressor genes: update].* Med Sci (Paris), 2007. 23(12): p. 1115-23.
247. McDermott, W.G., et al., *Nm23-H1 homologs suppress tumor cell motility and anchorage independent growth.* Clin Exp Metastasis, 2008. 25(2): p. 131-8.
248. Xu, L., et al., *Methylation-induced silencing of maspin contributes to the proliferation of human glioma cells.* Oncol Rep, 2016. 36(1): p. 57-64.
249. Chou, R.H., et al., *Suppression of the invasion and migration of cancer cells by SERPINB family genes and their derived peptides.* Oncol Rep, 2012. 27(1): p. 238-45.
250. Bussing, A., *Immune modulation using mistletoe (Viscum album L.) extracts Iscador.* Arzneimittelforschung, 2006. 56(6A): p. 508-15.
251. Elsasser-Beile, U., et al., *Antitumoral effect of recombinant mistletoe lectin on chemically induced urinary bladder carcinogenesis in a rat model.* Cancer, 2001. 91(5): p. 998-1004.
252. Fischer, S., A. Scheffler, and D. Kabelitz, *Stimulation of the specific immune system by mistletoe extracts.* Anticancer Drugs, 1997. 8 Suppl 1: p. S33-7.
253. Klingbeil, M.F., et al., *Cytotoxic effects of mistletoe (Viscum album L.) in head and neck squamous cell carcinoma cell lines.* Oncol Rep, 2013. 30(5): p. 2316-22.
254. Mulsow, K., et al., *Impact of Mistletoe Triterpene Acids on the Uptake of Mistletoe Lectin by Cultured Tumor Cells.* PLoS One, 2016. 11(4): p. e0153825.
255. Nazaruk, J. and P. Orlikowski, *Phytochemical profile and therapeutic potential of Viscum album L.* Nat Prod Res, 2016. 30(4): p. 373-85.
256. Rios, J.L., *Effects of triterpenes on the immune system.* J Ethnopharmacol, 2010. 128(1): p. 1-14.
257. Toniolo, A., et al., *Antiinflammatory and antioxidant effects of H2O2 generated by natural sources in Il1beta-treated human endothelial cells.* Prostaglandins Other Lipid Mediat, 2015. 121(Pt B): p. 190-8.

258. Ma, Z., et al., *Echinocystic Acid Inhibits IL-1beta-Induced COX-2 and iNOS Expression in Human Osteoarthritis Chondrocytes.* Inflammation, 2016. 39(2): p. 543-9.
259. Robson, R.L., J. Westwick, and Z. Brown, *Interleukin-1-induced IL-8 and IL-6 gene expression and production in human mesangial cells is differentially regulated by cAMP.* Kidney Int, 1995. 48(6): p. 1767-77.
260. Ricciotti, E. and G.A. FitzGerald, *Prostaglandins and inflammation.* Arterioscler Thromb Vasc Biol, 2011. 31(5): p. 986-1000.
261. Villeneuve, J., P. Tremblay, and L. Vallieres, *Tumor necrosis factor reduces brain tumor growth by enhancing macrophage recruitment and microcyst formation.* Cancer Res, 2005. 65(9): p. 3928-36.
262. Behrens, T.W. and D.L. Mueller, *Bcl-x and the regulation of survival in the immune system.* Immunol Res, 1997. 16(2): p. 149-60.
263. Chiu, T.L., et al., *AAV2-mediated interleukin-12 in the treatment of malignant brain tumors through activation of NK cells.* Int J Oncol, 2009. 35(6): p. 1361-7.
264. Vom Berg, J., et al., *Intratumoral IL-12 combined with CTLA-4 blockade elicits T cell-mediated glioma rejection.* J Exp Med, 2013. 210(13): p. 2803-11.
265. Muller, W.A., *Getting leukocytes to the site of inflammation.* Vet Pathol, 2013. 50(1): p. 7-22.
266. Hjortso, M.D. and M.H. Andersen, *The expression, function and targeting of haem oxygenase-1 in cancer.* Curr Cancer Drug Targets, 2014. 14(4): p. 337-47.
267. Tzima, S., et al., *Myeloid heme oxygenase-1 regulates innate immunity and autoimmunity by modulating IFN-beta production.* J Exp Med, 2009. 206(5): p. 1167-79.
268. Gandini, N.A., et al., *Heme oxygenase-1 expression in human gliomas and its correlation with poor prognosis in patients with astrocytoma.* Tumour Biol, 2014. 35(3): p. 2803-15.
269. Wick, W., U. Naumann, and M. Weller, *Transforming growth factor-beta: a molecular target for the future therapy of glioblastoma.* Curr Pharm Des, 2006. 12(3): p. 341-9.
270. Rosin, D.L. and M.D. Okusa, *Dangers within: DAMP responses to damage and cell death in kidney disease.* J Am Soc Nephrol, 2011. 22(3): p. 416-25.
271. Hajto, T., et al., *Immunomodulatory effects of Viscum album agglutinin-I on natural immunity.* Anticancer Drugs, 1997. 8 Suppl 1: p. S43-6.
272. Mockel, B., et al., *Effects of mistletoe lectin I on human blood cell lines and peripheral blood cells. Cytotoxicity, apoptosis and induction of cytokines.* Arzneimittelforschung, 1997. 47(10): p. 1145-51.
273. De Lau, W.B., et al., *HB4 antibody recognizes a carbohydrate structure on lymphocyte surface proteins related to HB6, CDw75, and CD76 antigens.* J Immunol, 1993. 150(11): p. 4911-9.
274. Bast, B.J., et al., *The HB-6, CDw75, and CD76 differentiation antigens are unique cell-surface carbohydrate determinants generated by the beta-galactoside alpha 2,6-sialyltransferase.* J Cell Biol, 1992. 116(2): p. 423-35.

275. Huber, R., et al., *Pharmacokinetics of natural mistletoe lectins after subcutaneous injection.* Eur J Clin Pharmacol, 2010. 66(9): p. 889-97.
276. Huber, R., et al., *Immunologic effects of mistletoe lectins: a placebo-controlled study in healthy subjects.* J Soc Integr Oncol, 2006. 4(1): p. 3-7.
277. Beuth, J., et al., *Behavior of lymphocyte subsets and expression of activation markers in response to immunotherapy with galactoside-specific lectin from mistletoe in breast cancer patients.* Clin Investig, 1992. 70(8): p. 658-61.
278. Beuth, J., et al., *[Comparative studies on the immunoactive action of galactoside-specific mistletoe lectin. Pure substance compared to the standardized extract].* Arzneimittelforschung, 1993. 43(2): p. 166-9.
279. Kheirollahi, M., et al., *Expression of cyclin D2, P53, Rb and ATM cell cycle genes in brain tumors.* Med Oncol, 2011. 28(1): p. 7-14.
280. Vecchio, D., et al., *Predictability, efficacy and safety of radiosensitization of glioblastoma-initiating cells by the ATM inhibitor KU-60019.* Int J Cancer, 2014. 135(2): p. 479-91.
281. Blake, S.M., et al., *Inactivation of the ATMIN/ATM pathway protects against glioblastoma formation.* Elife, 2016. 5.
282. Shimura, T., et al., *Cyclin D1 overexpression perturbs DNA replication and induces replication-associated DNA double-strand breaks in acquired radioresistant cells.* Cell Cycle, 2013. 12(5): p. 773-82.
283. Ahmad, M., et al., *How stemlike are sphere cultures from long-term cancer cell lines? Lessons from mouse glioma models.* J Neuropathol Exp Neurol, 2014. 73(11): p. 1062-77.
284. Ito, A., et al., *Degradation of interleukin 1beta by matrix metalloproteinases.* J Biol Chem, 1996. 271(25): p. 14657-60.
285. Schonbeck, U., F. Mach, and P. Libby, *Generation of biologically active IL-1 beta by matrix metalloproteinases: a novel caspase-1-independent pathway of IL-1 beta processing.* J Immunol, 1998. 161(7): p. 3340-6.
286. Ries, C., *Cytokine functions of TIMP-1.* Cell Mol Life Sci, 2014. 71(4): p. 659-72.

7. Acknowledgement

Firstly, I would like to thank my advisor Prof. Dr. Naumann for the support and assistance of my doctoral study and research, for her guidance and knowledge. Besides, I would like to thank my thesis committee Prof. Dr. Ruth, Prof. Dr. Feil, and Prof. Dr. Huber for their time and helpful comments.

Furthermore, I am grateful for the financial support from the ISUS innovation foundation, the Software AG, and the ISCADOR AG. I thank the ISCADOR AG for providing me with ISCADOR Qu and P. For the support with Aviscumine and also with ideas I thank Prof. Dr. Lentzen from MELEMA Pharma GmbH. In addition, I thank Dr. Heyder from Abnoba GmbH for providing native ML-1.

A special gratitude goes to our project partner Prof. Dr. Mittelbronn and his team in Frankfurt that helped me a lot with their knowledge, advice and active support.

I thank my colleagues Angela Armento, Rebecca Czolk, and Jacob Ehlers for the discussions and the fun we had in last years. Furthermore, I want to thank my students Linda Grimm, Felix Klostermann, Ahmed Yousif, Vivien Veninga, Miriam Hübner, and Jennifer T. Miemietz for helping me with the project.

I am grateful to my husband Jonas, my parents Gudrun and Ronald, and my brother Stefan for their love and emotional support in every situation during writing my thesis.

Last but not least, I want to thank all my friends, my parents-in-law, and my other family members for supporting me the last years.

Thanks for all the encouragement and help!